IDENTIFICATION OF *C. burnetii* TYPE IV SECRETION SUBSTRATES REQUIRED FOR INTRACELLLAR REPLICATION AND *Coxiella*-CONTAINING VACUOLE FORMATION

A Dissertation

by

MARY MARGARET WEBER

Submitted to the Office of Graduate and Professional Studies of
Texas A&M University
in partial fulfillment of the requirements for the degree of

DOCTOR OF PHILOSOPHY

Chair of Committee,	Jim Samuel
Committee Members,	Paul de Figueiredo
	Katja Mertens
	Vernon Tesh
Head of Department,	Jim Samuel

May 2014

Major Subject: Medical Sciences

ABSTRACT

Coxiella burnetii is a Gram-negative intracellular pathogen that encodes a specialized type IVb secretion system (T4SS) which is essential for intracellular replication, *Coxiella*-containing vacuole (CCV) formation, modulation of apoptosis, and effector translocation. To identify T4SS candidate substrates, we used an enhanced bioinformatics guided approach. Expression of 234 T4SS candidate substrates as TEM1 β-lactamase fusions identified 53 substrates that were translocated in a Dot/Icm-dependent manner. Large scale screens aimed at identifying localization and function revealed that several of these substrates traffic to distinct subcellular compartments and interfere with crucial host processes. To determine if any of these T4SS substrates are necessary for intracellular replication, we isolated 20 clonal T4SS substrate mutants using the *Himar1* transposon and transposase. Of these, 10 mutants exhibited defects in intracellular growth and CCV formation in HeLa and J774A.1 cells, but displayed normal growth in axenic culture. Given their confirmed role in intracellular replication and CCV formation, we named 5 of these substrates *CirA-E* (*Coxiella* effector for intracellular replication). To identify the pathways targeted by these crucial substrates, *S. cerevisiae* strains were co-transformed with pYEp13 yeast genomic library and the T4SS substrates. Using this approach we identified multiple members of the Rho family of GTPases as suppressors of Cbu0041 (CirA) toxicity. Overexpression in mammalian cells resulted in cell rounding, detachment, and reduced stress fibers. Collectively, these results indicate that *C. burnetii* encodes a large repertoire of T4SS substrates that play integral roles in host cell subversion and CCV formation.

DEDICATION

I would like to dedicate the work presented in this dissertation to Diana Weber. Without her unwavering love and support throughout the years none of this would have been possible. Thank you for always being there and for being the greatest mother in the world.

ACKNOWLEDGEMENTS

I would like to thank all current and former members of the Samuel lab for helpful discussion and critical review of the data presented in this dissertation. I would like to thank Gloria Galvan and Andres Tellez for their assistance with characterization of the nuclear effectors and William Wright for helping with the yeast suppressor screen. I would like to thank Chen Chen for conducting the bioinformatics and two-hybrid screen to identify T4SS candidates and for his guidance in setting up the large-scale screens to characterize the T4SS substrates. Thank you to Katja Mertens for adapting the *Himar1* transposon for use in *C. burnetii* and to Kristina Rowin and Anand Ganapathy for generating the *C. burnetii* transposon mutant library. I would also like to thank James Berg, Chris Dealing, Smita Singh, and Juanita McLachlan for maintaining the lab and assisting with experiments.

I would also like to thank Larry Dangott for LC/MS/MS assistance and Jane Miller for helping with the flow cytometry. I am extremely grateful to Kalli Landua, Ashish Aryal, and Steven Fullwood for extensive confocal training and for helping with image analysis.

I would especially like to thank Robert Faris for support encouragement, and for his help with experimental design and critical review of my data. Thanks to my friends and family for their support and encouragement over the years and for always being there no matter how apart we are.

Thank you to my committee members Paul de Figueiredo, Vernon Tesh, and Katja Mertens. Their advice, guidance, and support over the years has been invaluable and has helped my scientific development immensely.

Lastly I would like to thank James Samuel for his mentorship and for providing me a place to do research. I have learned a lot over the past 5 years and would not have been able to accomplish as much without his constant advice and support.

TABLE OF CONTENTS

LIST OF FIGURES

LIST OF TABLES

CHAPTER I

INTRODUCTION

The organism

Coxiella burnetii, a Gram-negative naturally obligate intracellular pathogen, is the etiological agent of Q fever, a zoonotic disease predominately associated with domestic livestock. The primary route of transmission occurs via inhalation of contaminated aerosols, resulting in an acute, flu-like illness that is typically self-limiting and readily resolves without antibiotic treatment. However, in rare instances chronic Q fever can develop that results in chronic endocarditis or hepatitis (81). The highly infectious nature, environmental stability, and ease of dissemination led to the classification of *C. burnetii* as a category B select agent and in 1999 it became a reportable disease by the CDC (64). Q fever is endemic and cases have been reported in virtually every region and major country in the world except New Zealand. While less than 1,400 cases were reported in the US between 1948 and 1986, the number of annually reported cases in the US has drastically increased since 2000. A recent outbreak of Q fever in the Netherlands resulted in over 4,000 documented cases with 20% of patients requiring hospitalization (105). Based on the incidence in other countries with a longer history of aggressive surveillance as well as common misdiagnosis of Q fever as the flu, suggests the incidence of this disease in the US may be significantly higher.

Prior to the development of genetic tools, the only known virulence factor of *C. burnetii* was lipopolysaccharide (71). Virulent phase I organisms, isolated from natural sources, express a complete O antigen whereas avirulent phase II organisms, obtained

from serial passage through embryonated eggs or tissue culture, express truncated LPS that often lacks the terminal O-antigen sugars (37).

Intracellular lifestyle of C. burnetii

Following inhalation, *C. burnetii* is capable of infecting a variety of host cell types with the primary respiratory tract target being alveolar macrophages. Binding of unknown bacterial ligand to $\alpha_v\beta_3$ integrin on the phagocytic cell leads to internalization by RAC1-dependent phagocytosis, however internalization of only phase I bacteria leads to dramatic reorganization of F-actin (69). While the receptor on nonprofessional phagocytes is not known, it is clear that invasion requires cytoskeletal rearrangements (69).

Following phagocytic uptake, the bacteria-containing nascent phagosome traffics through the default pathway to establish a *Coxiella*-containing vacuole (CCV) derived from the host lysosomal network. Five minutes after uptake, the nascent phagosome transitions from an early phagosome to a late phagosome, as evident by recruitment of the small GTPases, Rab5 and Rab7, markers of early and late endosomes, respectively (88). However, fusion with the lysosome is delayed by 2 hr compared to phagosomes containing latex beads which acquire lysosomal markers within five minutes of uptake. During this stall the phagosome engages the autophagic pathway as evident by decoration of the CCV membrane with light-chain 3 (LC3), a process that requires active bacterial protein synthesis (36, 88). Engagement of the autophagic machinery clearly benefits *C. burnetii* infection as induction of autophagy increases the number of infected cells and the size of the CCV (36). While the benefit to the pathogen by this initial stall

is unclear, it has been proposed that autophagic vesicles may deliver nutrients and membrane to the CCV and which could promote the transition from the small cell variant (SCV) to the large cell variant (LCV) (36, 88).

As the CCV matures into a late phagosome, it loses Rab5 but acquires Rab7, lysosome associated membrane glycoprotein 1 (LAMP-1), and vacuolar ATPase (vATPase). Acquisition of the vATPase serves to pump protons into the phagosome lumen, driving the pH from 5.4 to 5 (44). Finally, the CCV fuses with lysosomes, the vacuolar pH reduces to pH 4.5, and it acquires cathepsin D, acid phosphatases, and hydrolyases (88).

As the development of the CCV progresses, it can undergo homotypic fusions with other CCVs and heterotypic fusions with vesicles derived the autophagic (88), endocytic, or secretory (17) compartments. Multiple fusion events result in generation of a "spacious" CCV that often occupies the majority of the host cytoplasmic space. Generation of this spacious compartment is also dependent on the actin cytoskeleton and members of the Rho GTPase family since destabilization of actin or expression of GDP-locked RhoA results in formation of tight vacuoles that do not expand (1). Manipulation of these host processes is dependent on bacterial protein synthesis (44).

Surprisingly, expansion of the CCV does not affect host cell viability, suggesting *C. burnetii* prolongs cell viability by prevention of apoptosis and induction of pro-survival factors. *C. burnetii* infected cells are protected from staurosporin induced apoptosis and exhibit reduced cleavage of caspase-3, -9 and poly (ADP-ribose) polymerase (PARP) (112). Furthermore, tumor necrosis factor-α stimulation resulted in

reduced PARP cleavage (112). The bacteria also actively inhibit apoptosis by modulating the interplay between Beclin-1 and Bcl-2. Whereas Beclin-1 is recruited to the CCV and promotes bacterial replication and vacuole development, the number and size of the CCV is significantly reduced when Beclin-1 is unable to interact with Bcl-2 and this interaction is essential for apoptosis inhibition (107). *C. burnetii* also promotes host cell survival by promoting sustained activation of the pro-survival kinases Akt (110), Erk1/2 (110), and PKA (62, 63). Inhibition of these signaling cascades with pharmacological inhibitors drastically decreased the anti-apoptotic effect associated with the bacteria (48). Importantly, modulation of apoptosis through each pathway requires active bacterial protein synthesis and maybe mediated by the activity of bacterial effector proteins (62, 107, 110, 112).

Dot/Icm secretion system

Central to pathogenesis is a specialized type IVb secretion system that is closely related to that of *Legionella pneumophila*. This system was co-discovered by two lab groups that identified mutants with reduced intracellular multiplication (*icm*) (12) and a defect in organelle trafficking (*dot*), resulting in the dual nomenclature of Dot/Icm (10). In *Legionella* this system is composed of 26 components found on two distinct 20 kb regions of the chromosome. While the majority of these components lack homology to other *orfs*, 18 share homology to components of the bacterial conjugative DNA transfer systems (77).

In *Legionella* these components form a multi-protein apparatus that consists of several sub-complexes: the core complex, consisting of DotC, DotD, DotF, DotG and

DotH, serve to link the bacteria inner and outer membrane and a second complex composed of the coupling protein DotL, DotM, DotN, IcmS, IcmW (76, 106). This system also encodes an ATPase, DotB, whose activity is required for secretion (76).

Coxiella encodes 23 of the 26 components, lacking homologs of DotV, IcmR, DotJ (92). Functional similarity between the systems was demonstrated by cross-complementation of *Legionella* mutants with *Coxiella dotB, icmS, icmW*, and *icmT* (115), which suggested that *Legionella* could serve as a surrogate to study *Coxiella* secretion.

Identification of C. burnetii T4SS substrates

Until recently, a lack of genetic tools significantly hindered the ability to study T4SS in *C. burnetii*, necessitating use of *L. pneumophila* as a surrogate host. However the development of an acidified citrate cysteine media (ACCM) (80) for axenic culture of the organism, the development of *C. burnetii* shuttle vectors (20), and tools for random (7) and site-directed mutagenesis (8) have significantly advanced the field and allowed for confirmation of substrate secretion in *C. burnetii* (18, 20, 57, 109, 113). Importantly, the isolation of T4SS mutants have verified that, like the *Legionella* system, the Dot/Icm secretion system of *Coxiella* is essential for intracellular replication, CCV formation, effector translocation, and modulation of host apoptosis (6, 8, 18).

Numerous strategies have been employed to identify bacterial secretion substrates from intracellular pathogens such as *L. pneumophila.* Bacterial-two-hybrid (61) and bioinformatic guided approaches (15, 23, 43, 46, 83, 94) have led to the identification of over 250 T4SS substrates, representing approximately 10% of the

proteome. While significant homology exists between the two secretion systems, only a few of the effectors are conserved, which can be attributed to the vast differences between the intracellular niches. This suggests that *C. burnetii* may possess a unique repertoire of virulence factors. However, while homolog between the substrates is limited, many of the attributes of secretion substrates are similar and the tools used to identify *Legionella* substrates can be employed to identify *Coxiella* substrates.

DotF, a major component of T4SS core complex, was successful used to identify 8 *Legionella* T4SS substrates (61). Given the extensive homology between *Coxiella* and *Legionella* and the successful use of DotF as bait, a bacterial two-hybrid screen was employed to identify *Coxiella* T4SS substrates. Using this approach, 25 *orfs* were identified that were fused in frame with adenylate cyclase, 11 of which were eliminated based on their conservation among other Gram-negative bacteria (20). Use of established secretion assays such as CyaA and TEM1 translocation assay identified 6 substrates that were positive for translocation in both assays, representing a 42.9% (6/14) predictive success rate (20).

Bioinformatics has emerged as a powerful and effective tool for identifying potential bacterial effectors. A recent study by Burstein et al. (14) developed a novel computational approach that identified specific traits of bacterial effectors that could be exploited to identify candidate effector proteins. To identify *C. burnetii* T4SS substrates, we employed a similar strategy to generate a candidate list consisting of *C. burnetii orfs* that are paralogs to *L. pneumophila* substrates, harbor eukaryotic-like motifs, contain PmrA recognition sites (118) or E-block motifs (46).

While the intracellular niche occupied by *C. burnetii* is truly unique, it is possible that some of its effectors target the same host proteins as *Legionella* effectors. To identify paralogs, Chen et al. (20) conducted a genome wide screen using 134 *L. pneumophila* and 9 *C. burnetii* secretion substrates. After eliminating 12 substrates identified in a previous study (83), this approach identified 15 novel *orfs* that represent candidate substrates.

Many intracellular pathogens encode a large number of proteins that possess eukaryotic-like motifs that functionally mimic or antagonize host cell proteins to drive the infection process. Ankyrin-repeat domains comprise a diverse protein family that mediate protein-protein or protein-DNA interactions through the formation of a molecular scaffold (83). However, this motif is not restricted to eukaryotes, and has been found in several intracellular bacteria (60, 83, 84, 111) where it serves diverse functions including chromatin remodeling (84) and inhibition of apoptosis (60). In addition to ankyrin-repeat proteins, bioinformatic screening of the *C. burnetii* genome for proteins containing tetratricopeptide repeats (TRPs), coiled-coil domains (CCDs), leucine-rich repeats (LRRs), GTPase domains, F-boxes, kinases, and phosphatases domains lead to the identification of 24 novel candidate substrates (20).

Many virulent bacterial species encode two-component systems as sophisticated mechanisms for responding to specific environmental cues by modifying expression of virulence genes and regulating bacterial secretion. Using bioinformatics, Zusman et al. (118) identified a conserved regulatory element for five *C. burnetii dot/icm* genes that resembles the PmrA response regulator. Furthermore, using the consensus sequence

TTAA-N6-TTAA, they identified 35 *L. pneumophila* and 68 *C. burnetii orfs* that contain this conserved regulatory element. Secretion assays revealed that 3/5 *L. pneumophila orfs* tested were secreted in a Dot/Icm dependent manner, suggesting that PmrA may regulate specific actions of type IV secretion and could be used to identify putative secretion candidates (118). By modifying this consensus sequence we identified over 130 *orfs* (14, Chapter 2).

By examining traits (14) and sequences (54) from *Legionella* secretion substrates, two independent studies concluded that there is a biased toward specific amino acids in the last 20 residues of the C-terminus, however both studies were unable to identify a consensus sequence. By complementing sidCΔ100, a well characterized *Legionella* effector that lacks the C-terminal secretion signal, with codons from over 400 potential secretion candidates, Huang et al. (46) determined that the C-terminus of many *Legionella* substrates possess an E-block motif, characterized by 3-6 acidic residues in a region spanning 6-10 residues. Using the consensus sequences EExxE, ExE, or EEx the authors were able to identify 49 new T4SS substrates, suggesting that the presence of an E-block motif may be used to identify novel T4SS substrates (46). Using this motif, we identified over 50 *orfs* that represent potential secretion substrates (Chapter 2).

Characterization of C. burnetii T4SS substrates

To date, over one hundred novel T4SS substrates have been identified based on genomic (18), bacterial two-hybrid (20), or bioinformatics screens (20, 83, 109, 111). However, the function of the vast majority of these substrates remains undefined. Many of these substrates lack functional domains that serve as predictors of effector function.

To circumvent this, many large scale screens aimed at identifying subcellular localization and effector function have been employed to preliminarily characterize these substrates (13, 14, 73, Chapter 2).

Like *Legionella,* some redundancy appears to exist among *Coxiella* secretion substrates as three substrates, AnkG, CaeA, CaeB, act to independently promote host cell viability by modulating apoptosis. The ankyrin-repeat containing protein G (AnkG) binds the pro-apoptotic protein, p32, to inhibit apoptosis (60). Anti-apoptotic effector B (CaeB) inhibits apoptosis through a mitochondrial pathway whereas the nuclear effector CaeA was also noted to block apoptosis, however very limited data to suggest a molecular mechanism for this inhibition (52).

Finally *Coxiella* vacuolar protein A (CvpA), modulates clathrin-mediated vesicular trafficking. CvpA binds directly to AP2 and the clathrin heavy chain, both of which play integral roles in *Coxiella* replication as siRNA depletion of either significantly inhibited *C. burnetii* replication. Importantly, a Δ*cvpA* was significantly impaired in intracellular replication and vacuole development, highlighting the importance clathrin-mediated vesicular trafficking in *C. burnetii* pathogenesis (57).

CHAPTER II

IDENTIFICATION OF *C. BURNETII* TYPE IV SECRETION SUBSTRATES REQUIRED FOR INTRACELLLAR REPLICATION AND *COXIELLA*-CONTAINING VACUOLE FORMATION*

Summary

Coxiella burnetii, the etiological agent of acute and chronic Q fever in humans, is a naturally intracellular pathogen that directs the formation of an acidic *Coxiella*-containing vacuole (CCV) derived from the host lysosomal network. Central to its pathogenesis is a specialized Type IVB secretion system (T4SS) that delivers effectors essential for intracellular replication and CCV formation. Using a bioinformatics guided approach, 234 T4SS candidate substrates were identified. Expression of each candidate as a TEM-1 β-lactamase fusion protein led to the identification of 53 substrates that were translocated in a Dot/Icm-dependent manner. Ectopic expression in HeLa cells revealed that these substrates trafficked to distinct subcellular sites, including the endoplasmic reticulum, mitochondrion, and nucleus. Expression in yeast identified several substrates that were capable of interfering with yeast growth, suggesting these substrates target crucial host processes. To determine if any of these T4SS substrates are necessary for intracellular replication, we isolated 20 clonal T4SS substrate mutants using the *Himar1* transposon and transposase. Among these, ten mutants exhibited defects in intracellular

*Reprinted with permission from "Identification of *C. burnetii* type IV secretion substrates required for intracellular replication and *Coxiella*-containing vacuole formation**"** by Weber MM, Chen C, Rowin K, Mertens K, Galvan G, Zhi H, Dealing CM, Roman VA, Banga S, Tan Y, Luo Z-Q, Samuel JE. 2013. J. Bacteriol. **195**:3914–24., Copyright [2013] ASM Journals

growth and CCV formation in HeLa and J774A.1 cells, but displayed normal growth in bacteriological medium. Collectively, these results indicate that *C. burnetii* encodes a large repertoire of T4SS substrates that play integral roles in host cell subversion and CCV formation, and suggests less redundancy in effector function than found in the comparative *Legionella* Dot/Icm model.

Introduction

Coxiella burnetii, a Gram-negative naturally obligate intracellular pathogen, is the etiological agent of Q fever, a zoonotic disease predominately associated with domestic livestock. This highly infectious organism is usually acquired via inhalation of contaminated aerosols where it manifests as an acute, flu-like illness that is typically self-limiting and readily resolves without antibiotic treatment. However, in rare but serious instances chronic Q fever can develop, which generally presents as endocarditis or hepatitis (47).

Actin-dependent endocytosis of *C. burnetii* by macrophages leads to internalization in an early endosome and trafficking through the default endocytic pathway to ultimately establish an acidic C*oxiella*-containing vacuole (CCV) derived from the host lysosomal network (81). While the nascent CCV readily acquires Rab5 and Rab7, markers of early and late endosomes respectively, fusion with the lysosome is delayed compared to phagosomes harboring latex beads (44). During this initial stall, the *Coxiella*-containing phagosome undergoes repeated fusions with autophagosomes, an interaction that is believed to deliver nutrients to the organism (88). Following this delay, the phagosome fuses with the lysosome and the bacteria transition from a

nonreplicative small-cell variant (SCV) to the replicative large-cell variant (LCV) (21). As replication ensues, the *Coxiella*-containing vacuole expands to ultimately occupy most of the host cell cytoplasm and undergoes repeated fusions with autophagosomes, endolysosomes and at later time points, vesicles from the early secretory pathway (17, 88). Establishment of this intracellular niche is dependent on active bacterial protein synthesis (45) and requires manipulation of numerous host cell processes. This includes induction of autophagy (88), inhibition of apoptosis (60), modification of kinases and phosphatases (48, 110), modulation of the host transcriptome (65), and recruitment of secretory components (17).

Intracellular replication and CCV formation is dependent on a type IVB secretion system that is homologous to the Dot/Icm system of *Legionella pneumophila* (6, 18). In *Legionella,* this system is encoded by 27 *dot/icm* (defect in organelle trafficking/intracellular multiplication) genes (10, 66), 18 of which are homologous to components of the *tra/trb*-encoded DNA conjugative machinery (47). Together these components form a pilus-like structure that presumably spans across the inner and outer bacterial membranes and forms a translocation pore through the *Legionella*-containing vacuole (LCV), allowing delivery of bacterial effector proteins into the host cell cytosol (48). The Dot/Icm system of *Coxiella* consists of 24 of these Dot/Icm components, lacking homologs of IcmR, DotJ, and DotV (92).

These systems are functionally analogous, as demonstrated by cross-complementation of *Legionella* mutants with *Coxiella dotB, icmS, icmW*, and *icmT* (115). This similarity has successfully allowed researchers to use the genetically

tractable *L. pneumophila* as a surrogate host to identify *C. burnetii* T4SS substrates (20, 60, 83, 109). However only a few of the effectors are conserved, which is consistent with the different properties of the vacuoles occupied by these two pathogens. Whereas *C. burnetii* thrives in an acidic, autophagosome-like vacuole, *L. pneumophila* resides in a vacuole with a neutral pH derived from the host endoplasmic reticulum (47). Additionally, substantial differences in host range exist with *Legionella* predominately associated with protists and *Coxiella* being associated with a variety of mammalian species. To date, approximately 50 T4SS substrates have been identified in *C. burnetii* using bacterial two-hybrid (20), genomic (60), and ORFs with predicted eukaryotic-like domains (20, 83, 109, 111) for the ability to serve as Dot/Icm dependent secretion substrates.

The goal of the current study was to more comprehensively identify *C. burnetii* T4SS substrates using an enhanced bioinformatics-guided approach. The *C. burnetii* genome was screened for ORFs that contained a PmrA regulatory consensus sequence within the predicted promoter region (20, 118), E-block motif (46), or were homologs of known effectors. Using this approach, we identified 53 T4SS substrates, 46 of which have not been previously reported. Ectopic expression in mammalian cells and heterologous expression in yeast revealed that these substrates traffic to distinct subcellular compartments and modulate crucial host processes. The use of the *Himar1*-mediated random mutagenesis resulted in the generation of 20 clonal T4SS substrate mutants, ten of which were defective in intracellular replication and CCV formation. Overall the results of this study suggest that *C. burnetii* encodes a large repertoire of

secretion substrates that play integral roles in host cell subversion, intracellular replication, CCV formation and suggest less functional redundancy than the comparative *Legionella* model.

Materials and methods

Bacteria and host cell lines: Bacteria used for this study are listed in Table 2.1. *C. burnetii* Nine Mile phase II (NMII), clone 4 (RSA439) was propagated in ACCM-2 under microaerophilic conditions as previously described (80). When required, 350µg/ml kanamycin or 5µg/ml chloramphenicol was added. *L. pneumophila* strains Lp02 and Lp03 (*dotA*$^-$) were maintained on charcoal yeast extract (CYE) agar or ACES-broth yeast extract (AYE) broth and 5µg/ml chloroamphenicol was added, as needed.

HeLa, Hek293T, and J774A.1 cells were cultured in DMEM with 10% FBS. THP-1 and U937 cells were propagated in RPMI with 10% FBS. All cell lines were maintained at 37°C with 5% CO_2.

Table 2.1 Bacterial strains used in this study.

Strains	Phenotype or Description	References
C. burnetii		
RSA439	Phase II, Clone 4	(90)
RSA439 MK1	CBU0012::Tn, Cm^r	This study
RSA439 MK2	CBU0041::Tn, Cm^r	This study
RSA439 MK3	CBU0344::Tn, Cm^r	This study
RSA439 MK4	CBU0372::Tn, Cm^r	This study
RSA439 MK5	CBU0388::Tn, Cm^r	This study
RSA439 MK6	CBU0425::Tn, Cm^r	This study
RSA439 MK8	CBU0937::Tn, Cm^r	This study
RSA439 MK9	CBU1198::Tn, Cm^r	This study
RSA439 MK10	CBU1457::Tn, Cm^r	This study
RSA439 MK11	CBU1556::Tn, Cm^r	This study
RSA439 MK12	CBU1569::Tn, Cm^r	This study
RSA439 MK13	CBU1636::Tn, Cm^r	This study
RSA439 MK14	CBU1639::Tn, Cm^r	This study
RSA439 MK15	CBU1665::Tn, Cm^r	This study
RSA439 MK16	CBU2007::Tn, Cm^r	This study
RSA439 MK17	CBU2013::Tn, Cm^r	This study
RSA439 MK18	CBU2016::Tn, Cm^r	This study
RSA439 MK19	CBU2052::Tn, Cm^r	This study
RSA439 MK20	CBU2059::Tn, Cm^r	This study
RSA439 MK21	*icmX*::Tn, Cm^r	This study
L. pneumophila		
Lp02	Philadelphia-1 *rps*L *hsdR thyA* mutant	(10)
Lp03	Lp02 Δ*dotA*	(10)
E. coli		
DH5α	*F´(Φ80dΔ(lacZ)M15), recA1, endA1, gyrA96, thi1, hsdR17 (rk-mk+), supE44, relA1, deoR, Δ(lacZYA-argF), U169*	Stratagene
S. cerevisiae		
W303	*MATa ura3-1 leu2-3,112 his3-11,15 trpl-1 ade2-1 cad-100 rad5-535*	(29)

Bioinformatics analysis: For bioinformatic prediction of *C. burnetii* T4SS candidate substrates, RSA493 and *L. pneumophila* Philadelphia *1* genomes were acquired from the J. Craig Venter Institute Comprehensive Microbial Resource (http://cmr.jcvi.org/cgi-bin/CMR/GenomePage.cgi?org=). T4SS candidate substrates were selected based on the presence of one of the following three features: PmrA consensus regulatory sequence in promoter region, E block motif, or homolog to *Legionella* effector.

We recently reported the identification of 126 putative PmrA regulated *C. burnetii* ORF; however, only 35 of these candidate substrates were tested for Dot/Icm dependent translocation (20). We included 83 of the untested putative PmrA regulated genes in the current study.

We scanned the last 30 amino acids of all *C. burnetii* RSA493 encoding proteins for enrichment in glutamate, termed E-block motif (46). Using this algorithm, we identified 328 ORFs that encoded a similar motif. Among these, 122 ORFs encode hypothetical proteins that were retained in the candidate pool.

Lastly, we scanned the *C. burnetii* genome for similarity to the newly identified 70 *Legionella* effector proteins (117). To accomplish this, we used all-against-all searches of C. burnetii RSA 493 proteins using local BLAST-P. This approach resulted in the identification of 42 candidates, 29 were excluded based on their predicted function or conservation among Gram-negative bacteria

Plasmid construction: To examine Dot/Icm-dependent protein translocation in *C. burnetii*, we generated the kanamycin resistant TEM vector, pCC108, by removing

the chloroamphenicol resistance marker (Cm^R) and mCherry from pKM244 (Mertens et al., manuscript in prep.) using *Hind*III digestion and replaced it with a PCR amplified pHSP10-EGFP-pCbu1910-Kan^R selection marker cassette. pCbu1910-Flag tags-TEM1-BamHI cassette was assembled using SOEing PCR and the resulting cassette was cloned into the *Sac*I/*Sal*I sites to generate pCC108. Identified T4SS substrates were cloned into the *Bam*HI/*Sal*I site of pCC108 or pCBTEM to generate N-terminal TEM1 fusion proteins.

For ectopic expression and yeast toxicity experiments, all identified T4SS substrates were PCR amplified and cloned into *Bgl*II/*Sal*I sites of pEGFPC1 (BD Clontech, Mountain View, CA) to generate N-terminal EGFP fusions or *Bam*HI/*Sal*I sites of pYesNTA2 (Invitrogen, Carlsbad, CA). For substrates possessing *Bam*HI or *Sal*I sites in the target gene, *Bgl*II or *Xho*I was used (Table 2.2).

Table 2.2 Plasmids used in this study.

Plasmid		Description	References or Source
pKM225		pMW1650, *com1*p-Tn*A7*, *groES*p-mCherry, *com1*p-cat, Cm^R	Mertens et al. (Manuscript In Prep)
pKM244		pJB908a, *groES*p-mCherry, *com1*p-cat, Cm^R, Amp^R	Mertens et al. (Manuscript In Prep)
pCBTEM		pXDC61m, *groES*p-mCherry, *com1*p-cat, Cm^R,	(29)
	pCBTEM-1	pCBTEM:: Cbu0069	This study
	pCBTEM-2	pCBTEM:: Cbu0113	This study
	pCBTEM-3	pCBTEM:: Cbu0344	This study
	pCBTEM-4	pCBTEM:: Cbu0606	This study
	pCBTEM-5	pCBTEM:: Cbu01576	This study
pCC108		pKM244, HSP10p-EGFP, *com1*p-Flag-TEM, Kan^R	This study
	pCC108-1	pCC108::CBU0080	This study
	pCC108-2	pCC108::CBU0113	This study
	pCC108-3	pCC108::CBU0388	This study
	pCC108-4	pCC108::CBU0885	This study
	pCC108-5	pCC108::CBU1665	This study
	pCC108-6	pCC108::CBU1685	This study
	pCC108-7	pCC108::CBU1754	This study
pEGFP-C1		C-terminal fusion to EGFP, kan^r	Clontech
	pEGFP35	pEGFP-C1::CBU0012	This Study
	pEGFP36	pEGFP-C1::CBU0069	This study
	pEGFP37	pEGFP-C1::CBU0080	This study
	pEGFP38	pEGFP-C1::CBU0113	This study
	pEGFP39	pEGFP-C1::CBU0183	This study
	pEGFP40	pEGFP-C1::CBU0201	This study
	pEGFP41	pEGFP-C1::CBU0212	This study
	pEGFP42	pEGFP-C1::CBU0270	This study
	pEGFP43	pEGFP-C1::CBU0295	This study
	pEGFP44	pEGFP-C1::CBU0344	This study
	pEGFP45	pEGFP-C1::CBU0372	This study
	pEGFP46	pEGFP-C1::CBU0375	This study
	pEGFP47	pEGFP-C1::CBU0376	This study
	pEGFP48	pEGFP-C1::CBU0393	This study
	pEGFP49	pEGFP-C1::CBU0425	This study
	pEGFP50	pEGFP-C1::CBU0469	This study

Table 2.2 Continued

Plasmid	Description	References or Source
pEGFP52	pEGFP-C1::CBU0590	This study
pEGFP53	pEGFP-C1::CBU0606	This study
pEGFP54	pEGFP-C1::CBU0637	This study
pEGFP55	pEGFP-C1::CBU0665	This study
pEGFP55	pEGFP-C1::CBU0773	This study
pEGFP56	pEGFP-C1::CBU0885	This study
pEGFP57	pEGFP-C1::CBU1079	This study
pEGFP58	pEGFP-C1::CBU1102	This study
pEGFP59	pEGFP-C1::CBU1110	This study
pEGFP60	pEGFP-C1::CBU1150	This study
pEGFP62	pEGFP-C1::CBU1198	This study
pEGFP63	pEGFP-C1::CBU1434	This study
pEGFP64	pEGFP-C1::CBU1525	This study
pEGFP65	pEGFP-C1::CBU1566	This study
pEGFP66	pEGFP-C1::CBU1576	This study
pEGFP67	pEGFP-C1::CBU1594	This study
pEGFP68	pEGFP-C1::CBU1607	This study
pEGFP69	pEGFP-C1::CBU1620	This study
pEGFP71	pEGFP-C1::CBU1639	This study
pEGFP72	pEGFP-C1::CBU1665	This study
pEGFP73	pEGFP-C1::CBU1677	This study
pEGFP74	pEGFP-C1::CBU1685	This study
pEGFP75	pEGFP-C1::CBU1754	This study
pEGFP76	pEGFP-C1::CBU1789	This study
pEGFP77	pEGFP-C1::CBU1790	This study
pEGFP78	pEGFP-C1::CBU2007	This study
pEGFP79	pEGFP-C1::CBU2013	This study
pEGFP80	pEGFP-C1::CBU2016	This study
pEGFP81	pEGFP-C1::CBU2028	This study
pEGFP82	pEGFP-C1::CBU2059	This study
pEGFP83	pEGFP-C1::CBU2064	This study
pEGFP84	pEGFP-C1::CBU2076	This study
pEGFP85	pEGFP-C1::CBUA0015	This study
pEGFP86	pEGFP-C1::CBUA0019	This study

Table 2.2 Continued

Plasmid	Description	References or Source
pYES		
pYES1	pYES::CBU0041	This study
pYES2	pYES::CBU0129	This study
pYES3	pYES::CBU0175	This study
pYES4	pYES::CBU0410	This study
pYES5	pYES::CBU0414	This study
pYES6	pYES::CBU0794	This study
pYES7	pYES::CBU0801	This study
pYES8	pYES::CBU0814	This study
pYES9	pYES::CBU0881	This study
pYES10	pYES::CBU0937	This study
pYES11	pYES::CBU1045	This study
pYES12	pYES::CBU1217	This study
pYES13	pYES::CBU1314	This study
pYES14	pYES::CBU1379	This study
pYES15	pYES::CBU1406	This study
pYES16	pYES::CBU1425	This study
pYES17	pYES::CBU1457	This study
pYES18	pYES::CBU1460	This study
pYES19	pYES::CBU1461	This study
pYES20	pYES::CBU1524	This study
pYES21	pYES::CBU1543	This study
pYES22	pYES::CBU1556	This study
pYES23	pYES::CBU1569	This study
pYES24	pYES::CBU1599	This study
pYES25	pYES::CBU1636	This study
pYES26	pYES::CBU1751	This study
pYES27	pYES::CBU1769	This study
pYES28	pYES::CBU1823	This study
pYES29	pYES::CBU1825	This study
pYES30	pYES::CBU2052	This study
pYES31	pYES::CBU0012	This study
pYES32	pYES::CBU0080	This study
pYES33	pYES::CBU0113	This study
pYES34	pYES::CBU0183	This study

Table 2.2 Continued

Plasmid	Description	References or Source
pYES35	pYES::CBU0201	This study
pYES37	pYES::CBU0295	This study
pYES38	pYES::CBU0344	This study
pYES39	pYES::CBU0372	This study
pYES40	pYES::CBU0375	This study
pYES41	pYES::CBU0376	This study
pYES42	pYES::CBU0393	This study
pYES43	pYES::CBU0425	This study
pYES44	pYES::CBU0469	This study
pYES45	pYES::CBU0513	This study
pYES47	pYES::CBU0590	This study
pYES48	pYES::CBU0606	This study
pYES49	pYES::CBU0637	This study
pYES50	pYES::CBU0665	This study
pYES51	pYES::CBU0773	This study
pYES52	pYES::CBU0885	This study
pYES53	pYES::CBU1079	This study
pYES54	pYES::CBU1102	This study
pYES55	pYES::CBU1150	This study
pYES57	pYES::CBU1198	This study
pYES58	pYES::CBU1434	This study
pYES59	pYES::CBU1525	This study
pYES60	pYES::CBU1566	This study
pYES61	pYES::CBU1576	This study
pYES62	pYES::CBU1594	This study
pYES63	pYES::CBU1607	This study
pYES64	pYES::CBU1620	This study
pYES66	pYES::CBU1639	This study
pYES67	pYES::CBU1665	This study
pYES68	pYES::CBU1677	This study
pYES69	pYES::CBU1685	This study
pYES70	pYES::CBU1754	This study
pYES71	pYES::CBU1789	This study
pYES72	pYES::CBU2007	This study
pYES73	pYES::CBU2013	This study

Table 2.2 Continued

Plasmid	Description	References or Source
pYES74	pYES::CBU2016	This study
pYES75	pYES::CBU2028	This study
pYES77	pYES::CBU2064	This study
pYES78	pYES::CBU2076	This study
pYES79	pYES::CBUA0014	This study
pYES80	pYES::CBUA0015	This study
pYES81	pYES::CBUA0019	This study
pYES82	pYES::CBUA0020	This study

TEM translocation assays: TEM translocation assays for *L. pneumophila* and *C. burnetii*, in U937 or THP-1 cells, respectively, were conducted as previously described (20). *L. pneumophila* was transformed with pCBTEM and *C. burnetii* with pCC108 or pCBTEM. Individual colonies expressing the β-lactamase fusion protein were selected and propagated in AYE or ACCM-2 broth, respectively. Where needed, expression of fusion proteins was induced with 1 mM isopropyl β-D-1 thiogalactopyranoside (IPTG) for 48 h. Host cells were seeded at 10^5/ml in 24-well plates and were inoculated with a multiplicity of infection (MOI) of 30 and incubated for 3 h for infection with *L. pneumophila* or with an MOI of 100 and incubated for 48h for *C. burnetii*. The *L. pneumophila* or *C. burnetii* infected cells were loaded with 50 µl 6XCCF4/AM solution (LiveBLAzer-FRET B/G Loading Kit, Invitrogen) and incubated at room temperature for 2 h or 4 h, respectively. The percentage of blue cells was quantified using a Nikon A1 equipped with a chroma β-lactamase filter set (Chroma

#41031 excitation: 405 nm emission: 435 nm long-pass). For substrates exhibiting translocation rates above 10%, approximately 1000 cells were counted; however for substrates exhibiting low translocation rates (less than 10%) approximately 5000 cells were counted. Results are presented as mean values from triplicate wells from at least two independent experiments.

Ectopic expression in HeLa cells: To determine subcellular localization of *C. burnetii* T4SS substrates, HeLa cells were seeded in 24-well glass bottom dishes at a density of 10^5/ml. Where indicated, cells were infected at an MOI of 100 with mCherry expressing *C. burnetii*-pKM244. At 72 h post infection, infected or uninfected cells were transiently transfected with EGFP fusion constructs using Lipofectamine (Invitrogen) following the guidelines outlined by the manufacturer. Twenty four hours post-transfection, cells were fixed with 4% formaldehyde, permeabilized with ice-cold methanol, and nuclei were stained with 1X Hoechst. For colocalization analysis, primary antibodies were diluted in 1% BSA and used at the following concentrations: 1:250 anti-CoxIV (GenScript, Piscataway, NJ) and 1:250 anti-Calnexin (GenScript). Primary antibodies were detected using 1:1000 Alexa Fluor 555 (Cell Signaling, Boston, MA) diluted in 1% BSA. To assess colocalization with autophagosomes, cells were co-transformed with EGFP-tagged substrates and pmRFP-LC3 (Addgene, Cambridge, MA). Fluorescence images were acquired with a Nikon-A1 microscope using the 60X oil immersion object and images were processed using NIS-Elements Software. Similar results were obtained from at least three independent experiments with at least 100 transfected cells per experiment.

Yeast toxicity assay: To assess toxicity of *C. burnetii* T4SS substrates in yeast, each ORF was cloned into pYesNTA2 as *Bam*HI/*Sal*I PCR fragments, and the resulting constructs were transformed into *S. cerevisiae* strain W303 using a standard transformation protocol (33). Transformants were plated on uracil dropout media, supplemented with glucose, and incubated for 72 h at 30°C. Five colonies from each transformation were expanded and toxicity was assessed by serially diluting and spotting onto the appropriate dropout media (95). Toxicity results were determined from at least three independent experiments.

Secreted embryonic alkaline phosphatase (SEAP) assay: To identify T4SS substrates that disrupt the secretory pathway, Hek293T cells were co-transformed with pSEAP and pEGFP constructs expressing the T4SS substrates. Twenty-four hours post-transfection, cells were washed with 1X phosphate-buffered saline (PBS) and incubated for an additional 8 h. Following the allotted incubation period, the culture supernatant was collected to calculate the extracellular SEAP. For determination of intracellular SEAP, cells were lysed (114) and fractions measured for alkaline phosphatase activity using the Phospha-Light System (Invitrogen) as described by the manufacturer. Results were tabulated from at least 2 independent experiments with at least 3 replicates per experiment.

Generation of *C. burnetii* transposon mutants: *C. burnetii*, axenically cultured in ACCM-2, was washed twice and resuspended in destilled water to an approximate concentration of 10^9/ml. Bacteial cells were mixed with 1 µg of pKM225 plasmid DNA and electroporation was performed as previously described (80). After 7 d, individual

colonies were picked and expanded in ACCM-2. Genomic DNA was isolated for rescue cloning using GenElute Bacterial Genomic DNA Kit (Sigma, St. Louis, MO). Purified DNA was digested with *Hind*III (New England Biolabs, Ipswich, MA), ligated with T4 DNA ligase (New England Biolabs), and transformed into chemically competent *E. coli* DH5α. To determine genomic insertion site of *Himar1* transposon, three colonies per transformation were sequenced using ColE1-R (5'-CTTTCCTGCACTAGATCCCC-3') and CatF (5'-GTACTGCGATGAGTGGCAG-3').

Growth curve analysis of T4SS substrate mutants: For growth curve comparison of *C. burnetii* T4SS substrate mutants, the concentration of *C. burnetii* strains axenically cultured in ACCM-2 was determined using qPCR with *IS1111*gene specific primers (51). To first verify that mutants had comparable growth rates in axenic culture, curves in ACCM-2 were conducted by inoculating 20 ml ACCM-2 with 10^6/ml of RSA439, RSA439 *icmX*::Tn, or RSA439 specific T4SS substrate mutants. At 1 d, 4 d, and 7 d post-inoculation, 1 ml of culture was removed, pelleted, and resuspended in 200 µl DNA lysis solution with 10 µl of 20 mg/ml proteinase K (13). For cell culture comparison, J774A.1 or HeLa cells were seeded in 24-well plates to a density of 10^5/ml. Cells were infected at an MOI of 50 with *C. burnetii* (RSA439), RSA439 *icmX*::Tn, or RSA439 specific T4SS substrate mutants in triplicate. Four hours post-infection, cells were washed twice with 1X PBS to remove uninternalized bacteria, fresh media was added to each well, and cultures were incubated at 37°C with 5% CO_2. At 1 d, 4 d, and 7 d, cells were harvested using trypsinization (HeLa) or scraped (J774A.1), and resuspended in 200 µl DNA lysis solution with 10 µl of 20 mg/ml proteinase K (13).

DNA was isolated from the infected cells and ACCM-2 cultures using High Pure PCR Template Prep Kit (Roche Applied Sciences, Indianapolis, IN), and purified DNA was quantified using qPCR with TaqMan and primers specific for *IS1111* (51). At least three independent growth curves for axenic and cell culture were conducted with at least three samples per experiment.

Coinfection: For coinfection experiments, HeLa cells were seeded at a density of 10^5/ml onto glass bottom 24-well plates. Cells were infected at an MOI of 100 with either wild-type RSA439, specific T4SS substrate mutants, or coinfected with wild-type and mutant strains with 1:1 ratio. Four hours post-infection, non-internalized bacteria were removed by washing twice with 1X PBS and fresh culture media was added. Cultures were propagated for an additional 7 d. Following infection, cells were washed, fixed with 4% formaldehyde, and DNA was stained with 1X Hoechst. Fluorescence images were acquired with a Nikon-A1 microscope using the 60X oil immersion object and images were processed using NIS-Elements Software. Similar results were obtained from three independent experiments with at least 50 infected cells per experiment.

Results

Identification of novel *C. burnetii* T4SS substrates by bioinformatics screen: *In silicon* analyses have succeeded in the prediction of putative secretion substrates in bacterial pathogens (14, 20, 46). The use of these computational tools allows one to narrow down the number of candidates to experimentally manageable levels. In the current study, we have expanded the number of *C. burnetii* type IV substrates using

three new parameters: consensus promoter element in PmrA regulation (20, 118), an E-block motif (46), and homology to known effectors (117).

The two component regulatory system PmrA/B regulates several *dot*/*icm* genes and genes encoding T4SS substrates (118). A recent study revealed that 35 *L. pneumophila* and 68 *C. burnetii* ORFs contain the PmrA regulatory elements TTAA-N6-TTAA (118). In *L. pneumophila* some of these ORFs code for *bona fide* Dot/Icm substrates, suggesting the usefulness of this prediction. Using 5 *dot*/*icm* genes (*icmD, icmQ, icmV, icmW,* and *dotD*) and several confirmed *Coxiella* secretion substrates (including Cbu1751, AnkB, AnkJ, AnkM), we identified a consensus sequence (TTAATATTTTCTTAAGGTTTXTGXGXTAXAAT) (Table 2.3) distinct from that reported by Zusman et al. (118). A genome-wide search with this element allowed us to obtain 126 candidates, 35 of which have been previously tested (20), and the remaining 83 (Table 2.3) were tested in the current study.

Table 2.3 Predicted PmrA regulated ORFs.

ID	5' End	Putative PmrA binding site	3' End	Strand	Distance of predicted binding site to ATG
CBU0013	13016	TTAAGGTAACTTTAATATTTCTTGGTTAA--ACT	12985	-	29
CBU0021	18235	TTAATATTTCCTTAACCTAATGAAGTTATT--CT	18266	+	71
CBU0023	22399	TTAATTTTATCTTAAGATAAGGAAATCTTT-ACT	22367	-	48
CBU0051	49435	CTCATACTTCCTTAAGGTTTTTTGGAGAT--ACT	49404	-	72
CBU0069	63320	CTAAGATTATCTTAATTTTAACTTGATAGC-A-T	63351	+	31
CBU0077	71460	TTAAAATTAAATTAA--TCAATTAATATTGACCT	71491	+	82
CBU0084	75607	TTAATATTATCTTAAGGTTATTGGGTTATT-C-T	75638	+	0
CBU0119	111571	TTAAGAAATCTTTAATCTCGCAGTGGTATG-C-T	111540	-	79
CBU0144	131010	TTAAGTTTGTTTTAATATCGATGTGTCAA--GAT	131041	+	38
CBU0183	172128	TTAAGAGTATTTTAAGTTTATGCAGATAT--AAT	172159	+	104
CBU0201	190143	TTAATATTATTTTTA-ATCTTACCTTTAAAAAAT	190111	-	70
CBU0213	197619	TTAAGATTGAATTAATTTTTGGATATTAC--TTT	197588	-	28
CBU0215	200426	TTAACAGAAAATTAA--TTTTAGGGATTTCACCT	200395	-	136
CBU0273	245187	TTAATATTATTTTAACCTTTCGTCCCTAAA-A-T	245156	-	32
CBU0326	293301	TTAAGAAAATCTTAAATTTTATCGATGATT--CA	293270	-	52
CBU0343	310482	TTCATATTCACTTAATCTTATTGTAGTAAC-T-T	310513	+	88
CBU0355	322015	CTAAGATTCTCTTAATCTCATTACAGAATGA--T	322046	+	31
CBU0361	327063	TTAAGAAAAACTTAAGGAAGAATAGAAAGT--TT	327032	-	106
CBU0388	348481	TTAATATTCCCCTAAGCTTTATTCGTTACA-C-T	348512	+	72
CBU0393	357811	TTAATAAAGGTTTAATGTTTTAGAGGTATT-C-T	357780	-	47
CBU0436	388876	TTAATATTTAATTAAGTTTATTTGTTTAGA-C-T	388845	-	94
CBU0505	445857	TTAATATTCCCTTAAGTTTTAAGCTTTATA-A-T	445826	-	44
CBU0600	547351	TTAACTTTACCTTAACAAAACCTGATTAT--ACT	547382	+	35
CBU0619	565992	TTAATCTTTTCTTAAGGTTTTTGGCTTATA-C-T	565961	-	141
CBU0625	569123	TTAAGAATTCCTTAATAAATGAATGATAAG-A-T	569154	+	127
CBU0637	586648	TTAATTTTTACTTAATTTTT-TAATCGACT-TCT	586617	-	123
CBU0665	606974	TTAATATTTTCTTAATACCGCGATGGTATT-C-T	607005	+	13
CBU0690	636458	TGAACATGATTTTAA-ATCTTATGGTGTTATGCT	636490	+	82
CBU0790	737321	TTAATAATTCCCTAATTTCTCAGTGTTATC-C-T	737352	+	83
CBU0860	816692	TTAATAAATCATTAATATTGTTGTTGGATA-A-T	816723	+	46
CBU0978	930285	TTAAGCTTTTTTTAATAATAAAATGTTAG--ACT	930316	+	34
CBU0992	940945	TTAAGATTTTCCTAAGGGTTATGAAGTACT-A-T	940914	-	35
CBU1017	962048	TTAATTTTATTTTTA--TCTTATTGAT-TTTATT	962078	+	158
CBU1033	975307	TTAAGAGTTCTTTAAGGTTCGCCCGCTAC--ACT	975338	+	165

Table 2.3 Continued

ID	5' End	Putative PmrA binding site	3' End	Strand	Distance of predicted binding site to ATG
CBU1059	1005087	TTTAGATTATTTTAATTTAAAAAGTTTAG--AGG	1005056	-	147
CBU1098	1047078	TTAATAAATTCTTAAGATTAAGCTGTTATT-C-T	1047047	-	39
CBU1103	1051114	TTAATATTCTCTTAAGGTTGATGAGGTAGA-T-T	1051083	-	30
CBU1110	1056911	TTAATGAAGCTTTAACAATAGAGCGATAT--ACT	1056880	-	23
CBU1114	1059926	TTCATACTTTTTTAAGCAAACGTTGATAT--CCT	1059895	-	37
CBU1167	1110630	TTAATATTCTCTTAATAGCTTCATCCAATAA--T	1110599	-	72
CBU1178	1119864	TTAAAATTTCTTTAATAAACTTCTACTAA--ACT	1119895	+	117
CBU1198	1142178	TTAAGGCTACGTTAAGTTGAAGGGAGTAA--GAT	1142209	+	44
CBU1213	1157000	TTAAGATTGATTTAATGTCTGGCGGTTAG--AAT	1157031	+	36
CBU1216	1161120	TTAATTTTATTTTAATTTATTTCGGATAC--ACT	1161089	-	33
CBU1226	1176853	TTAATTTTGCTTTAA--ATGCAAGCATTTTTATT	1176822	-	41
CBU1252	1204114	TTAACGGTAATTTAAGGTTTCTTTTCTAAA-A-T	1204083	-	21
CBU1253	1204021	TTCAGGTTCACTTAAGTTTAAAAGGTTAA--TTT	1204052	+	235
CBU1288	1242627	TTAACTTTCTTCTAAGAAAAGACTGTTAT--AGT	1242596	-	44
CBU1291	1245983	TTAATGGAAACTTAAGCTTTCTTCATTACA-A-T	1246014	+	41
CBU1368	1318196	TTAATATTTTCTTAATTCCAATTCAGTGTGC--A	1318165	-	94
CBU1369	1318222	TTAAGCGTAATTTAATATTATGCCCTTAT--AAT	1318253	+	17
CBU1370	1320557	TTAATTTTTTCATAATGTAGGAATTATAT--ACT	1320526	-	51
CBU1387	1336989	TTCATATAGCCTTAA--TATGGTTACTGTAAAAT	1337020	+	48
CBU1409	1359599	TTAAGGTTAACCTAAGCTTGAGTTGTTAGA-A-T	1359630	+	133
CBU1420	1369171	CTAATATTCCCTTCAGTTTATATTGATAAC-A-T	1369202	+	17
CBU1523	1471228	TTAAGATTAATTTAC--TCTTGTTATTATTTACA	1471259	+	88
CBU1530	1481188	TTAATATATTTTTAAGTTTCATACATTAAC-A-T	1481157	-	36
CBU1535	1484881	TTAAGATTTGTTTAAGCAGGCTGCCCTAT--ACT	1484850	-	45
CBU1564	1512170	ATCAGATTCCGTTAATAATTCGGCAGTAT--ACT	1512139	-	43
CBU1576	1522991	TTCATATTTCTTTAATTTTTCAGCGCTATC-A-T	1523022	+	43
CBU1611	1555499	TTAATATTTTATTAAGTTTATCGATTTATA-G-T	1555468	-	48
CBU1618	1557905	TTAATATTAAATTAATATTAAGAAAT-AGA-A-T	1557935	+	101
CBU1624	1563565	TTAATATTTCCTTAAGGTAAGGAAGGTATA--GT	1563534	-	41
CBU1639	1579897	TTAATTTTGCTTTAAGTTTAACGCGCTAAC-A-T	1579866	-	58
CBU1649	1589543	TTAATACTGTCTTAAGGAAGTGGTGCTAGC-A-T	1589512	-	42
CBU1650	1589620	TTAATATTTCGTTAAGGTTAGTGGGCTATT-C-T	1589651	+	48
CBU1685	1616231	TTAATTTTTCTTTAA--TTAATTTTAATAATATT	1616262	+	18
CBU1701	1634450	CTAATATTCCCTTAACTTCCTTCTGGTAGG-A-T	1634481	+	33

Table 2.3 Continued

ID	5' End	Putative PmrA binding site	3' End	Strand	Distance of predicted binding site to ATG
CBU1757	1688680	TCAAGACTTAATTAA--TTTATTTTATTTATATG	1688649	-	39
CBU1775	1705606	CTAAGGTTAGTTTAATCTTGCTAAGGTAA--TAT	1705637	+	65
CBU1780	1708193	TTCATTTTTCTTTAAGTTTTGATTGATAAC-A-T	1708224	+	129
CBU1794	1725403	TTAAGGTTTTCTTAATAAAGGCTGTTTAT--ACT	1725434	+	26
CBU1818	1748733	TTTATTTACATTTAA--TTAAAATCATTTATTAT	1748764	+	51
CBU1822	1753234	TTAGGATTAAATTAACATGCAGGTGTTAA--GAT	1753203	-	88
CBU1863	1793470	TTAATATTTTTTTAATATTTGGATTTTAAG-A-T	1793439	-	69
CBU2013	1920851	TTAATAATTTGTTAATATCGGTTTGGTAAT-A-T	1920820	-	20
CBU2051	1957518	TTCATATATTTTTAAGCATGGCTTGGTAC--ACT	1957487	-	36
CBUA0007	4919	TTAATTCTTCTTTAATAATATACTGATAT—CCT	4888	-	34

In the second method, we used the E-block feature found in a large number of Dot/Icm substrates of *L. pneumophila* (46). One of the three consensus sequences, EExxE, ExE, or EEx, was found in 49 Dot/Icm substrates of Coxiella, indicating the usefulness of this motif as a reliable predictor of substrate candidates. Using this feature, we identified 328 ORF*s* that possess a similar motif. Of these, 122 ORF*s* encode hypothetical proteins that were retained in the candidate pool (Table 2.4).

Table 2.4 *C. burnetii* T4SS candidates possessing an E block motif.

ID	E position
CBU0012	E_Position = [16,19,21]
CBU0050	E_Position = [3,6,9,28]
CBU0061	E_Position = [1,15,16,17,19]
CBU0067	E_Position = [18,22,26,28]
CBU0080	E_Position = [0,1,7,18,19,20]
CBU0092	E_Position = [5,20,21]
CBU0113	E_Position = [11,18,19,20,21]
CBU0115	E_Position = [3,7,12,13,23]
CBU0122	E_Position = [6,8,9,10,11,18,22]
CBU0134	E_Position = [14,16,25]
CBU0150	E_Position = [11,18,19]
CBU0211	E_Position = [5,8,10]
CBU0212	E_Position = [3,8,21,22,23]
CBU0270	E_Position = [9,13,15,26]
CBU0295	E_Position = [9,10,13,15,19]
CBU0328	E_Position = [1,15,18]
CBU0339	E_Position = [4,14,18,19]
CBU0340	E_Position = [3,8,15,24,25]
CBU0344	E_Position = [0,1,18,20]
CBU0360	E_Position = [6,9,11,15,19,23]
CBU0372	E_Position = [0,7,8,11,20,24]
CBU0375	E_Position = [6,8,27]
CBU0376	E_Position = [12,16,18,20,27]
CBU0377	E_Position = [3,13,16,20,21]
CBU0425	E_Position = [13,14,17]
CBU0469	E_Position = [2,5,10,26]
CBU0470	E_Position = [4,12,13,26]
CBU0498	E_Position = [2,13,16]
CBU0507	E_Position = [0,8,15,24,25]
CBU0510	E_Position = [5,12,16,17,24,25]
CBU0513	E_Position = [4,6,22,24]
CBU0562	E_Position = [1,3,4,7]
CBU0590	E_Position = [16,22,25]
CBU0606	E_Position = [1,10,11,13]
CBU0651	E_Position = [3,14,16,22,27]

Table 2.4 Continued

ID	E position
CBU0654	E_Position = [0,13,14]
CBU0656	E_Position = [10,23,27,28]
CBU0658	E_Position = [4,5,6,9,12]
CBU0698	E_Position = [0,1,6,15]
CBU0699	E_Position = [0,2,9]
CBU0705	E_Position = [7,11,22,24]
CBU0706	E_Position = [3,13,14,15]
CBU0710	E_Position = [1,4,5]
CBU0719	E_Position = [2,17,18]
CBU0756	E_Position = [12,26,28]
CBU0773	E_Position = [11,16,17,24]
CBU0879	E_Position = [6,8,9,12,15,18,20]
CBU0885	E_Position = [10,12,14,16,18,20,21]
CBU0891	E_Position = [11,15,16,20,23]
CBU0910	E_Position = [7,9,18,19]
CBU0941	E_Position = [6,8,19,27]
CBU0957	E_Position = [0,1,10]
CBU0970	E_Position = [11,13,16]
CBU0972	E_Position = [4,7,26]
CBU0985	E_Position = [3,4,6,14,17,25]
CBU1044	E_Position = [3,4,13,20,24]
CBU1065	E_Position = [2,3,8]
CBU1069	E_Position = [12,15,27,28]
CBU1079	E_Position = [14,18,19,25]
CBU1088	E_Position = [7,8,11]
CBU1102	E_Position = [9,10,11,15,17]
CBU1107	E_Position = [7,11,15,17,20]
CBU1108	E_Position = [6,10,14,15,16,18,20,21]
CBU1124	E_Position = [13,16,23,26]
CBU1150	E_Position = [11,12,24,28]
CBU1164	E_Position = [3,4,5,21]
CBU1209	E_Position = [8,11,12,13,14,19]
CBU1215	E_Position = [14,15,25,27]
CBU1219	E_Position = [0,3,10,17]

Table 2.4 Continued

ID	E position
CBU1224	E_Position = [2,5,27]
CBU1234	E_Position = [3,8,10,25]
CBU1295	E_Position = [0,10,11,16]
CBU1328	E_Position = [2,3,19]
CBU1354	E_Position = [2,4,6]
CBU1367	E_Position = [9,12,28]
CBU1377	E_Position = [10,11,17]
CBU1434	E_Position = [0,17,19,28]
CBU1463	E_Position = [2,4,6,19]
CBU1479	E_Position = [3,5,18]
CBU1496	E_Position = [5,6,19,21]
CBU1525	E_Position = [4,5,13,15,22,23]
CBU1533	E_Position = [1,5,19,22]
CBU1546	E_Position = [6,8,20,25]
CBU1566	E_Position = [0,7,10,26,27]
CBU1603	E_Position = [12,24,25]
CBU1607	E_Position = [11,15,17,20,23]
CBU1611	E_Position = [0,12,24,25,27]
CBU1616	E_Position = [7,10,12,22]
CBU1620	E_Position = [4,9,11,12,14,16,18]
CBU1659	E_Position = [7,20,21]
CBU1660	E_Position = [3,9,10,13,16,23,28]
CBU1662	E_Position = [5,7,16,26]
CBU1665	E_Position = [21,22,26]
CBU1667	E_Position = [6,7,17]
CBU1673	E_Position = [5,8,9,22]
CBU1677	E_Position = [6,10,12,15,19,22]
CBU1680	E_Position = [11,20,21]
CBU1686	E_Position = [11,15,21,22]
CBU1705	E_Position = [3,7,14,16,25,28]
CBU1733	E_Position = [6,8,9,28]
CBU1754	E_Position = [2,9,15,17]
CBU1776	E_Position = [2,4,11,12,14,15,18]
CBU1789	E_Position = [1,3,24]
CBU1790	E_Position = [9,12,13,14,15]

Table 2.4 Continued

ID		E position
CBU1883		E_Position = [1,9,10,17,22]
	CBU1954	E_Position = [7,25,28]
	CBU1999	E_Position = [9,11,17]
	CBU2007	E_Position = [7,9,11,19]
	CBU2010	E_Position = [15,25,28]
	CBU2016	E_Position = [2,7,10,16,19,21]
	CBU2023	E_Position = [8,15,18,23,25]
	CBU2028	E_Position = [4,5,6,10]
	CBU2033	E_Position = [5,21,22]
	CBU2034	E_Position = [4,11,12]
	CBU2057	E_Position = [3,8,15,24,25]
	CBU2059	E_Position = [8,10,16,20]
	CBU2060	E_Position = [0,2,6,16]
	CBU2064	E_Position = [3,4,6,11,14,18,20]
	CBU2076	E_Position = [6,7,15,25]
	CBUA0015	E_Position = [8,12,14,16,17,18]
	CBUA0019	E_Position = [1,9,11]
	CBUA0020	E_Position = [10,19,22]

Lastly, we scanned the *C. burnetii* genome for homologs of the recently identified *L. pneumophila* Dot/Icm substrates (117) leading to the identification of 42 candidates, 29 (Table 2.5) of which were tested in the current study.

Table 2.5 *L. pneumophila* effectors used for the identification of homologs in *C. burnetii*

Hit	Query	Hit description	E value
CBU0001	lpg1924	chromosomal replication initiator protein DnaA (dnaA) {Coxiella burnetii RSA 493}	0.29
CBU0026	lpg1888	ribose 5-phosphate isomerase (rpiA) [5.3.1.6] {Coxiella burnetii RSA 493}	0.24
CBU0027	lpg1106	acyltransferase family protein {Coxiella burnetii RSA 493}	0.17
CBU0111	lpg1106	2-amino-3-ketobutyrate coenzyme A ligase (kbl) [2.3.1.2...	0.33
CBU0147	lpg1684	preprotein translocase, SecA subunit (secA) {Coxiella burnetii RSA 493}	0.32
CBU0235	lpg0021	translation elongation factor G (fusA) {Coxiella burnetii RSA 493}	0.56
CBU0530	lpg1716	TPR domain protein {Coxiella burnetii RSA 493}	0.16
CBU0676	lpg2539	NAD dependent epimerase/dehydratase {Coxiella burnetii RSA 493}	0.2
CBU0682	lpg0021	conserved domain protein {Coxiella burnetii RSA 493}	0.69
CBU0693	lpg1670	dehydrogenase, E1 component, alpha subunit [1.2.4.1] {Coxiella burnetii RSA 493}	0.52
CBU0753	lpg0260	transporter, AcrB/AcrD/AcrF family {Coxiella burnetii RSA 493}	0.49
CBU0845	lpg1692	UDP-glucose/GDP-mannose dehydrogenase family {Coxiella ...	0.59
CBU0902	lpg1667	hypothetical protein {Coxiella burnetii RSA 493}	0.3
CBU1049	lpg1959	hypothetical protein {Coxiella burnetii RSA 493}	0.12
CBU1108	lpg0130	hypothetical protein {Coxiella burnetii RSA 493}	0.26
CBU1160	lpg2148	TPR domain protein {Coxiella burnetii RSA 493}	0.35
CBU1282	lpg2826	carbamoyl-phosphate synthase, small subunit (carA) [6.3...	0.15
CBU1292	lpg1083	ankyrin repeat domain protein {Coxiella burnetii RSA 493}	0.25
CBU1341	lpg2826	GMP synthase (guaA) [6.3.5.2] {Coxiella burnetii RSA 493}	0.5
CBU1363	lpg1171	exodeoxyribonuclease I, putative {Coxiella burnetii RSA 493}	0.15
CBU1370	lpg1639	hypothetical protein {Coxiella burnetii RSA 493}	0.95
CBU1387	lpg2546	hypothetical protein {Coxiella burnetii RSA 493}	0.054
CBU1494	lpg2555	pyridoxal phosphate biosynthetic protein PdxJ (pdxJ) {Coxiella burnetii RSA 493}	0.82
CBU1535	lpg0375	hypothetical protein {Coxiella burnetii RSA 493}	0.88
CBU1594	lpg2359	GatB/Yqey domain protein {Coxiella burnetii RSA 493}	4.00E-30
CBU1603	lpg2912	conserved hypothetical protein {Coxiella burnetii RSA 493}	0.13
CBU1852	lpg2826	hypothetical protein {Coxiella burnetii RSA 493}	0.072
CBU2057	lpg2546	conserved hypothetical protein {Coxiella burnetii RSA 493}	0.33

T4SS-dependent translocation of candidate substrates: To determine Dot/Icm-dependent translocation of these candidates, each of the 234 genes was fused to the C-terminal end of β-lactamase on pCBTEM (20). Plasmids that direct the expression of the β-lactamase fusion proteins were transformed into Lp02 (10), a *L. pneumophila* strain with a functional Dot/Icm apparatus. The resulting transformants were used to infect U937 cells at an MOI of 30, and protein translocation was determined by β-lactamase-mediated cleavage of the fluorescence dye CCF4-AM. Fifty-three proteins were found to cause more than 1% of U937 cells to display blue fluorescence. While the majority of these secretion substrates exhibited a low translocation rate of <10%, four substrates (Cbu0425, Cbu2007, Cbu1620, and CbuA0015) exhibited a high translocation rate of 90%. When expressed in the *dotA* mutant of *L. pneumophila*, none of these proteins was able to promote the delivery of the β-lacmatase into host cytosol (Fig. 2.1). Collectively, these results support the designation of these 53 proteins as substrates of the Dot/Icm T4SS substrates.

Figure 2.1 Dot/Icm-dependent translocation of *C. burnetii* T4SS substrates by *L. pneumophila*. *L. pneumophila* WT strain Lp02 or Δ*dotA* Lp03 expressing β-lactamase fused T4SS substrates were used to infect U937 cells at an MOI of 30. Infected cells were loaded with CCF4/AM and substrate translocation was determined by counting the number of blue cells. For substrates exhibiting translocation rates above 10%, approximately 1000 cells were counted; however for substrates exhibiting low translocation rates (less than 10%) approximately 5000 cells were counted. Results are presented as mean values from triplicate wells from at least two independent experiments.

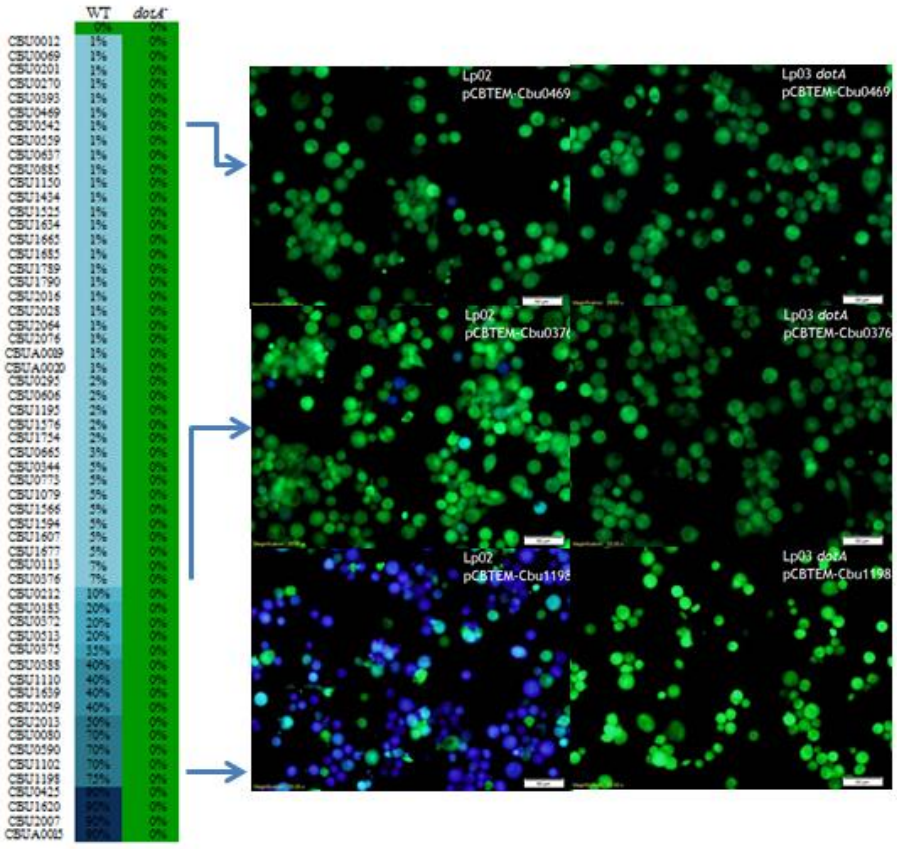

To determine whether the protein substrates identified with the *L. pneumophila* surrogate host can also be recognized by the Dot/Icm transporter of *C. burnetii*, *C. burnetii* RSA439 or *icmX*::Tn was transformed with β-lactamase TEM1 fusions listed in Table 2.2 and the resulting transformants were used to infect THP-1 cells. Forty-eight hours post-infection, cells were loaded with CCF4-AM and incubated for an additional 4h prior to imaging. RSA439 expressing β-lactamase TEM-1 each of the substrate fusions was positive for translocation as evident by the presence of at least 1% blue cells (Fig. 2.2A) for each tested substrate. Using the constitutive pCC108 and the inducible vector pCBTEM we were able to demonstrate translocation of eleven substrates by *C. burnetii*; however we did observe lower expression (data not shown) and lower translocation using the constitutive pCC108 vector, suggesting this may be due to weaker promoter than in comparative *C. burnetii* TEM vectors [8, 20]. Notably Cbu0069, Cbu0113, and Cbu0885 exhibited a higher translocation when expressed in the natural host *C. burnetii.* No β-lactamase translocation was observed in host cells infected with the RSA439 *icmX*::Tn (Fig. 2.2B), indicating that translocation of these *C. burnetii* T4SS substrates is dependent on a functional secretion system suggesting they are *bona fide C. burnetii* T4SS substrates.

Figure 2.2 Newly identified secretion substrates are secreted by *C. burnetii*. THP-1 cells were infected for 48 h with *C. burnetii* expressing β-lactamase fusion constructs and subsequently loaded with CCF4/AM as described in materials and methods. (A) Confocal imaging of wild-type infected cells revealed the presence of blue cells (B) translocation of selected substrates was absent in cells infected with the *icmX*::Tn, indicating the identified substrates are translocated into host cells in a Dot/Icm-dependent manner.

A.

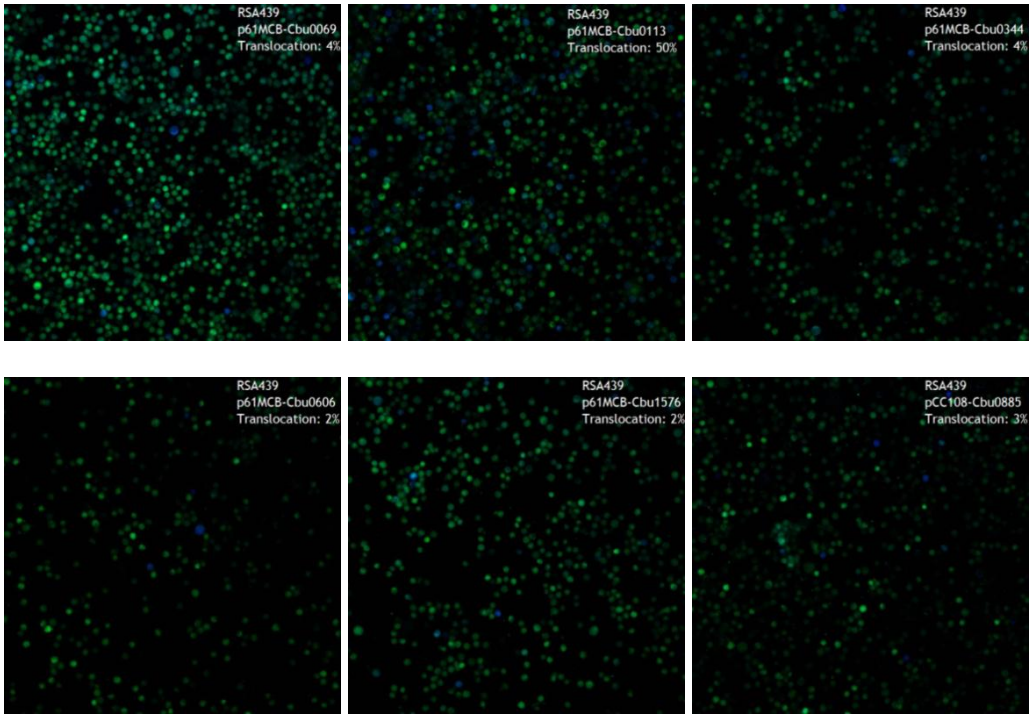

Figure 2.2 Continued

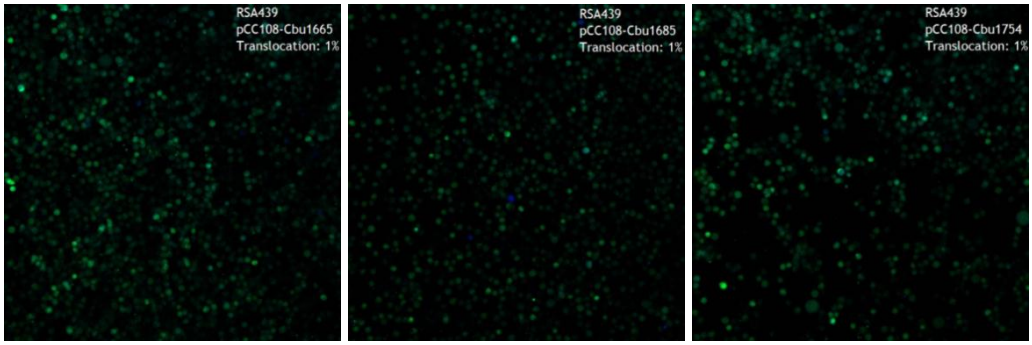

B.

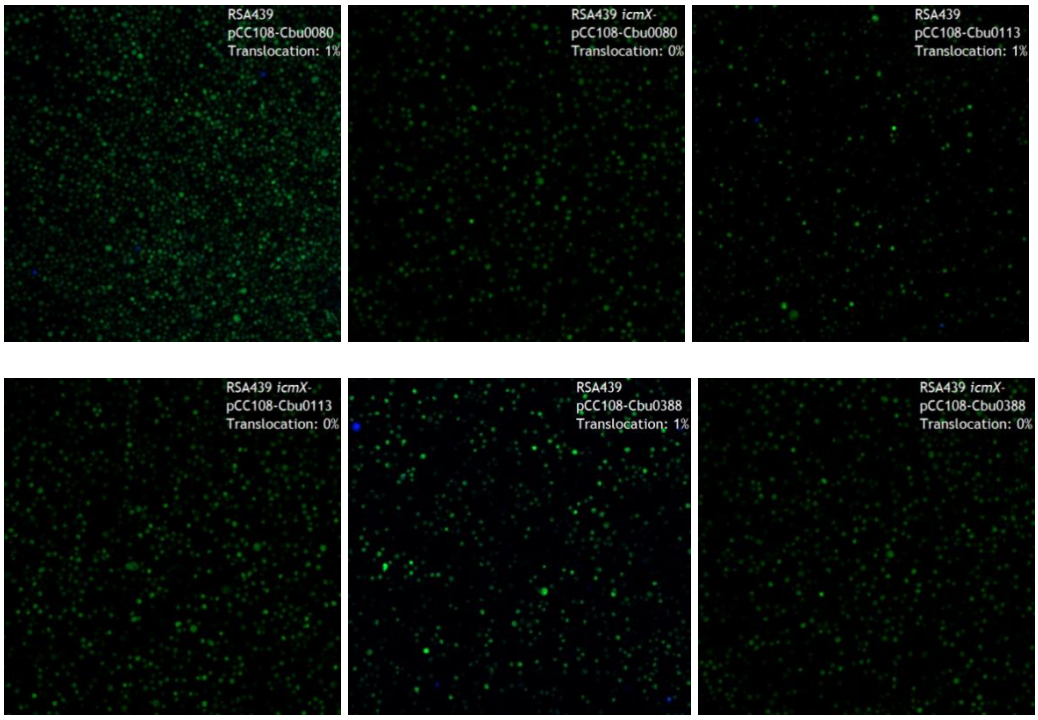

Newly identified *C. burnetii* Dot/Icm substrates exhibit significant plasticity among bacterial isolates: Different isolates of *C. burnetii* are associated with unique disease states characterized by distinct pathological features. For instance, the Dugway (D) rodent isolate is avirulent when compared to NMI (99), whereas the Graves (G) and Kearns (K) isolates establish an infection characterized by less inflammation and dissemination (89). Comparison of these different isolates revealed that many effector proteins are intact in specific group isolates but disrupted in other isolates, suggesting different effector proteins may be responsible for different host cell responses and consequently distinct disease states (9, 18, 111).

To compare the heterogeneity of the newly described effectors, genome information for NM, D, K, and G isolates was compared using PATRIC (34). Among the proteins identified in this study, only 12 (Cbu0270, Cbu0469, Cbu0637, Cbu0773, Cbu1079, Cbu1434, Cbu1566, Cbu1754, Cbu1789, Cbu2007, Cbu2016, and Cbu2076) are fully conserved among all isolates (Table 2.6). Further comparison between the isolates showed that the highest conservation exists between NMI and Dugway isolates, with an additional 11 substrates fully conserved.

Table 2.6 Genome comparisons of T4SS substrates identified in this study. Brackets after each ORF indicate an alternative start (AS), an N-terminal (NT) and/or C-terminal (CT) truncation, or frame shift (FS) compared to corresponding NMI ORF. Numbers following abbreviation denote length of AS, amount truncated from N- or C- terminus, or site of frameshift.

Gene Locus in NMI	Alias in isolates			Domain
	K	G	Dugway	
Cbu0012	CbuK0201 (AS 242bp)	CbuG0281 (AS 242bp)	CbuD0136 (AS 242bp)	P-loop
Cbu0069	CbuK1982/CbuK1983 (NT 21bp, FS 137bp)		CbuD2035 (NT 29bp, FS 343bp)	HRDC-like
Cbu0080	CbuK1976 (AS 506bp,)	CbuG1937 (AS 506bp, CT 102bp)	CbuD2028	HLH DNA-binding domain
Cbu0113		CbuG1899	CbuD1994	PH-domain
Cbu0183	CbuK0377 (CT 7bp)	CbuG1822 (CT 86bp)	CbuD1910	
Cbu0201	CbuK0392 (NT 77bp)	CbuG1805 (NT 77bp)	CbuD1894 (NT 77bp)	Ankyrin repeat
Cbu0212	CbuK0401 (AS 1019bp)	CbuG1796 (AS 1019bp)	Cbu1884 (AS 1019bp)	
Cbu0270	CbuK0462	CbuG1738	CbuD1824	
Cbu0295	CbuK0492 (NT 272bp, CT 305bp)	CbuG1710 (NT 272bp)	CbuD1787 (NT 17bp)	SEL1
Cbu0344	CbuK0540 (AS 455bp)	CbuG1663 (NT 69bp)	CbuD1734 (AS 455bp)	Coiled-coil
Cbu0372	CbuK0563 (FS 621bp)	CbuG1637 (FS 700bp)	CbuD1711	Fic, transmembrane domain
Cbu0375	CbuK0569 (NT 209bp)	CbuG1634 (NT 209bp)	CbuD1704 (FS 468)	

Table 2.6 Continued

Gene Locus in NMI	K	G	Dugway	Domain
Cbu0376	CbuK0569 (AS 27bp)	CbuG1634 (AS 27bp)	CbuD1704 (AS 515bp)	
Cbu0388	CbuK1672/CbuK1673/CbuK1674 (NT 11bp, FS 975bp)	CbuG1619 (NT 11bp, FS 2044bp)	CbuG1679/CbuG1680 (NT 11bp, FS 1588bp)	
Cbu0393	CbuK1668 (FS 287bp)	CbuG1615 (NT 142bp, FS 559bp)	CbuD1674 (FS 559bp)	RPT1 domain
Cbu0425 (*cirB*)	CbuK1643 (AS 116bp, CT 539bp)	CbuG1587 (AS 116bp)	CbuD1648 (AS 116bp, CT 59bp)	
Cbu0469	CbuK1391	CbuG1544	CbuD1609	
Cbu0513	CbuK1341 (NT 71bp, CT	CbuG1498	CbuD1562	
Cbu0637	CbuK1619	CbuG1367	CbuD0648	
Cbu0665	CbuK1593 (NT 21bp)	CbuG1341 (NT 21bp, CT 85bp)	CbuD0675 (AS 92bp)	
Cbu0773	CbuK0643	CbuG1228	CbuD0821	
Cbu0885	CbuK0750	CbuG1117	CbuD0949 (NT 86bp)	HAD-like
Cbu1079	CbuK0945	CbuG0924	CbuD1181	
Cbu1102	CbuK0972 (AS 404bp, FS 1053)	CbuG0900 (CT 111bp)	CbuD1204 (AS 404bp)	
Cbu1110	CbuK0977 (FS 166bp)		CbuD1210 (NT 53bp, FS 166bp)	
Cbu1150	CbuK1017 (AS 57bp)	CbuG0859 (AS 476bp)	CbuD1247 (AS 476bp, CT 26bp)	Transmembrane helix hairpin
Cbu1198	CbuK1062 (NT 140bp)	CbuG0811 (NT 140bp)	CbuD1287	
Cbu1434	CbuK0601	CbuG0575	CbuD0561	
Cbu1525	CbuK1752 (AS 152bp)	CbuG0485 (NT 459bp, FS 924bp)	CbuD0461 (AS 1900bp)	YebC-like
Cbu1566	CbuK1793	CbuG0446	CbuD0422	

Table 2.6 Continued

Gene Locus in NMI	K	G	Dugway	Domain
Cbu1576	CbuK1806 (NT 129bp)	CbuG0435/CbuG0436 (FS 902bp)	CbuD0410	GatB/YqeY motif
Cbu1594	CbuK1823		CbuD0395	Transmembrane helix
Cbu1607	CbuK1834 (NT 242bp)	CbuG0407 (NT 242bp, CT 13bp)	CbuD0383 (NT 242bp)	
Cbu1620	CbuK1842 (FS 240bp)	CbuG0403 (AS 171bp)	CbuD0378 (AS 296bp, FS 240bp)	
Cbu1639	CbuK1862	CbuG0383 (FS 309bp)	CbuD0358	
Cbu1665	CbuK0343 (FS 897bp)		CbuD0334	
Cbu1677	CbuK0333	CbuG0344	CbuD0324	
Cbu1685	CbuK0326 (FS 1060bp)	CbuG0337	CbuD0317 (NT 35bp, FS 427bp)	
Cbu1754	CbuK0252	CbuG0136	CbuD0247	
Cbu1789	CbuK0083	CbuG0170	CbuD0015	SGL-like
Cbu1790	CbuK0084 (FS 924bp)	CbuG0171 (FS 1685bp)	CbuD0016 (FS 1263bp)	PRR domain
Cbu2007	CbuK2058	CbuG2016	CbuD2108	
Cbu2013	CbuK2064 (NT 50bp)	CbuG2022 (NT 50bp)	CbuD2113 (NT 50bp)	
Cbu2016	CbuK2067	CbuG2025	CbuD2117	
Cbu2028	CbuK2080 (AS 68bp, FS 46bp)	CbuG2038 (AS 51bp, FS 361bp)	CbuD2129 (AS 51bp)	WW domain-like
Cbu2059 (*cirE*)	CbuK2105 (AS 389bp, CT 615bp)	CbuG2063 (NT 182bp, FS 313bp)	CbuD2154 (AS 389bp)	
Cbu2064	CbuK2107 (AS 1233bp)	CbuG2065 (NT 22bp, CT 112bp)	CbuD2156 (NT 22bp)	
Cbu2076	CbuK2121	CbuG2077	Cbu2172	
CbuA0015				Coiled coil
CbuA001				

Table 2.6 Continued

Gene Locus in NMI	K	G	Dugway	Domain
CbuA0020		CbuG2038 (CT 447bp)	CbuDA0049 (CT 101bp)	

It is well established that the T4SS translocation signal resides in the last 100 residues of the C-terminus of secretion substrates. Genome comparison of these isolates revealed that many of these substrates have C-terminal truncations, suggesting that these substrates may not be translocated by specific isolates, further supporting the idea of different effector pools for specific *C. burnetii* pathotypes. Many of the substrates have undergone frameshifts, resulting in the creation of several pseudogenes. For example, Cbu0388 has undergone several frameshifts, leading to the generation of three separate pseudogenes in K and two pseudogenes in D. Similarly, Cbu0375 and Cbu0376 have undergone several mutations resulting in two separate genes in NMI, but one gene in the other three isolates. Such variations may correlate with the requirement of different effector pools at disease states during infection.

Table 2.7 Phenotypes associated with *C. burnetii* T4SS substrates.

Cbu Number	Screen/Reference Number[1]	LP TEM[2]/CB TEM	Ectopic Localization[3]	Yeast Toxicity	SEAP[5]	Transposon Mutant/ Replication Defect[6]
Cbu0012*	E-block	1%	No Pattern	No Phenotype	No Phenotype	Yes/ Slight Defect[a]
Cbu0041 (*cirA*)	18	70%	Punctate	**Toxic**	No Phenotype	Yes/ No Intracellular Replication
Cbu0069	PmrA	1%	No Pattern	No Phenotype	No Phenotype	
Cbu0080	E-block, 12	70%/1%	No Pattern	No Phenotype	No Phenotype	
Cbu0113	E-block	7%/50%	No Pattern	No Phenotype	No Phenotype	
Cbu0129	18	70%	Nucleus	No Phenotype	No Phenotype	
Cbu0175	18	20%	No Pattern	No Phenotype	No Phenotype	
Cbu0183	PmrA	20%	No Pattern	No Phenotype	No Phenotype	
Cbu0201*	PmrA	1%	No Pattern	No Phenotype	No Phenotype	Yes/ No Defect
Cbu0212	E-block	10%	No Pattern	No Phenotype	No Phenotype	
Cbu0270*	E-block	1%	No Pattern	No Phenotype	No Phenotype	
Cbu0295*	E-block, 12	2%	No Pattern	No Phenotype	No Phenotype	
Cbu0344	E-block	5%/4%	No Pattern	No Phenotype	No Phenotype	Yes/ No Defect
Cbu0372	E-block	20%	Endoplasmic Reticulum	No Phenotype	No Phenotype	Yes/ No Defect
Cbu0375	E-block	35%	No Pattern	No Phenotype	No Phenotype	
Cbu0376	E-block	7%	No Pattern	No Phenotype	No Phenotype	
Cbu0388	PmrA	40%/1%	Nucleus	No Phenotype	No Phenotype	Yes/ No Intracellular Replication[a]
Cbu0393*	PmrA	1%	Nucleus	No Phenotype	No Phenotype	
Cbu0410	18	45%	ND	No Phenotype	No Phenotype	
Cbu0414	18	45%	No Pattern	No Phenotype	No Phenotype	
Cbu0425 (*cirB)*	E-block, 12	90%	Cytoplasmic	No Phenotype	No Phenotype	Yes/ No Intracellular Replication
Cbu0469*	E-block	1%/4%	No Pattern	No Phenotype	No Phenotype	

Table 2.7 Continued

Cbu Number	Screen/Reference Number[1]	LP TEM[2]/CB TEM	Ectopic Localization[3]	Yeast Toxicity	SEAP[5]	Transposon Mutant/ Replication Defect[6]
Cbu0606	E-block	2%/2%	Cytoplasmic	**Toxic**	No Phenotype	
Cbu0665	PmrA	3%	Cytoplasmic	No Phenotype	No Phenotype	
Cbu0773	E-block	5%	No Pattern	No Phenotype	No Phenotype	
Cbu0794	18	80%	Nucleus	No Phenotype	No Phenotype	
Cbu0801	18	10%	No Pattern	No Phenotype	No Phenotype	
Cbu0814	18	10%	No Pattern	No Phenotype	No Phenotype	
Cbu0881	18	80%	ND	No Phenotype	No Phenotype	
Cbu0885	E-block	1%/3%	Cytoplasmic	**Toxic**	No Phenotype	
Cbu0937 (*cirC)*	18	2%	Cytoplasmic	No Phenotype	No Phenotype	Yes/ No Intracellular Replication
Cbu1045	18	40%	No Pattern	No Phenotype	No Phenotype	
Cbu1079	E-block	5%	No Pattern	No Phenotype	No Phenotype	
Cbu1102	E-block	70%	No Pattern	No Phenotype	No Phenotype	
Cbu1110	PmrA	40%	No Pattern	No Phenotype	No Phenotype	
Cbu1150*	E-block	1%	No Pattern	No Phenotype	No Phenotype	
Cbu1198	PmrA	75%	No Pattern	No Phenotype	No Phenotype	Yes/ Slight Defect[a]
Cbu1217	18	10%	No Pattern	No Phenotype	No Phenotype	
Cbu1314	18	2%	Nucleus	No Phenotype	No Phenotype	
Cbu1379*	18	1%	No Pattern	No Phenotype	No Phenotype	
Cbu1406	18	40%	Cytoplasmic	No Phenotype	No Phenotype	
Cbu1425*	18	1%	Mitochondria	No Phenotype	No Phenotype	
Cbu1434*	E-block	1%	Cytoplasmic	No Phenotype	No Phenotype	
Cbu1457	18	2%	ND	No Phenotype	No Phenotype	Yes/ Slight Defect[a]
Cbu1460	18	40%	ND	No Phenotype	No Phenotype	
Cbu1461	18	2%	Cytoplasmic	No Phenotype	No Phenotype	
Cbu1524	12, 18	10%	Nucleus	**Toxic**	No Phenotype	
Cbu1525	E-block, 12		Cytoplasmic	No Phenotype	No Phenotype	
Cbu1543	18	25%	Punctate	No Phenotype	No Phenotype	

Table 2.7 Continued

Cbu Number	Screen/Reference Number[1]	LP TEM[2]/CB TEM	Ectopic Localization[3]	Yeast Toxicity	SEAP[5]	Transposon Mutant/ Replication Defect[6]
Cbu1556	18	50%	Cytoplasmic	No Phenotype	**0.23 ± 0.01**	Yes/ No Defect
Cbu1566	E-block	5%	No Pattern	No Phenotype	No Phenotype	
Cbu1576	PmrA	2%/2%	Endoplasmic Reticulum	No Phenotype	No Phenotype	
Cbu1594	Homolog	5%	No Pattern	No Phenotype	No Phenotype	
Cbu1607	E-block	5%	No Pattern	No Phenotype	No Phenotype	
Cbu1620	E-block	90%	No Pattern	No Phenotype	No Phenotype	
Cbu1636	18	1%	Punctate	No Phenotype	No Phenotype	Yes/ No Defect
Cbu1639	PmrA	4%	No Pattern	No Phenotype	No Phenotype	Yes/ No Defect
Cbu1665*	E-block	1%/1%	No Pattern	No Phenotype	No Phenotype	Yes/ No Defect
Cbu1677	E-block	5%	No Pattern	No Phenotype	No Phenotype	
Cbu1685	PmrA	1%/1%	No Pattern	No Phenotype	No Phenotype	
Cbu1751	18	50%	No Pattern	No Phenotype	No Phenotype	
Cbu1754	E-block	2%/1%	No Pattern	No Phenotype	No Phenotype	
Cbu1769	18	1%	No Pattern	No Phenotype	No Phenotype	
Cbu1789*	E-block	1%	No Pattern	No Phenotype	No Phenotype	
Cbu1790*	E-block	1%	Cytoplasmic	No Phenotype	No Phenotype	
Cbu1823	12, 18	50%	No Pattern	No Phenotype	No Phenotype	
Cbu1825	12, 18	40%	Mitochondria	No Phenotype	**1.70 ± 0.01**	
Cbu2007	E-block	90%	Cytoplasmic	No Phenotype	No Phenotype	Yes/ No Defect
Cbu2013	PmrA	50%	Cytoplasmic	No Phenotype	No Phenotype	Yes/ Slight Defect[a]
Cbu2016*	E-block	1%	No Pattern	**Toxic**	No Phenotype	Yes/ No Defect
Cbu2028*	E-block	1%	No Pattern	No Phenotype	No Phenotype	
Cbu2052 (*cirD*)	12, 18	90%	Cytoplasmic	**Toxic**	No Phenotype	Yes/ No Intracellular Replication
Cbu2059 (*cirE*)	E-block, 12	40%	Cytoplasmic	No Phenotype	No Phenotype	Yes/ No Intracellular Replication
Cbu2064*	E-block, 12	1%	No Pattern	No Phenotype	No Phenotype	
Cbu2076*	E-block	1%	No Pattern	No Phenotype	No Phenotype	

Table 2.7 Continued

Cbu Number	Screen/Reference Number[1]	LP TEM[2]/CB TEM	Ectopic Localization[3]	Yeast Toxicity	SEAP[5]	Transposon Mutant/ Replication Defect[6]
Cbu2078	12	10%	ND	No Phenotype	No Phenotype	
CbuA0014	12, 20	10%	No Pattern	No Phenotype	No Phenotype	
CbuA0015	E-block, 20	90%	No Pattern	No Phenotype	No Phenotype	
CbuA0020*	E-block	1%	Mitochondria	No Phenotype	No Phenotype	

***C. burnetii* T4SS substrates target distinct subcellular compartments in mammalian cells:** Following translocation into a host cell, many effector proteins target specific subcellular compartments or decorate the CCV membrane where they interact with host proteins (20, 60, 61, 109, 111). To determine host subcellular compartments targeted by the herein identified *C. burnetii* T4SS substrates, *C. burnetii* infected or uninfected HeLa cells were transiently transfected with each substrate expressed as a fusion of EGFP. Imaging of 52 ectopically expressed substrates identified 17 substrates that displayed a pattern distinct from EGFP. Most of these EGFP fusions were diffusely localized throughout the cytosol and were excluded from the nuclei (Fig. 2A, Table 2.7). All of the tested substrates displayed similar localization in infected and uninfected cells and no protein was co-localized with the *Coxiella*-containing vacuole (data not shown).

Interestingly, we identified two substrates, Cbu0393 and Cbu0388, that traffic to the nucleus, indicated by colocalization with the marker Hoechst (Fig. 2.3A). Bioinformatic analysis of these nuclear substrates identified a potential nuclear

localization signal, PPTKRPRGL, in its N-terminal region beginning at the 11th residue for Cbu0393 (53) and KKPSKKVKIKKSKPKKKK beginning at the 922nd residue for Cbu0388.

To better determine the subcellular organelles targeted by these EGFP patterned substrate fusions, we conducted colocalization analysis with markers of relevant organelles. Two substrates, Cbu0372 and Cbu1576, localized to the endoplasmic reticulum (ER) as evident by colocalization with the ER marker calnexin (Fig. 2.3B). EGFP-CbuA0020 targeted the mitochondria as evident by colocalization with the mitochondrial marker CoxIV (Fig. 2.3B).

Overexpression of several substrates interferes with yeast growth: Due to its genetic tractability and the high level conservation of many cellular processes with mammalian cells, *Saccharomyces cerevisiae* has evolved as a useful model for studying bacterial effector proteins (104). A large number of bacterial effectors have been identified based on their ability to interfere with yeast growth (15, 18, 95) or by their ability to alter vesicle trafficking (23, 95). To determine whether any of the *C. burnetii* T4SS substrates are toxic to yeast, we inserted each of these genes, as well as previously reported substrates (20), into the galactose inducible vector pYesNTA2. *S. cerevisiae* W303, carrying *C. burnetii* substrates, were grown in Uracil dropout media, serially diluted, and spotted onto appropriate dropout agar. Using this approach we identified six substrates that severely impaired growth (Fig. 2.4).

Figure 2.3 *C. burnetii* secretion substrates target distinct subcellular compartments when ectopically expressed in HeLa cells. Each T4SS substrate was expressed as a C-terminal fusion to EGFP and used for transfection of HeLa cells. (A) A diffuse cytoplasmic signal that excluded the nuclei or co-localization with the nucleus, here shown for Cbu2059 and Cbu0393, respectively, could be demonstrated. (B) Colocalization analysis identified two substrates (Cbu0372 and Cbu1576) that colocalize with the endoplasmic reticulum marker calnexin and one substrate (CbuA0020) that colocalizes with the mitochondrial marker CoxIV. Scale bar in merged images represents 10 µm. Arrows denote location chosen for inset.

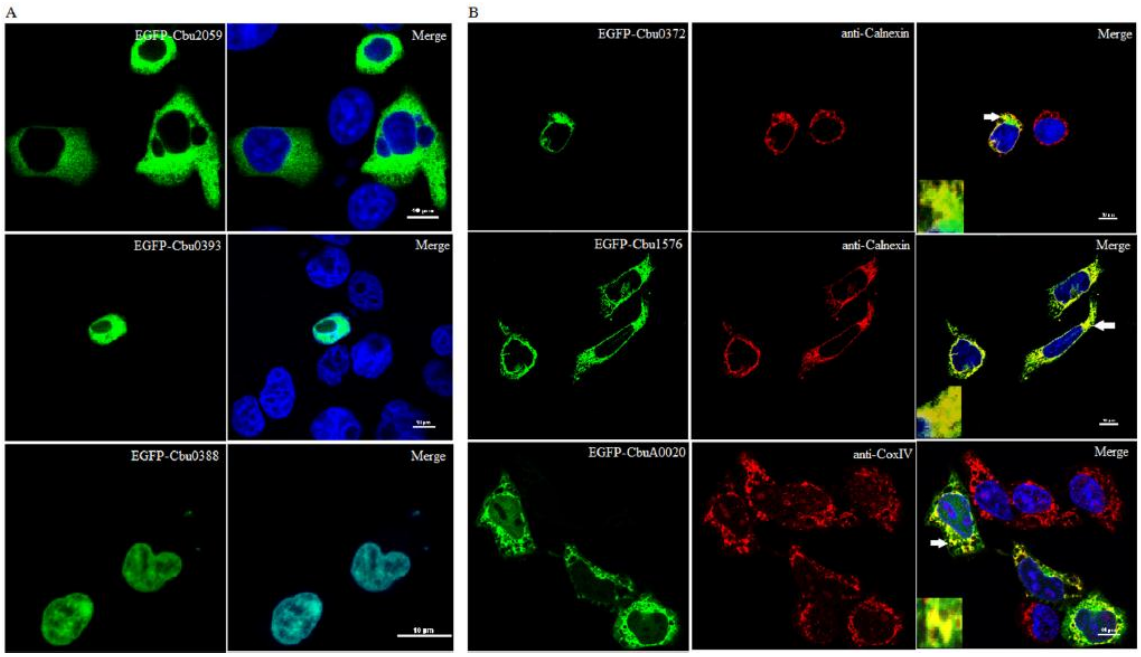

Figure 2.4 *C. burnetii* T4SS substrates interfere with yeast growth. *S. cerevisiae* W303 expressing *C. burnetii* T4SS substrates were diluted to an OD_{600} of 0.2 serially diluted and on spotted onto dropout media containing 2% glucose or 2% galactose. All strains exhibited similar growth under noninducing conditions, in presence of glucose, but exhibited significantly diminished growth on galactose containing media.

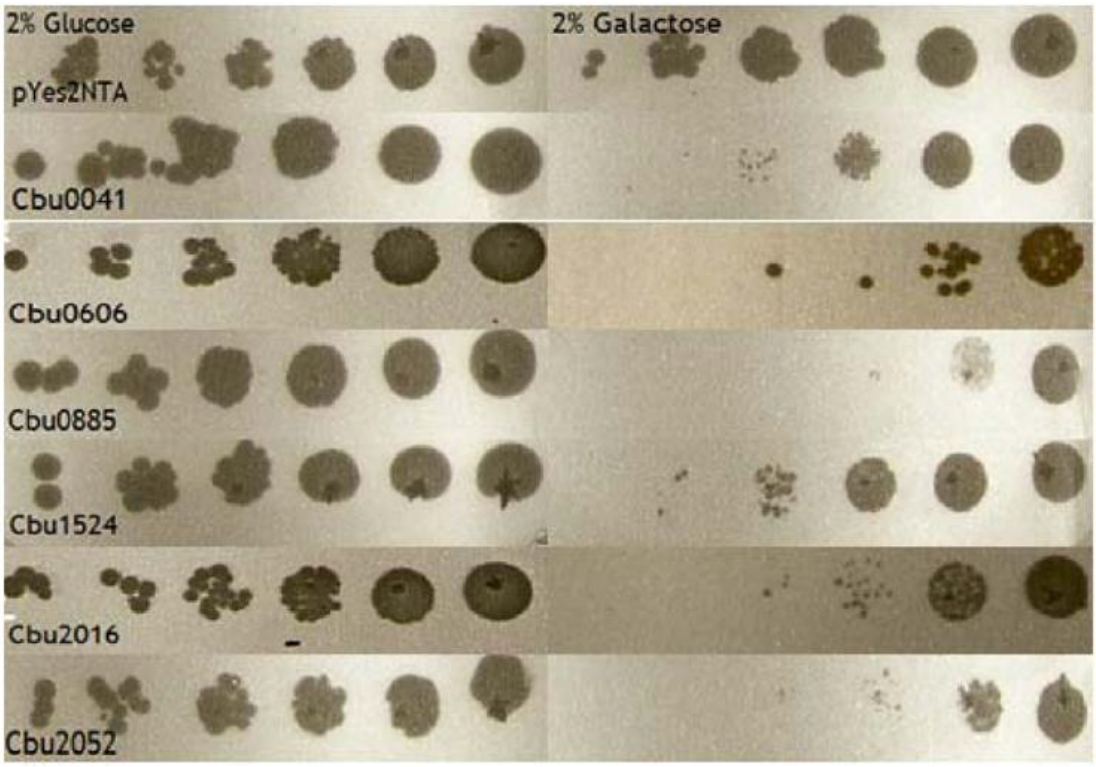

Overexpression of *C. burnetii* secretion substrates interferes with the host secretory pathway: One *C. burnetii* T4SS effector has been shown to interfere with vesicle trafficking by disrupting membrane trafficking using the secreted embryonic alkaline phosphatase (SEAP) assay (18). To determine whether other Coxiella Dot/Icm substrates interfere with the secretory pathway of eukaryotic cells, Hek293T cells were transiently transfected to express both the SEAP protein and EGFP substrate fusions. The ratio of extracellular to intracellular SEAP activity was calculated (Table 2.7 and Fig. 2.5). Three substrates, Cbu1556, Cbu1825, and CbuA0019 exhibited an extracellular/intracellular ratio of 0.23 ± 0.01 ($P<0.0001$), 1.70 ± 0.01 ($P=0.0004$), and 1.36 ± 0.04 ($P=0.0002$) respectively, which was significantly reduced compared to the vector alone ratio of 4.32 ± 0.16, indicating that these *C. burnetii* effectors interfere with the host secretory pathway.

***C. burnetii* T4SS substrates are essential for intracellular replication and CCV formation:** The *Legionella pneumophila* Dot/Icm system is estimated to deliver over 250 proteins into the host cell cytosol. In the *L. pneumophila* model, loss of a single effector generally doesn't diminish bacterial intracellular replication, suggesting a degree of functional redundancy (79). To determine whether individual *C. burnetii* T4SS substrates are necessary for intracellular replication and CCV maturation, we generated a pool of mutants using the mariner-based *Himar1* transposon for random mutagenesis. Rescue cloning and sequencing analysis led to the isolation of 20 unique T4SS substrate mutants (Table 2.7 and Fig. 2.6).

Figure 2.5 *C. burnetii* secreted effectors interfere with host protein secretion. Hek293T cells were co-transfected with pSEAP and GFP-tagged T4SS substrates or vector control. Twenty-four hours post-transfection, external and internal SEAP was calculated. A significant decrease in SEAP activity was noted for Cbu1556 ($P<0.0001$), CbuA0019 ($P=0.0002$), and Cbu1825 ($P=0.0004$) compared to the vector control.

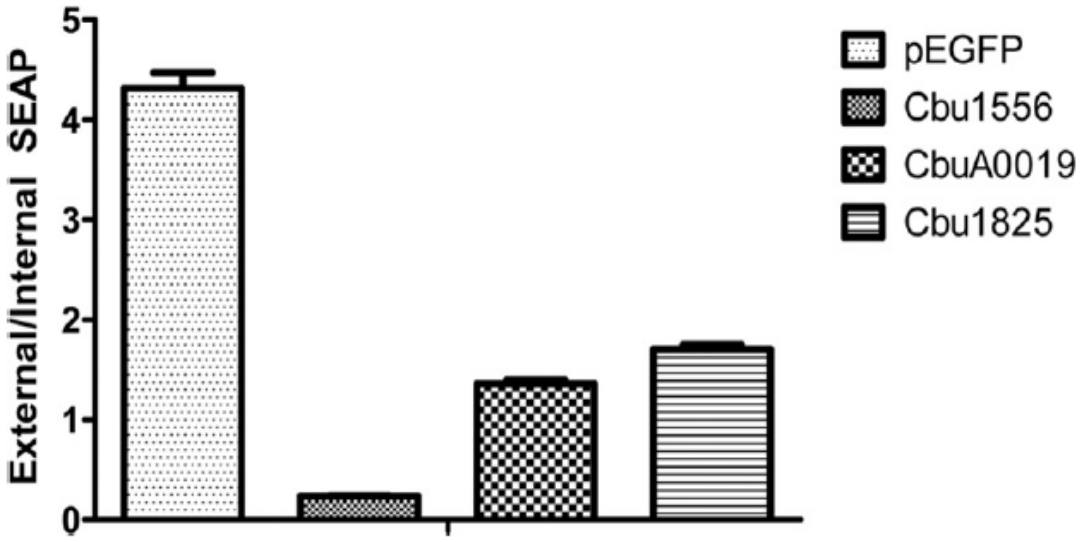

Figure 2.6 *Himar1* transposon insertion into *C. burnetii* T4SS substrate genes. To generate a large pool of *C. burnetii* Tn mutants, NMII was transformed with pKM225, and the resulting transformants were expanded and rescue cloned and three *E. coli* colonies were sequenced per transformation. The schematic shows the insertion of the *Himar1* transposon (blue) into the T4SS substrate genes (purple)

CBU0012

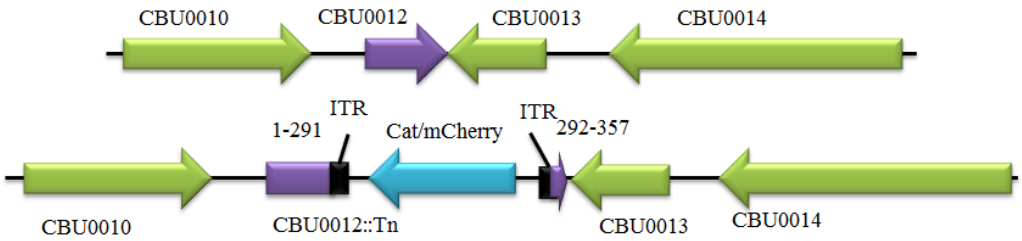

CBU0041 (*cirA*)

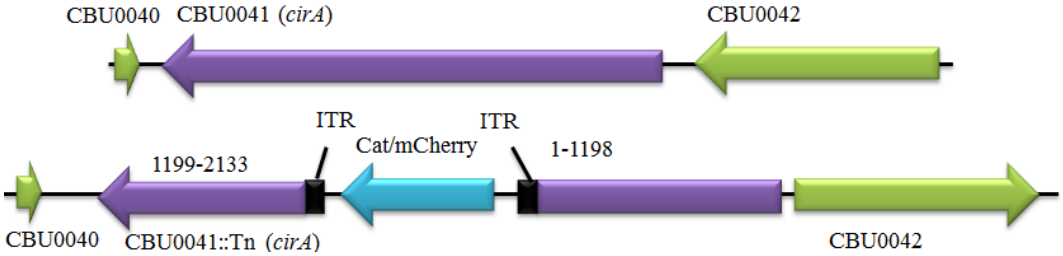

CBU0201

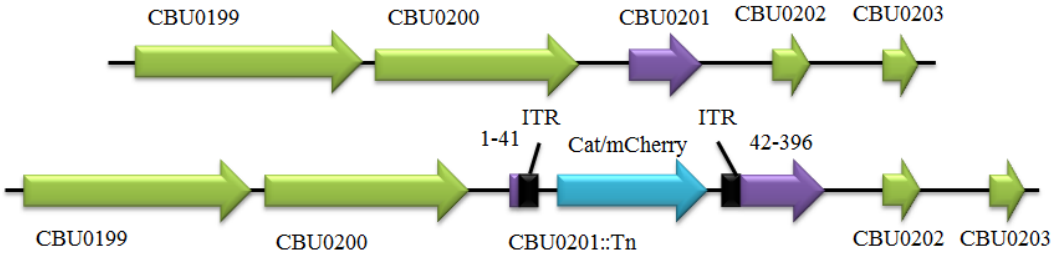

Figure 2.6 Continued

CBU0344

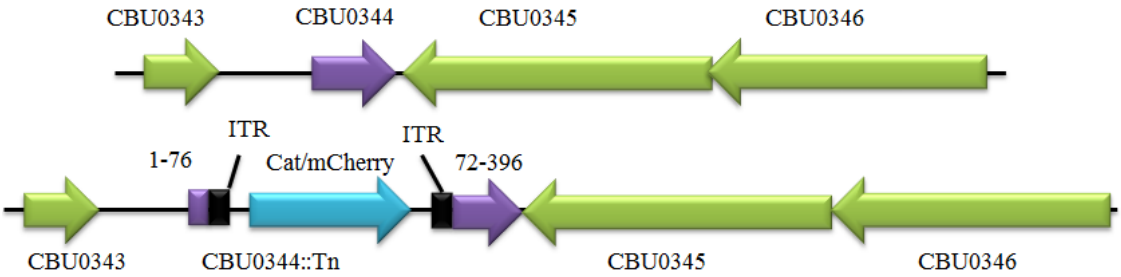

CBU0372

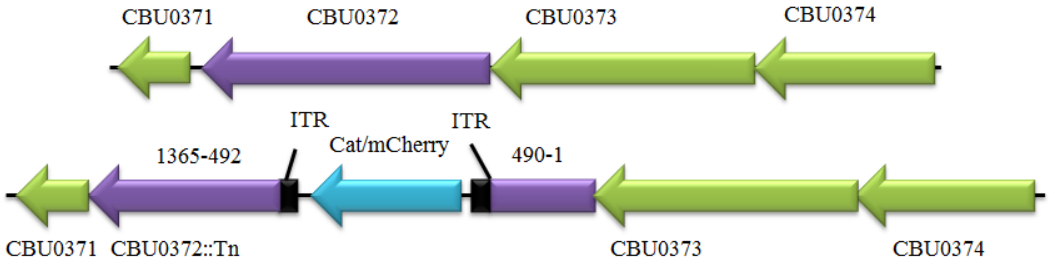

CBU0388

CBU0425 (*cirB*)

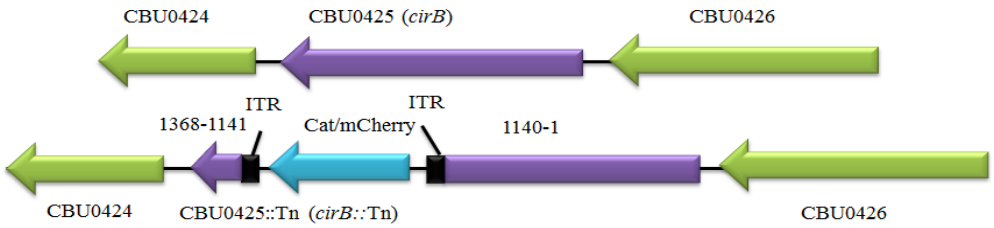

Figure 2.6 Continued

CBU0937 (*cirC*)

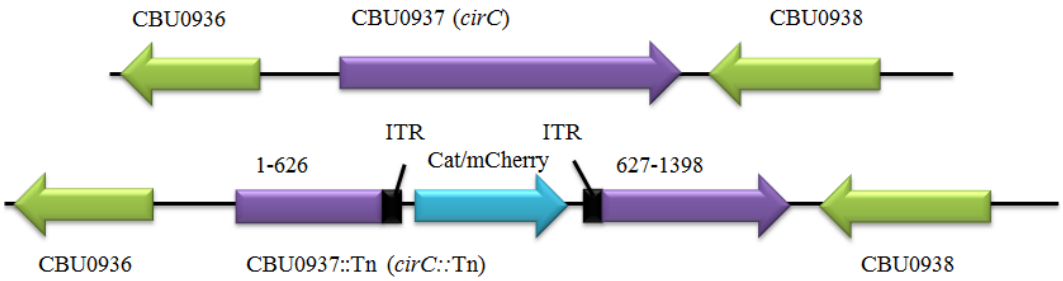

CBU1198

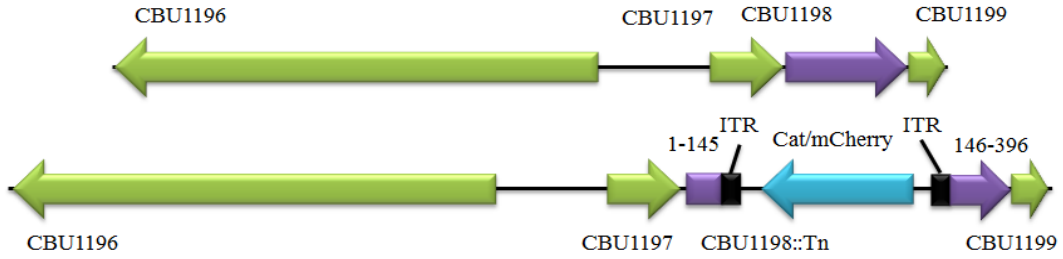

CBU1457

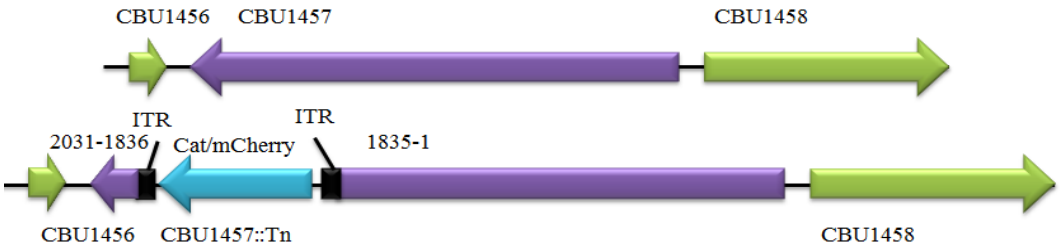

CBU1556

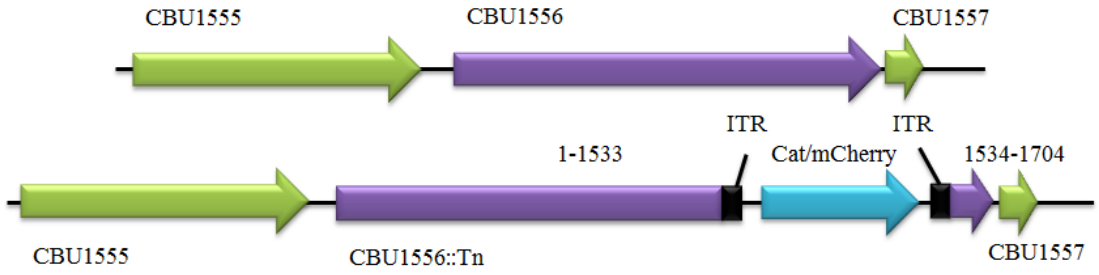

Figure 2.6 Continued

CBU1569

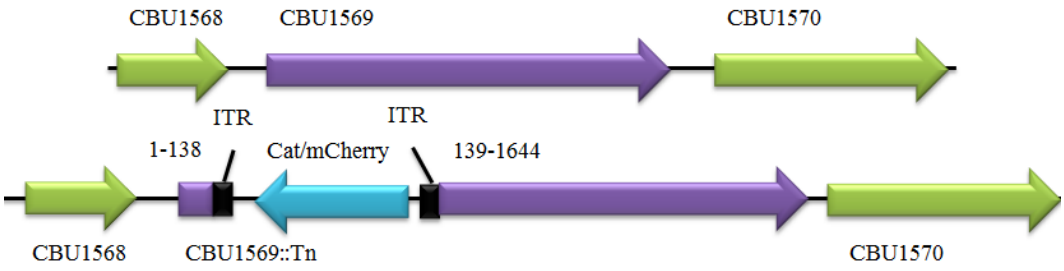

CBU1636

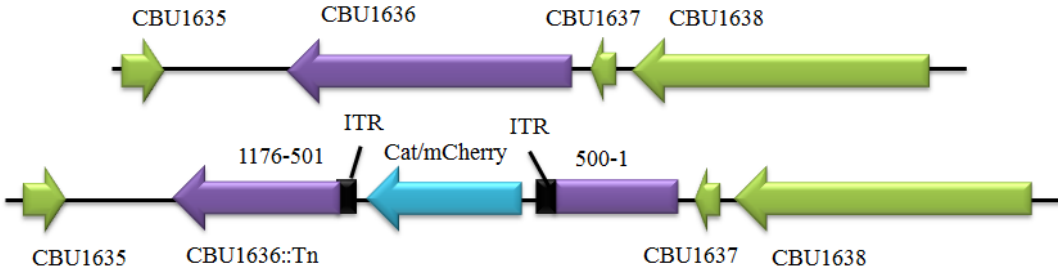

CBU1639

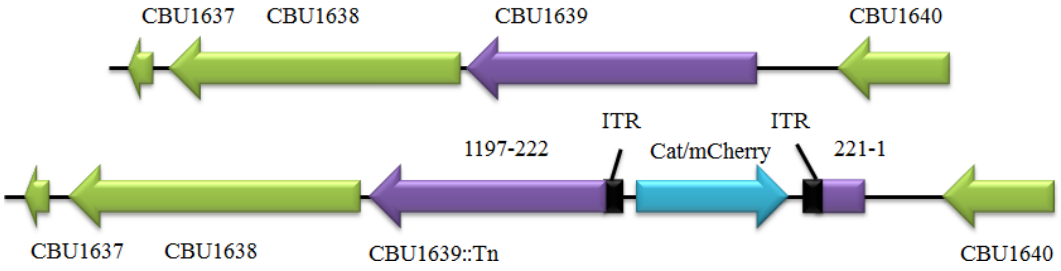

CBU1665

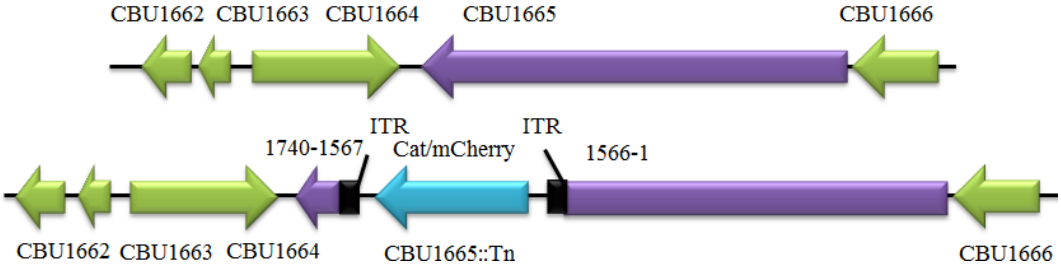

Figure 2.6 Continued

CBU1639

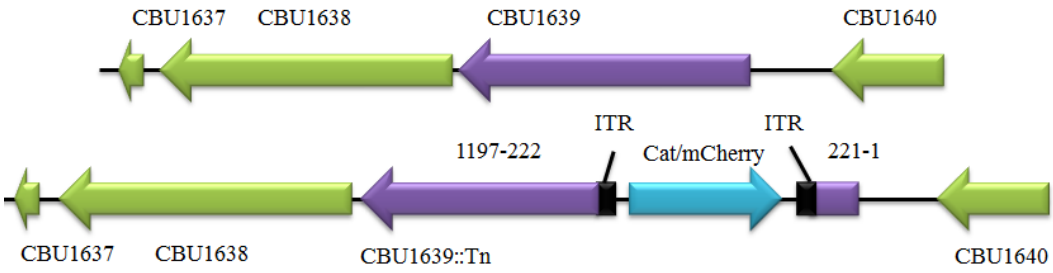

CBU2007

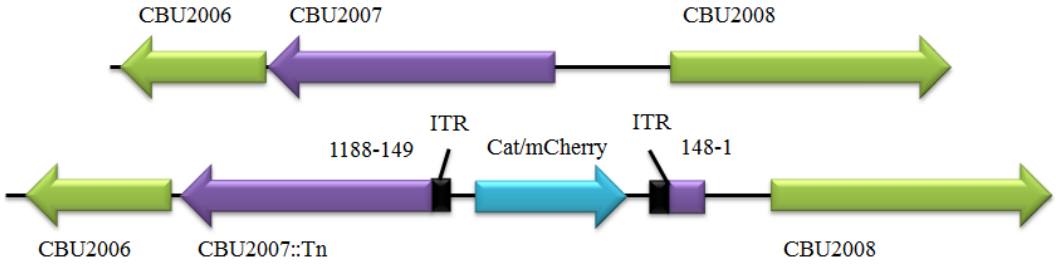

CBU2013

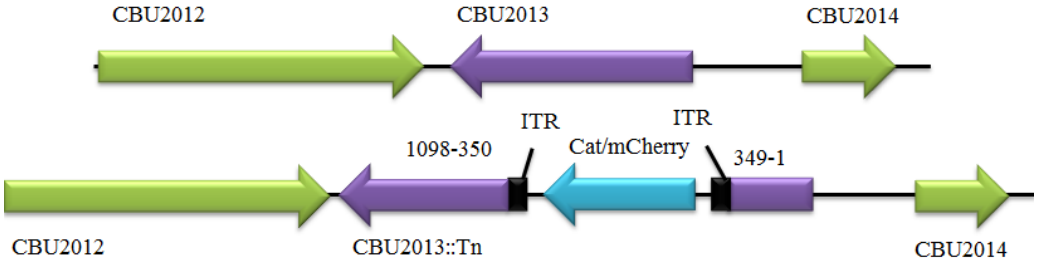

CBU2016

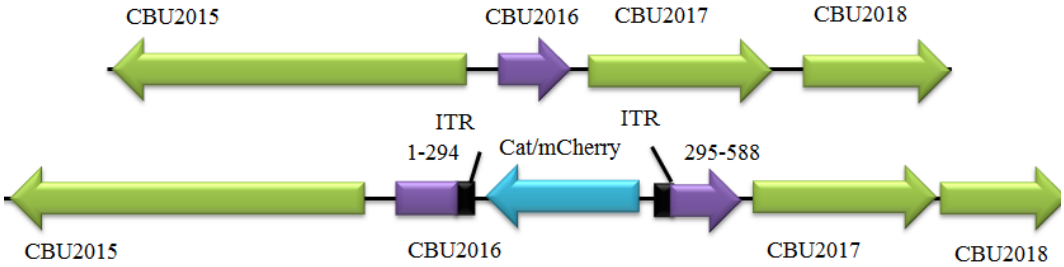

Figure 2.6 Continued

CBU2052 (*cirD*)

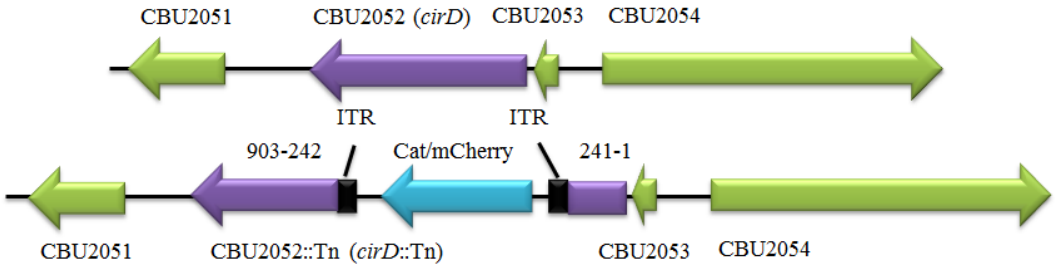

CBU2059 (*cirE*)

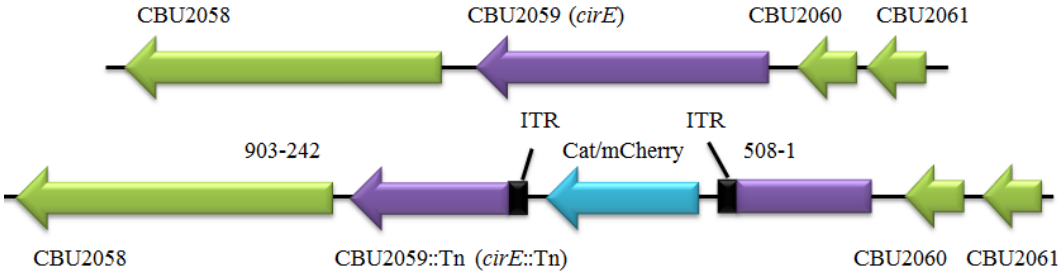

CBU1652 (*icmX*)

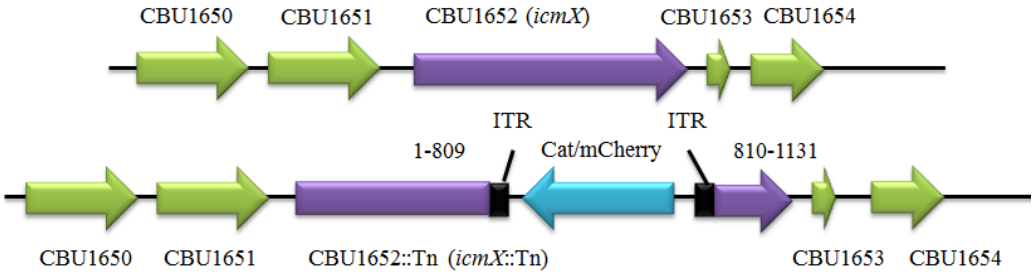

To determine the effects of each of these mutations on bacterial intracellular replication or CCV formation, we infected J774A.1 and HeLa cells with these mutants and monitored bacterial growth. Whereas several of the substrates were dispensable for intracellular replication, six substrate mutants (Cbu0041, Cbu0388, Cbu0425, Cbu0937, Cbu2052, and Cbu2059) were unable to replicate in J774A.1 (Fig. 2.7A) or HeLa cells (data not shown). These mutants displayed a growth phenotype similar to that of the RSA439 *icmX*::Tn strain. An additional four substrate mutants (Cbu0012, Cbu1198, Cbu1457, and Cbu2013) were capable of replication in J774A.1; however, the bacterial yield was significantly reduced compared to the parental RSA439 (Fig. 2.7B). None of these mutants were capable of forming the characteristic large CCV and instead resided in a tight fitting vacuole that did not expand even at late timepoints following infection (Fig. 2.7C). None of these mutants displayed a growth defect when cultured axenically in ACCM-2 (Fig. 2.8A), indicating that the growth defect is not caused by impairment in general bacterial physiology, but likely the inability of the mutants to properly interact with host cellular processes necessary for the establishment of replicative niche.

Figure 2.7 Individual *C. burnetii* effector proteins are essential for intracellular replication and CCV formation. NMII *C. burnetii* was transformed with the *Himar1* transposon and the resulting clonal substrate mutants were used to infect J774A.1 Tn insertion into Cbu0041 *(cirA*), Cbu0388, Cbu0425 (*cirB*) Cbu0937 *(cirC*), Cbu2052 *(cirD*), and Cbu2059 (*cirE)* resulted in an inability to replicate intracellularly; however (B) Tn insertion into Cbu0012, Cbu1198, Cbu1457, and Cbu2013 resulted in reduced intracellular replication compared to RSA439. To determine if co-infection with parental NMII would rescue the Tn mutants' growth defect, HeLa cells were infected with an MOI of 100 of each strain and incubated for seven days. Images were captured using a Nikon A1 confocal microscope and at least 100 infected cells were imaged per experiment. Co-infection with wild-type resulted in significant replication for both wild-type and Tn substrate mutant whereas cells only infected with the substrate mutant did not exhibit significant replication. Scale bars represent 6µM.

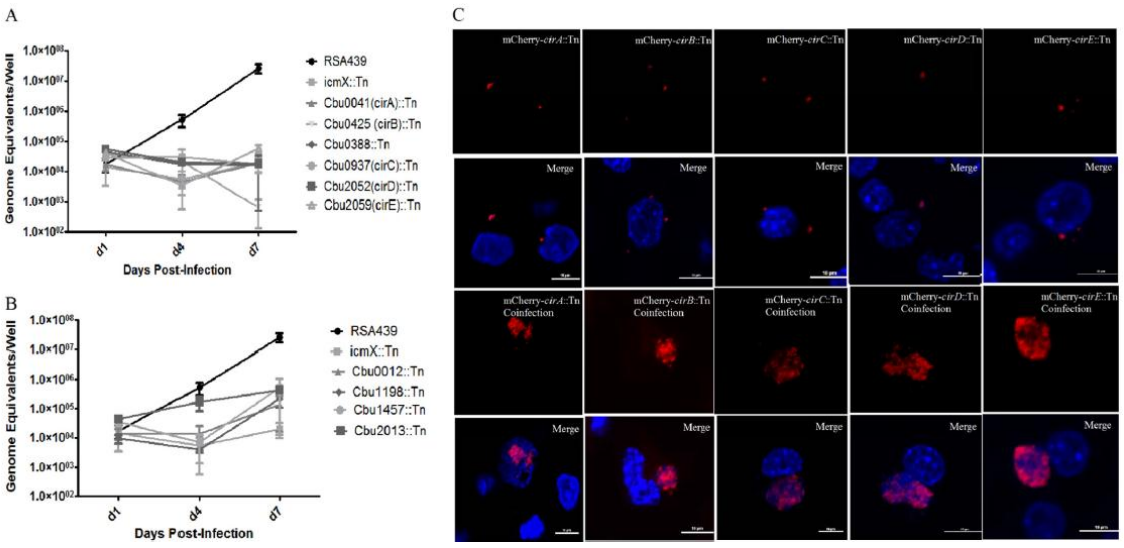

Ten substrate mutants exhibited an inability to productively infect host cells. It was recently demonstrated that co-infection of an *icmD*::Tn with the isogenic NMII rescues this growth defect by supplying the T4SS functions in *trans* (6). If the inability of these effector mutants to replicate intracellularly is due to the loss of an individual effector function, supplying the effector function *in trans* should similarly rescue their growth defect. Confocal images of cells infected with individual substrate mutants resulted in the formation of tight fitting vacuoles that do undergo expansion at late time points of infection (Fig. 2.7C). However, co-infection of Cbu0041, Cbu0388, Cbu0937, Cbu2052, Cbu2059, Cbu0425, and Cbu1457 effector mutants with the isogenic NMII resulted in the formation of CCVs that consisted of roughly equivalent numbers of substrate mutant (red) and NMII (blue) (Fig. 2.7C), indicating that these *Tn* effector mutants are capable of replicating in a vacuole co-inhabited by the parental strain. No co-infected cells were observed for Cbu0012, Cbu1198, and Cbu2013. Therefore, at this time, we were unable to confirm that these individual substrates are necessary for intracellular replication and CCV formation.

To further verify that the affected substrate genes in these mutants are responsible for the observed phenotypes, we tested three additional *Himar1* insertions each for Cbu0041, Cbu0425, Cbu0937, Cbu2052, and Cbu2059 that were inserted in the same position (Fig. 2.8B), but were obtained from separate individual transformations. Growth curve analysis of each mutant in J774A.1 resulted in no intracellular replication (Fig. 2.8), suggesting that the observed growth defect is due to the loss of that individual effector protein and is unlikely the result of a random point mutation at a secondary site

or due to polar effects. Given their crucial role in intracellular replication and CCV formation, we renamed Cbu0041, Cbu0425, Cbu0937, Cbu2052, Cbu2059, as *cirA-E* (*Coxiella* effector for intracellular replication), respectively. Overall these results indicate that the growth defect observed for *cirA-E* is due to the loss of an individual effector protein and thus results in the inability of the mutant bacteria to form the proper CCV.

Discussion

Using multiple bioinformatics predictions and analyses, we obtained 234 candidates for substrates of the Coxiella Dot/Icm T4SS. Translocation assays with *L. pneumophila* as surrogate host resulted in the identification of 53 substrates that were secreted in a Dot/Icm-dependent manner, representing a 22.6% success rate for substrate identification. Seven substrates identified using this screen (Cbu0080, Cbu0295, Cbu0425, Cbu1525, Cbu2059, Cbu2064, and CbuA0015) were previously identified as Dot/Icm secretion substrates in two independent studies based on genomic (18) and plasmid QpH1 (109) screens. The identification of 46 novel substrates highlights the effectiveness of using computational approaches. However, the use of a PmrA consensus sequence and E-block motifs did not rediscover many of the previously reported substrates (18, 20, 83, 109, 111). This suggests that the features governing the recognition of substrate secretion by the Dot/Icm complex is highly diverse and that their expression regulation differs significantly.

Cbu0201 (*ankC*) was previously reported as negative for secretion (83, 111); however, we observed a 1% translocation rate for this substrate using *L. pneumophila* as

Figure 2.8 *C. burnetii* growth defects are due to the loss of individual effector proteins. (A) *C. burnetii* T4SS substrate mutants were used to inoculate ACCM-2 using 1.0 X 10^6 bacteria/ml. Loss of individual effectors had no effect on axenic culture. (B) To verify that the growth defect is due to loss of individual effector proteins, three additional mutants obtained from separate transformations were used to infect J774A.1 cells at an MOI of 100. Genome equivalents were calculated at d1, d4, and d7. Each isolated Tn mutant exhibited a similar phenotype, indicating the inability to replicate intracellularly is due to the loss of a specific individual effector and is not likely attributable to another mutation at a secondary site.

A

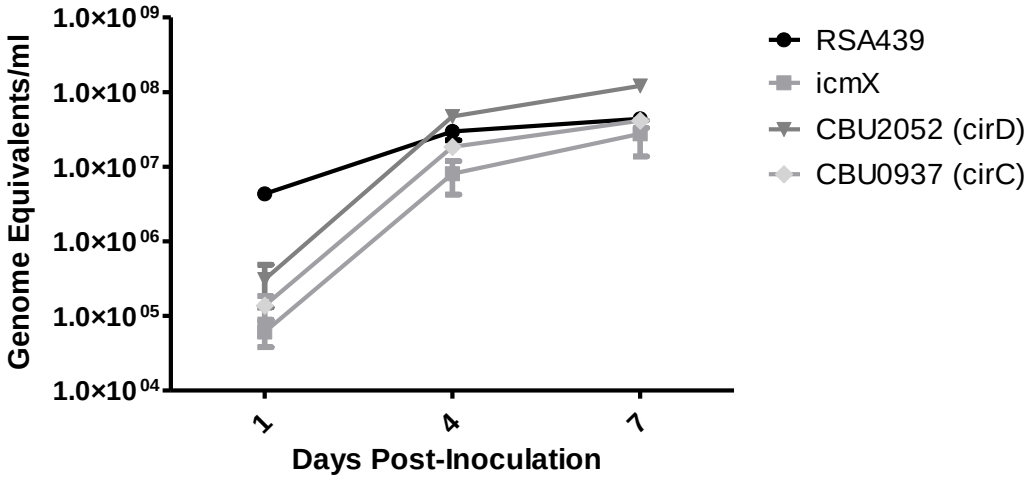

Figure 2.8 Continued

B.

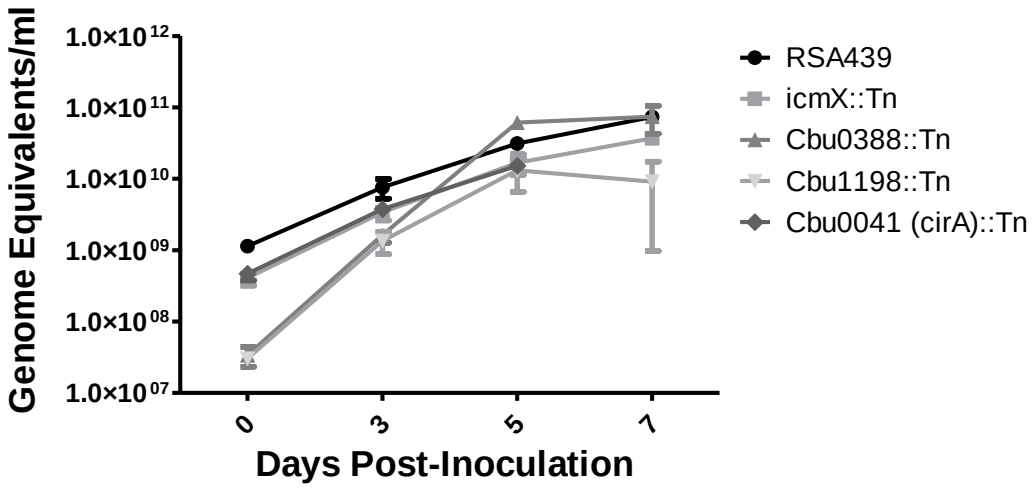

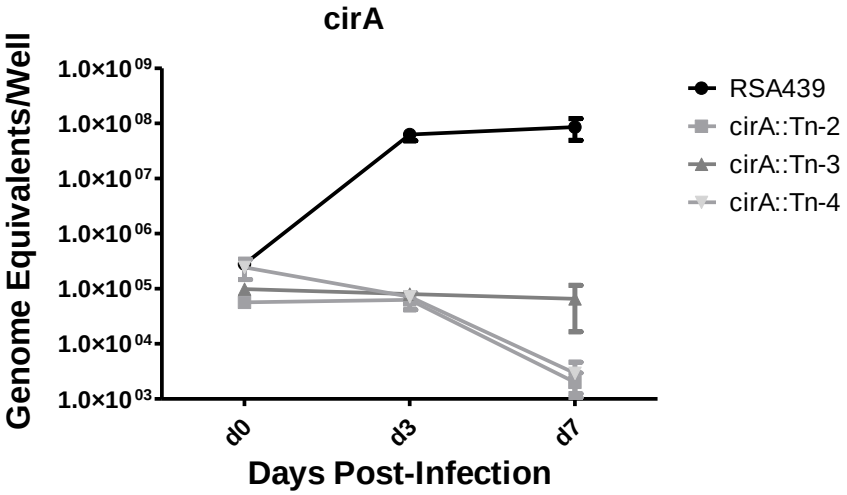

Figure 2.8 Continued

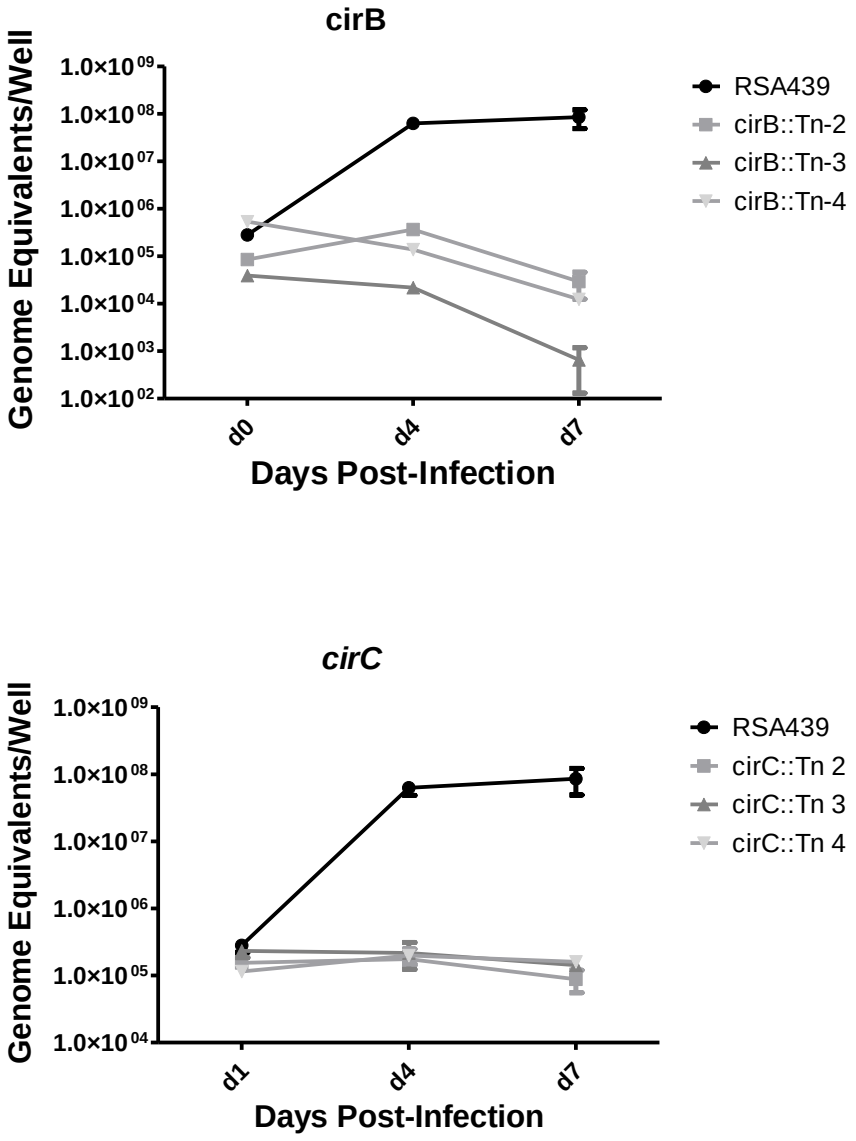

Figure 2.8 Continued

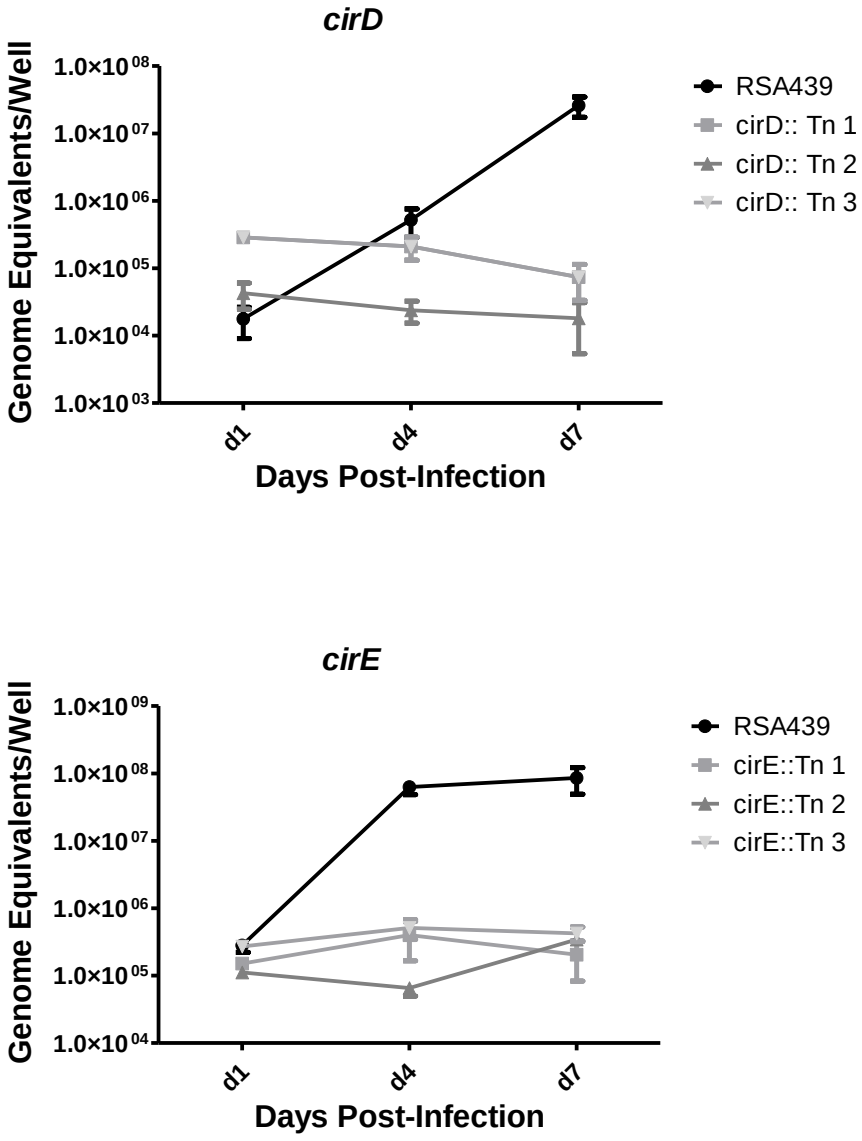

a surrogate host. The discrepancies between these studies can most likely be attributed to a difference in secretion assays used. Here we used the β-lactamase TEM-1 assay and observed a 1% translocation, whereas the previous studies used a CyaA assay (83, 111). The different results obtained between these studies highlight the importance of using multiple translocation approaches to more comprehensively define protein substrates of the Dot/Icm system. Although our results suggest *ankC* is T4SS substrate of Coxiella, further verification using independent secretion assays in *C. burnetii* is needed.

Following translocation into the host cell, many proteins traffic to specific subcellular compartments where they modulate the activity of specific host proteins. Subcellular localization has been used in numerous studies as an important starting point for elucidating effector function (15, 18, 23, 109). We transiently transfected infected and uninfected HeLa cells with EGFP-tagged T4SS substrates. Of the 52 substrates examined, 16 fusions displayed a pattern distinct from EGFP. Whereas the vast majority of these patterns were evenly distributed throughout the cytosol, distinct localization of several substrates was observed.

The long-standing coexistence between bacterial pathogens and eukaryotic host has facilitated the evolution of novel methods for subverting the host innate immune response (40). In the past decade, several bacterial effectors have been identified that traffic to the nucleus where they provoke histone modifications and facilitate chromatin remodeling (32, 39, 85, 116), suggesting that targeting host gene expression is a conserved mechanism used by intracellular pathogens to combat the host defense. Given that many intracellular pathogens secrete nuclear effector proteins, we assessed

colocalization of our T4SS substrates with the nuclear marker Hoechst. We identified two substrates, Cbu0393 and Cbu0388, which trafficked to the nucleus and encoded a predicted nuclear localization signal. Interestingly several additional studies recently identified three other *C. burnetii* nuclear substrates; Cbu1524 (*caeA*), Cbu1314, and CbuK1976, suggesting *C. burnetii* encodes a large repertoire of nuclear effectors (18, 20, 52).

C. burnetii has been shown to overcome host defense and to inhibit host cell death by actively promoting host cell viability by inducing pro-survival pathways. Modulation of the interplay between Beclin 1 and Bcl-2 (107) and sustained activation of Akt and Erk1/2 (110), have been proposed to be mediated by T4SS effectors. This hypothesis is supported by the characterization of AnkG, a *C. burnetii* T4SS effector that was found to inhibit apoptosis by modulating p32 (60). An additional 2 effector proteins, nuclear localized *caeA* (Cbu1524) and mitochondrial localized *caeB* (Cbu1532), were similarly found to prevent host cell apoptosis (52). In the current study we identified another substrate, CbuA0020 that colocalized with the mitochondrial marker CoxIV. It will be interesting to determine whether this mitochondrial-localized protein is similarly capable of inhibiting host cell apoptosis.

Ectopic expression in yeast has been routinely used to study bacterial effector proteins. For example, 79 *Legionella* effectors are able to significantly impair yeast growth (43), a phenotype that has been exploited to analyze their biochemical function (35, 100, 108). The identification of Coxiella T4SS substrates capable of inhibiting yeast growth will provide additional tools in determining their role in infection. Similarly,

specific targeting of these proteins to distinct host organelles will facilitate future functional analysis.

Recent advances in the field, including the ability to culture the bacteria axenically in ACCM-2 (80), to genetically manipulate the pathogen using a *Himar1* transposon (7), and recently the adaptation of a loop-in-loop-out mediated site-directed mutagenesis (8) have significantly advanced our understanding of *C. burnetii* pathogenesis. By applying these tools to our study we were able to successfully generate and isolate a pool of transposon mutants which included 20 T4SS substrate mutants. Growth curve analysis of each mutant revealed that ten of these substrates mutants were unable to replicate intracellularly or form a characteristic CCV. This intriguing finding suggests less functional redundancy than observed for the comparable *L. pneumophila* model in which only a few effectors, including SdhA (56) and AnkB (2), have been shown to be essential for intracellular replication in mammalian cells. Furthermore, a recent study by O' Connor et al. (79) demonstrated that deletions of large segments of the *L. pneumophila* genome results in no impairment in mammalian intracellular replication, however these mutants were significantly impaired in replication in 3 amoeba species. The differences in effector redundancy between these two related bacterial species can mostly be attributed to the fact that *L. pneumophila* is an accidental human pathogen that has developed a large effector repertoire for growth in a diverse array of protozoa species, whereas *C. burnetii* is a highly adapted mammalian pathogen that is capable of replicating in numerous vertebrate species (79).

Each of the *cirA-E*::Tn mutants were observed to be incapable of efficient intracellular replication, unless in cells coinfected with the isogenic NMII. Recent studies have shown that coinfection of *L. pneumophila ankB* mutant with wild-type *L. pneumophila* was able to rescue the growth defect associated with this mutant by supplying the effector in *trans*, highlighting the importance of individual effector proteins in generating the appropriate intracellular niche. Similarly, it was demonstrated that the growth defect associated with a *C. burnetii icmD*::Tn mutant could also be rescued by coinfection with the wild-type (6). The ability of NMII to rescue the specific Tn mutants supports the hypothesis that the growth defect observed is the result of the mutants inability to form the appropriate CCV that results from the loss of an individual effector protein. This is an intriguing finding and highlights the importance of individual effector proteins in modulating interactions with the host to facilitate the appropriate intracellular niche.

Genome comparison for *cirA-E* revealed that only four substrates (*cirA*, *cirB, cirC*, and *cirD*,) are fully conserved among the different *C. burneti* pathotypes (20), whereas significant heterogeneity exist among *cirE*. However, *cirE* has undergone several frameshifts, raising the question is this substrate secreted by other *C. burnetii* pathotypes? It will be interesting to determine if each of these substrates are translocated by each of the pathotypes and if the RSA439 mutants can be complemented by the corresponding K, G, or D DNA.

In conclusion we show that *C. burnetii* encodes a large, unique repertoire of T4SS substrates that traffic to distinct subcellular compartments and potentially interfere

with crucial host cell processes. Through the use of a *Himar1* transposon, we isolated 20 individual T4SS substrate mutants, ten of which were found to be essential for efficient intracellular replication and CCV formation, indicating a lack of effector functional redundancy. Further study of these effectors, including mutant complementation, generation of site-directed mutants, and identification of host binding partners, is currently underway to better address how each effector facilitate bacterial pathogenesis

CHAPTER III

TARGETING OF RHO GTPASES BY CIRA, A T4SS SUBSTRATE OF *COXIELLA BURNETII* ESSENTIAL FOR INTRACELLULAR REPLICATION

Summary

Coxiella burnetii, the etiological agent of acute and chronic Q fever in humans, is an intracellular pathogen that replicates in an acidified parasitophorous vacuole derived from host lysosomes. Central to pathogenesis is a specialized Dot/Icm secretion system that delivers bacterial virulence proteins, termed effector proteins, into the host cell cytosol. Recently we reported the identification of 85 T4SS substrates, 6 of which were toxic to yeast. Of these toxic substrates, Cbu0041 (CirA), was determined to be necessary for intracellular replication and CCV formation. To identify the pathway targeted by CirA, *S. cerevisiae* overexpressing CirA was co-transformed with pYEp13 yeast genomic library. Using this approach we identified Rho GTPases as suppressors of CirA toxicity. In mammalian cell, ectopically expressed CirA localized to the plasma membrane, induced cell rounding, and disrupted the actin cytoskeleton. Phage display analysis identified Rho GTPase activating protein 29 as a potential binding partner of CirA. The finding that a *Coxiella* effector protein targets specific Rho GTPases is consistent with a recent study that demonstrated F-actin and the active forms of both RhoA and Cdc42 are recruited to the CCV and is essential for formation of the characteristically spacious CCV.

Introduction

Coxiella burnetii is a naturally obligate intracellular pathogen that is the causative agent of Q fever in humans. The primary route of infection is through inhalation of contaminated aerosols, which typical results in acute Q fever, a debilitating flu-like illness that is generally self-limiting and readily resolves without antibiotic treatment. However, in rare circumstances persistent infection can lead to chronic Q fever that presents as endocarditis or hepatitis (106). While the number of reported cases of acute Q fever in the United States is relatively low, a marked increase occurred in 1999 when Q fever became a reportable disease and a recent outbreak of Q fever in the Netherlands resulted in over 4,000 confirmed cases with 20% of patients requiring hospitalization (105). The dramatic increase in reported cases suggests *C. burnetii* is an emerging pathogen and highlights our lack of understanding of *C. burnetii* virulence factors.

Inhalation of *C. burnetii* by a mammalian host results in actin-dependent endocytosis and internalization in an early endosome. While numerous intracellular pathogens actively subvert the default endocytic pathway to establish a unique host-derived vacuole, *C. burnetii* generally follows the default trafficking pathway to establish a *Coxiella*-containing vacuole (CCV) derived from the host lysosomal network. Generation of this unique replicative compartment requires active bacterial protein synthesis for homotypic and heterotypic fusions associated with generation of spacious CCV that occupies the majority of the host cytoplasmic space (17, 45, 88).

Central to pathogenesis is a specialized type IVB secretion system (T4SS) that is homologous to the Dot/Icm secretion system of *L. pneumophila*. In *Legionella* this system is composed of 26 *dot*/*icm* (defect in organelle trafficking/intracellular multiplication) genes that together form a pilus-like structure that spans the bacterial inner and outer membrane to deliver bacterial virulence proteins into the host cell cytoplasm. *Coxiella* encodes 23 of these Dot/Icm components. Recent advances including axenic culture (80) and genetic manipulation (7, 8) have confirmed that, like the *Legionella* system, the Dot/Icm system of *C. burnetii* is essential for intracellular replication, CCV formation, effector translocation, and modulation of host apoptosis (6, 18).

To date over a hundred T4SS substrates have been identified in *C. burnetii* using bacterial-two-hybrid (20), bioinformatics (20, 57, 83, 113), plasmid localization (67, 109) and genomic assays (18). Large-scale screening of these substrates has demonstrated that these substrates traffic to distinct subcellular compartments, interfere with crucial host processes, and importantly are less functionally redundant when compared to the *Legionella* model (18, 20, 57, 67, 109, 113). While phenotypes identified using these large scale screens can aid in effector characterization, the function of many of these substrates remains unknown. Three effector proteins CaeA, CaeB, and AnkG, were recently reported to play a role in modulating host survival by interfering with apoptosis (52, 60) whereas a fourth effector, CvpA, was recently shown to engage the clathrin mediated transport pathway (57).

The Rho family of small GTPases is found in all eukaryotic organisms and plays an integral role in actin organization, cell adhesion, vesicle trafficking, and migration (86). These molecules act as molecular switches that cycle between an active GTP-bound form and an inactive GDP-bound form (86, 101). Cycling between these forms is tightly regulated by 3 families of proteins: 1) guanine nucleotide exchange factors (GEFs) active Rho GTPases by displacing Mg^{2+} to promote GDP release and GTP binding, 2) GTPase activating proteins (GAPs) inactivate Rho GTPase by inserting a water molecule into the catalytic pocket to stimulate intrinsic GTPase activity, and 3) guanine nucleotide-dissociation inhibitors (GDIs) control subcellular localization to inhibit interaction with downstream targets (86, 96, 101).

In the current study we demonstrate that the toxicity of CirA is suppressed by overexpression of small Rho GTPases including Rho1, Rho2, Rho4, and Cdc42. Furthermore, overexpression of CirA in mammalian cells resulted in cell rounding, cytoskeleton disruption, and ultimately apoptotic cell death. Phage display analysis revealed that CirA targets Rho GAP 29, suggesting that CirA acts upstream of the Rho GTPase.

Materials and methods

Bacteria and host cell lines: Bacteria and yeast used for this study are listed in Table 3.1. *C. burnetii* Nine Mile phase II (NMII), clone 4 (RSA439) was propagated in ACCM-2 under microaerophilic conditions as previously described (80). When required, 350 µg/ml kanamycin or 5 µg/ml chloramphenicol was added.

Table 3.1 Bacterial and yeast strains used in this study.

Strains	Phenotype or Description	References
C. burnetii		
RSA439	Phase II, Clone 4 (NMII)	(90)
RSA439 MK2	CBU0041::Tn, Cm^r	(113)
RSA439 MK21	*icmX*::Tn, Cm^r	(113)
RSA439 MK22	Intergenic Cbu0179-Cbu0180::Tn, Cm^r	This study
E. coli		
DH5α	*F´(Φ80dΔ(lacZ)M15), recA1, endA1, gyrA96, thi1, hsdR17 (rk-mk+), supE44, relA1, deoR, Δ(lacZYA-argF), U169*	Stratagene
S. cerevisiae		
W303	*MATa ura3-1 leu2-3,112 his3-11,15 trpl-1 ade2-1 cad-100 rad5-535*	(29)

HeLa, Hek293T, and J774A.1 cells were cultured in DMEM with 10% FBS. All cell lines were maintained at 37°C with 5% CO_2.

Complementation of CirA::Tn: The 1169^P-Kan^R cassette was PCR amplified from pMiniTn7-Kan (8) and cloned into pKM244 (113) to generate pKM244-Kan^R. The ORF Cbu0041 (*cirA*) was PCR amplified and cloned into the *SalI/KpnI* of pCMV-DYKDDDDK-C (Clontech) to generate a C-terminal fusion to Flag-tag. The resulting fusion protein was amplified and cloned into the *SalI*/*SphI* site of pKM244-Kan^R to generate pMW-*cirA*.

Axenically cultured RSA439 MK2 (Cbu0041::Tn) (113) was washed twice and re-suspended in distilled water to approximately 10^{10}/ml. Electrocompetent bacteria were mixed with 10 μg pMW-Cbu0041 and electroporated as previously described (80).

After 7 d, individual colonies were expanded in ACCM-2 and screened by Western blotting for expression of the Flag-tagged fusion.

To determine if plasmid complementation of RSA439 MK2 rescued the observed growth defect, HeLa cells where seeded into 24-well glass bottom plates at 10^5/ml. After 24 hr, cells were infected in triplicate with an MOI of 50 with *C. burnetii* (RSA439), RSA439 Ig0179::Tn, RSA439 *icmX*::Tn, RSA439 *cirA*::Tn, or RSA439 *cirA*::Tn pMW-*cirA*. At 7 d post-infection, cells were fixed with 4% formaldehyde for 10min and nuclei were visualized with 1X Hoechst.

Immunofluorescence: To assess localization of CirA, HeLa cells where seeded in triplicate into 24-well glass bottom plates at 10^5/ml. Cells were transfected with Lipofectamine following the manufactures instructions. Twenty-four hr post-transfection, cells were fixed with 4% formaldehyde for 10 min, permeabilized with 0.1% triton-X 100 for 5 min, and nuclei were visualized with 1X Hoechst. To assess co-localization with RhoA and Cdc42, cells were co-transfected and stained with anti-myc antibodies (Thermo) and Alexa Fluor® 555 secondary antibodies (Cell Signaling). Actin was visualized using Alexa Fluor® 555 or Alexa Fluor® 647 conjugated Phalloidin (Life Technologies). Fluorescence images were acquired with a Nikon-A1 microscope using the 60X oil immersion object and images were processed using NIS-Elements Software. Results were tabulated from triplicate wells with at least 50 transfected cells per experiment. Similar results were obtained from at least 3 independent experiments.

Yeast suppressor screen to identify host proteins capable of suppressing CirA toxicity: *CirA* was introduced into pYesNTA2 as *BamHI/SalI* fragments and

toxicity was assessed by serially diluting and spotting on uracil dropout media containing galactose as the carbon source (113, Table 3.2). The pYEp13 genomic library (ATCC no. 37323) was introduced into *S. cerevisiae* W303 (pGal::*cirA*) and the resulting transformants were plated on uracil leucine dropout media containing galactose as previously described (100). From a transformation yielding 2.0 X 10^6 transformants, 53 potential suppressors were isolated. To verify suppression, plasmids were isolated, and retransformed into *S. cerevisiae* W303 (pGal::*cirA*). Of these, 11 (pSup1-pSup11) consistently suppressed the toxicity of CirA. Suppressor plasmids were sequenced using pYEp13 seq F (ACTACGCGATCATGGCGA) and pYEp13 seq R (TGATGCCGGCCACGATGC) and results were analyzed using the yeast genome database (http://yeastgenome.org).

Individual ORFs from the plasmids that consistently suppressed toxicity (pSup1-pSup7) or members of the Rho GTPase family (Rho1-5, Cdc42) were introduced into p415ADH (73) as *BamHI/SalI* or *PstI/SmaI* fragments. Individual plasmids were transformed into W303 (pGal::*cirA*) and the resulting transformants were serially diluted and spotted on uracil leucine dropout media.

Table 3.2 Plasmids used in the study.

Plasmid	Description	References or Source
pKM225	pMW1650, *com1*p-Tn*A7*, *groES*p-mCherry, *com1*p-cat, Cm^R	Mertens et al. (Manuscript In Prep)
pKM244	pJB908a, *groES*p-mCherry, *com1*p-cat, Cm^R, Amp^R	Mertens et al. (Manuscript In Prep)
pKM244Kan	pJB908a, *groES*p-mCherry, *com1*p-cat, Cm^R, Amp^R, p1169-Kan^R	This study
pMW-CirA	pKM244Kan-CirA	This study
Ectopic expression plasmids		
pEGFP-C1	C-terminal fusion to EGFP, kan^r	Clontech
pEGFP-CirA	pEGFP-C1::Cbu0041	(20)
pRK5-myc-RhoA WT	pRK5-myc::RhoA, $carb^r$	Addgene 12962
pRK5-myc-RhoA CA	pRK5-myc::RhoA Q63L, $carb^r$	Addgene 12964
pRK5-myc-RhoA DN	pRK5-myc::RhoA T19N, $carb^r$	Addgene 12963
pRK5-myc-Cdc42 WT	pRK5-myc::Cdc42, $carb^r$	Addgene 12972
Yeast toxicity plasmids		
p415ADH	pGal, $carb^R$, Leu2	(73)
P415ADH-Rho1	P415ADH::*rho1*	This study
P415ADH-MRP2	P415ADH::*mrp2*	This study
P415ADH-Met16	P415ADH::*met16*	This study
P415ADH-Nut2	P415ADH::*nut2*	This study
P415ADH-Jip5	P415ADH::*jip5*	This study
P415ADH-Rho2	P415ADH::*rho2*	This study
P415ADH-Rho3	P415ADH::*rho3*	This study
P415ADH-Rho4	P415ADH::*rho4*	This study
P415ADH-Rho5	P415ADH::*rho5*	This study
P415ADH-Cdc42	P415ADH::*cdc42*	This study
pYESNTA	pGal, $Carb^R$, Ura	(113)
pYESNTA-CirA	pYESNTA::CirA	(113)

Phage display: To identify the mammalian target of CirA, we employed a modified pull-down phage display. Hek293 cells were transfected using Lipofectamine with EGFP-CirA or EGFP alone per the guidelines outlined by the manufacture. Twenty-four hr post-transfection, cells were lysed with lysis buffer (50 mM Tris HCl, pH 7.4, 150 mM NaCl, 1 mM EDTA, and 1% TRITON X-100) and incubated at 4°C overnight with protein G magnetic beads (Invitrogen). Immunoprecipitation (IP) reactions were washed and blocked with 3% BSA. A 8mer cyclic phage library was incubated with EGFP alone and following 1 hr incubation, the pre-cleared library was incubated with the CirA IP. Two hr post-inoculation the beads were washed with 0.01% Tween in PBS, eluted using 10 mM glycine pH3.1, and the eluent was used to infect an *E. coli* K91 culture. Twenty-four hr post-inoculation, the phage was purified from the *E. coli* K91 culture using NaCl/PEG precipitation. The purified phage was used to re-pan IPs for a total of 3 rounds. During RII and RIII, 50 plaques were picked, PCR amplified, and sequenced. Results were tabulated by calculating enrichment between RII and RIII.

Phagocytosis assay: To rule out differences in uptake between the strains, bacteria were stained with CFSE following the manufactures guidelines (Life Technologies). Bacteria were enumerated as previously described (113) and an MOI of 1 was used to infect J774A.1 macrophages seeded at 10^5/ml in glass bottom 24-well dishes. Four hr post-infection, cells were washed 3 times with PBS and extracellular fluorescence was quenched using trypan blue. Cells were counted using a Nikon-A1 microscope using the 60X oil immersion objective lens. At least 200 cells were counted per well with at least 3 wells per experiment. Similar results were obtained from at least

3 independent experiments. Percent infection was tabulated by counting the number of infected cells compared with the total number of cells.

Results

CirA is necessary for intracellular replication and CCV formation: We previously reported the identification of over 80 T4SS substrates, 10 of which exhibited a growth defect in cell culture (113). Co-infection with wild-type bacteria rescued the growth defect for 5 of these Tn mutants, suggesting the observed growth defect is due to the loss of an individual effector protein. Plasmid complementation of *cirA*::Tn mutant rescued intracellular replication and CCV formation (Fig. 3.1). These results indicate that CirA is a T4SS effector that is essential for intracellular replication and CCV formation.

Overexpression of the small GTPases Rho1 and Cdc42 suppress the toxicity CirA: To identify the host proteins targeted by CirA, we conducted a yeast suppressor screen to identify proteins that, when overexpressed, were capable of suppressing CirA toxicity. *S. cerevisiae*, expressing CirA from a galactose inducible promoter, was transformed with the pYEp13 yeast genomic library. From a transformation yielding 2.0 X 10^6 transformants, 53 colonies were isolated, 11 of which consistently suppressed the toxicity of CirA (Fig. 3.2A). Sequencing of each pSup revealed that over half of these clones contained identical plasmids (pSup1-pSup7), each encoding 5 full yeast *orfs* and a truncated *mms1* (Fig. 3.2B). Individual expression of each full-length *orf* found in pSup1-7 revealed that only the small GTPase Rho1 was capable of suppressing CirA, suggesting Rho1 is the cellular target of CirA (Fig. 3.2C).

Figure 3.1 Plasmid complementation of *cirA*::Tn rescues both intracellular replication and CCV formation. (A) Confocal images of HeLa cells infected at an MOI of 50 with an intergenic Tn mutant (Ig0179-0180), *cirA*::Tn, and complemented *cirA*::Tn pMW-CirA for 7 d. Images were captured with a Nikon A1 confocal microscope, with a least 100 infected cells observed per experiment.

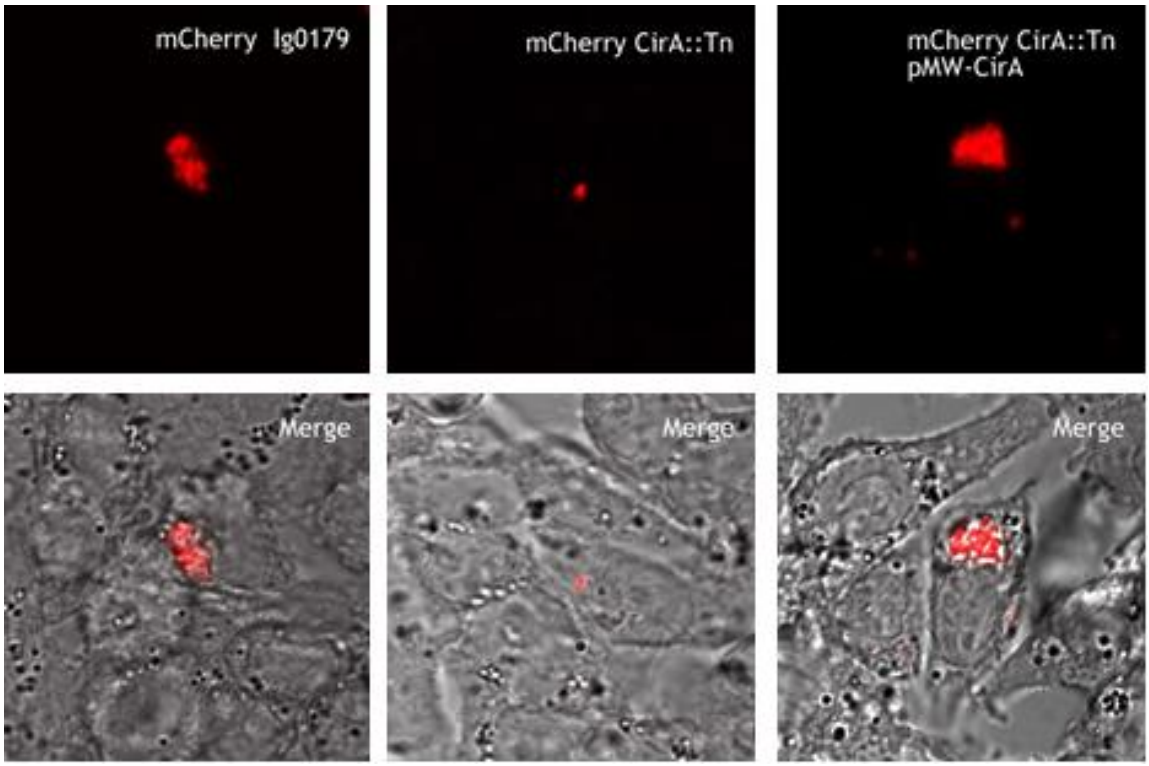

Figure 3.2 Overexpression of the small GTPases suppress the toxicity of CirA. (A) *S. cerevisiae* W303, overexpressing CirA from a galactose-inducible promoter, was transformed with the yeast genomic library pYEp13. Eleven clones (pSup1-pSup11) were isolated that consistently suppressed the toxicity of CirA. (B) Sequencing of the suppressor plasmids revealed that 7 of these plasmids (pSup1-pSup7) were identical and predicted to contain 5 full-length yeast *orfs* and a truncated *mms1*. (C) Each *orf* from pSup1 were PCR amplified and cloned into p415-ADH and the resulting constructs were transformed into CirA expressing yeast. Only expression of Rho1 was capable of suppressing CirA toxicity. (D) To determine if suppression is specific to Rho1, each Rho GTPase from *S. cerevisiae* was independently expressed in CirA harboring yeast. Only the GTPases Rho1, 2, 4, and Cdc42 were able to suppress CirA toxicity.

A.

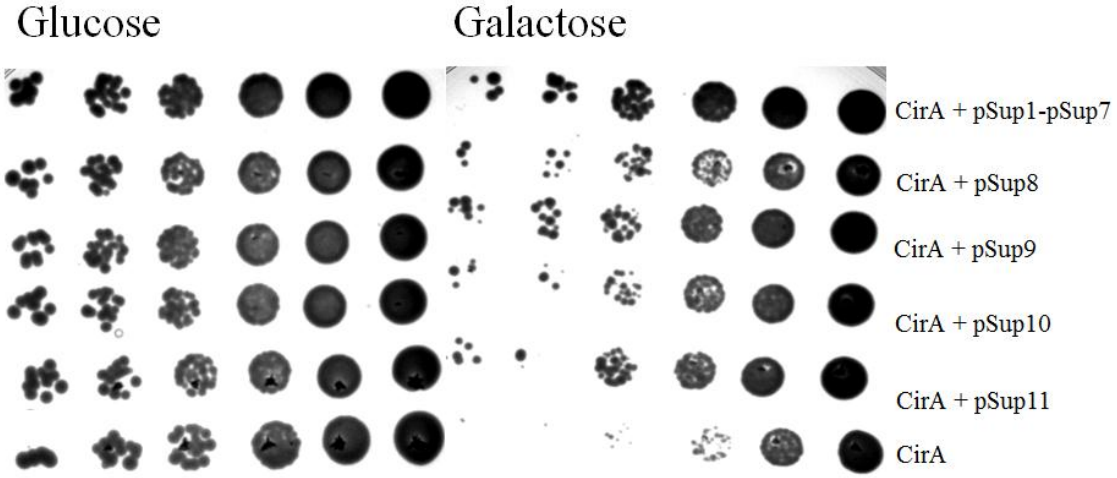

Figure 3.2 Continued

B.

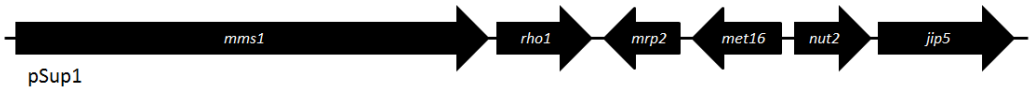

C.

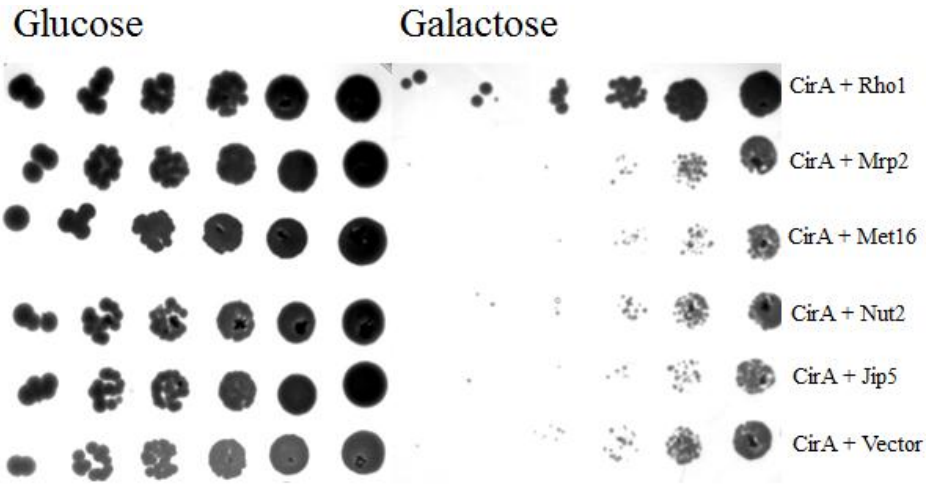

D.

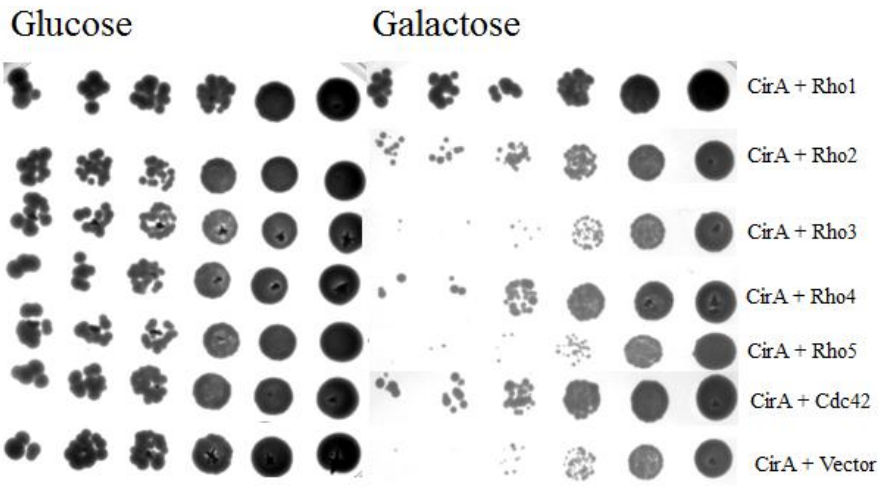

While the majority of the isolated suppressor plasmids contained Rho1, 1 plasmid (pSup8), contained the Rho GTPase Cdc42. The finding that another suppressor plasmid contained alternate Rho GTPase capable of suppressing CirA toxicity suggested CirA might target multiple members of the Rho GTPase family. *S. cerevisiae* encodes 6 Rho GTPases (Rho1-5 and Cdc42) of which only Rho1 and Cdc42 are essential. To determine if CirA targets multiple Rho GTPases, we independently expressed each Rho GTPase in the CirA expressing yeast. Expression of only Rho1, Rho2, Rho4, or Cdc42 was able to suppress the toxicity of this effector protein (Fig. 3.2D).

CirA co-localizes with F-actin and the small GTPases RhoA and Cdc42: Suppression of CirA toxicity by members of the Rho family of GTPases suggest that these are the cellular targets of CirA. Mammals encode 22 Rho GTPases, of which RhoA, Cdc42, and Rac1 are the most widely studied (86). To identify subcellular localization in mammalian cells, CirA was expressed as a C-terminal fusion to EGFP and the resulting construct was used to transiently transfect HeLa cells. EGFP-CirA predominately localized to the plasma membrane (Fig. 3.3A). To better assess the localization of CirA, cells were co-transfected with either myc-RhoA (mammalian homologue to Rho1) or myc-Cdc42 and F-actin was visualized by phalloidin staining. CirA co-localized with both F-actin (Fig. 3.3B) and the Rho GTPases RhoA (Fig. 3.3C) and Cdc42 (Fig. 3.3D). No co-localization was noted between EGFP alone and F-actin or Rho GTPases RhoA and Cdc42 (Fig. 3.3B-D).

Figure 3.3 Ectopically expressed EGFP-CirA localizes to the plasma membrane and co-localizes with F-actin and Rho GTPase RhoA and Cdc42. (A) CirA was expressed as a C-terminal fusion to EGFP and used to transiently transfect HeLa cells. (B) Representative micrographs of HeLa cells transfected with EGFP-CirA (green) and immunostained with Alexa Fluor 555 Phalloidin or co-transfected with myc-tagged RhoA or Cdc42 (red). White boxes denote the area used for insets.

A.

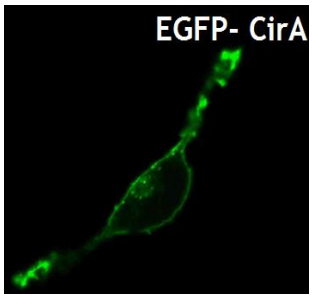

B.

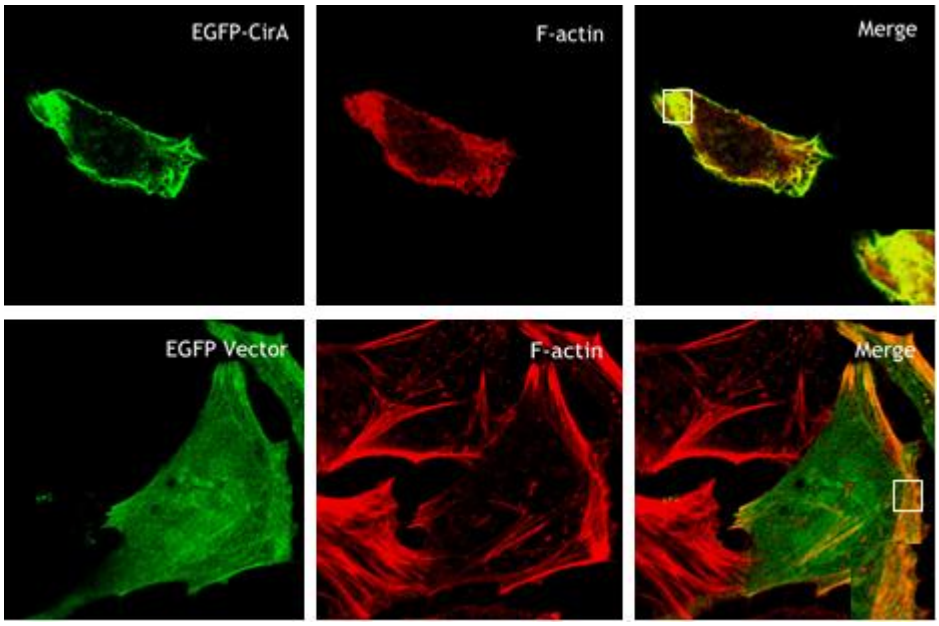

Figure 3.3 Continued

C.

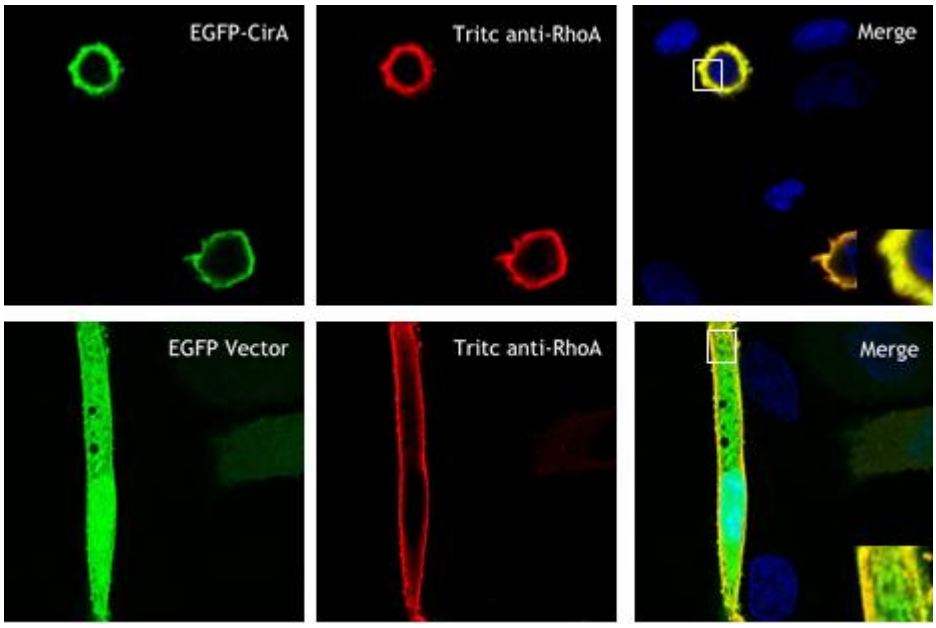

D.

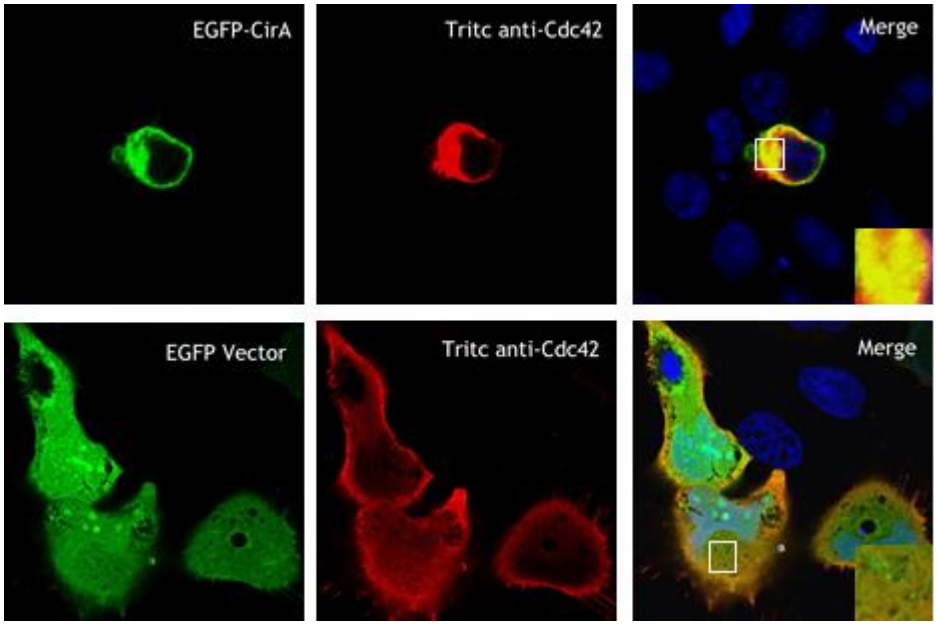

Overexpression of CirA leads to cell rounding and disruption of the actin cytoskeleton: To better explore the impact of CirA on the mammalian host cytoskeleton, cells were transfected and scored for phenotypes associated with perturbation of the actin cytoskeleton. Overexpression of CirA in HeLa cells (Fig. 3.4A) and Hek293 cells (data not shown) resulted in cell rounding and detachment from the culture dish. By 24 hr post-transfection, 86% of CirA expressing cells were rounded and detached, whereas only 8% of cells transfected with the negative control, EGFP alone, were rounded by this timepoint. Phalloidin staining revealed that cells transfected with CirA possessed reduced stress fibers whereas cells transfected with EGFP alone exhibited robust stress fibers (Fig. 3.3B and 3.4B). Only 24% of CirA transfected cells possessed stress fibers whereas 85% of cells transfected with the negative control exhibited normal stress fiber formation. Collectively these results suggest that overexpression of CirA perturbs the actin cytoskeleton of the host cell.

Phage display identified RhoGAP 29 as the mammalian target of CirA: The use of a yeast suppressor screen successfully identified a pathway targeted by CirA, however we have been unable to successfully detect an interaction between CirA and RhoA (mammalian homology of Rho1) or Cdc42 using co-immunoprecipitation reactions. This suggests that it may directly interact with another protein in the Rho pathway that regulates stress fiber formation To address this hypothesis, we used a modified phage display procedure (5). Following RII and RIII of panning, we sequenced 50 plaques and compared enrichment between rounds. Following RIII, 73% of the plaques contained the peptide consensus RRNDLGTE compared to 42% following RII.

Figure 3.4 Overexpression of CirA leads to cell rounding and disruption of the actin cytoskeleton. (A) Cells overexpressing EGFP-CirA or EGFP alone were scored for rounding at 24 hr post-transfection. (B) Stress fibers were visualized by staining with Alexa Fluor 555 phalloidin. (A, B) Rounding and stress fiber disruption was determined by counting at least 50 transfected cells from triplicate wells. Data are representative of at least 3 independent experiments. Statistical analysis were tabulated using t-test and generated a statistically difference of $P<0.0005$.

A.

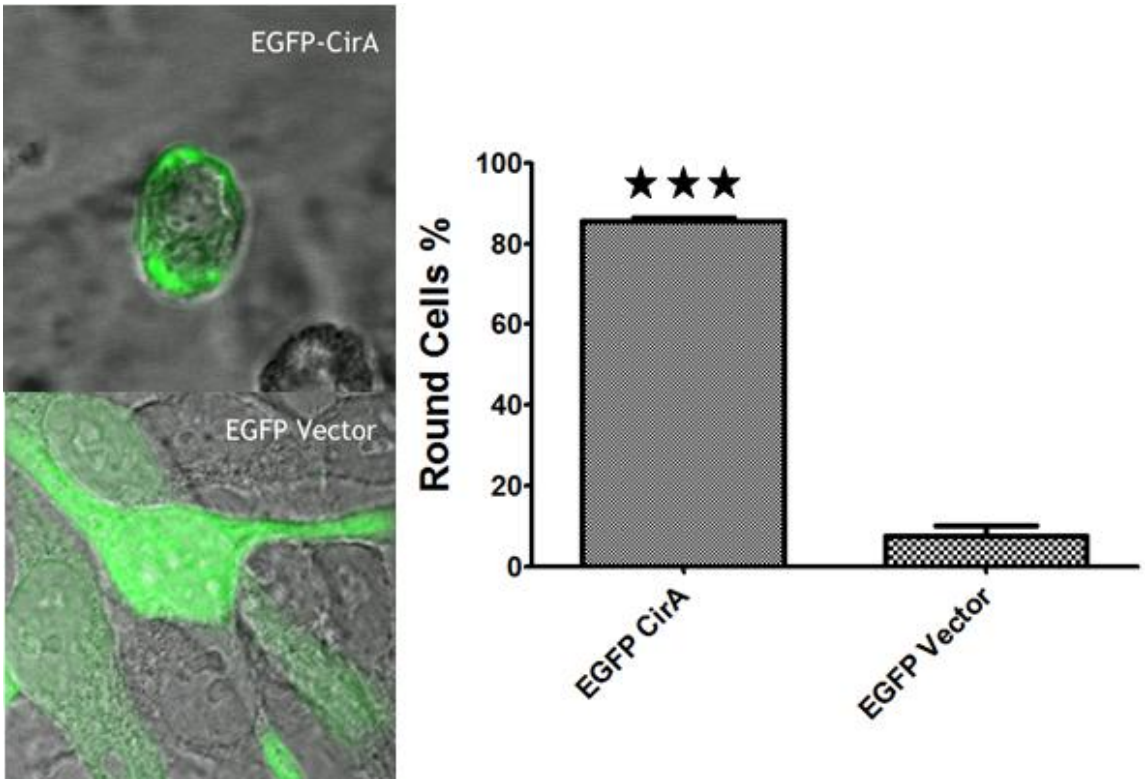

Figure 3.4 Continued

B.

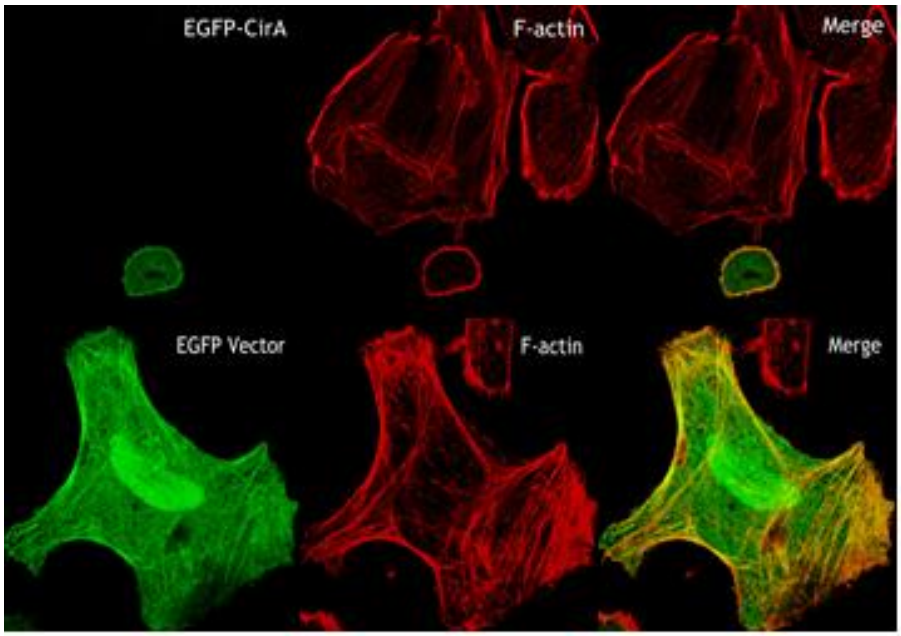

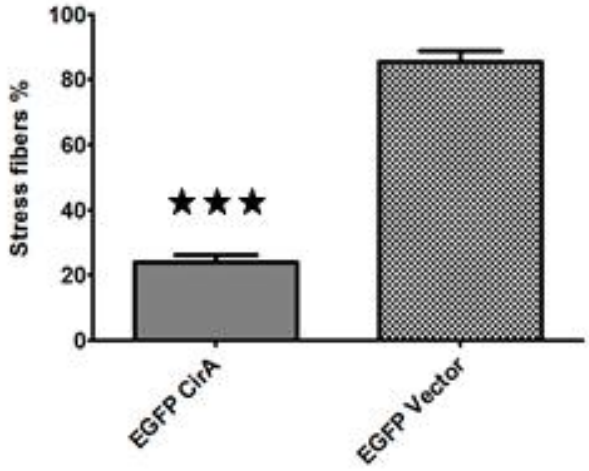

No other sequences were enriched between RII and RIII. BLAST analysis identified Rho GTPase activating protein 29 (RhoGAP 29), also known as PTPL1-associated RhoGAP protein 1 (PARG1), as a potential target. These results suggest the mammalian binding partner of CirA maybe Rho GAP 29.

CirA is dispensable for bacterial uptake: Several pathogenic bacteria secrete effector proteins that modulate phagocytic uptake (11, 27, 70). However, a recent study by Newton et al. (78) suggested the T4SS of *C. burnetii* is not active until at least 8 hr post-infection and requires CCV acidification and endocytic maturation, which precludes CirA from being involved in bacterial uptake. To validate this hypothesis, we compared uptake of CFSE labelled bacteria by J774Al.1 macrophages. No difference in uptake was noted between the strains (Fig. 3.5). These results indicate that CirA does not engage Rho GTPases to modulate bacterial uptake.

Discussion

CirA is a T4SS effector that was previously demonstrated to be essential for intracellular replication and CCV formation (113). This effector lacks conserved domains and is not homologous to other known proteins; however it is highly conserved among *C. burnetii* pathotypes, suggesting it may be important for pathogenesis. In the current study we employed a yeast suppressor screen to identify the cellular pathway targeted by this effector. Using this approach we identified Rho GTPases as suppressors of CirA toxicity.

Figure 3.5 CirA is not involved in bacterial uptake. J774A.1 macrophages were infected with an MOI of 1 with CFSE labeled bacteria. No difference in uptake was noted between the strains. Data are representative of 3 independent experiments with at least 600 cells from triplicate samples.

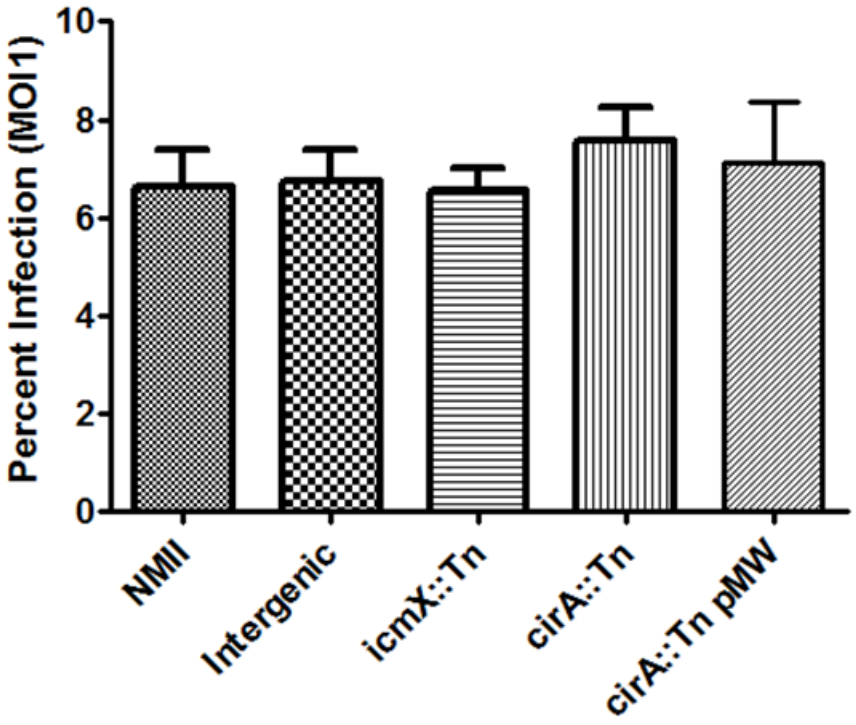

Saccharomyces cerevisiae has emerged as a popular model to characterize bacterial virulence factors due to the conservation of many pathways between yeast and mammals, genetic tractability, and ease of use (104). Heterologous expression of bacterial effector proteins in yeast has been exploited in numerous studies to identify effectors that impair crucial host processes (4, 18, 100, 113, 114). In an attempt to understand the function of these toxic effectors, yeast genetic screens have been employed to identify host proteins that when overexpressed, suppress the toxicity of the effector protein (35, 100, 108). Principally the lethality associated with *L. pneumophila* AnkX was overcome by overexpression of components involved in membrane trafficking and allowed the investigators to determine that it modifies Rab1 by phosphorylcholination (100). This screening tool has since been extended to characterize two other effectors: LecE, an effector that manipulates phospholipid biosynthesis (108), and Ceg14, an effector that inhibits actin polymerization (35).

Based on its successful use to characterize 3 *Legionella* effectors, we employed this screening tool to identify the host pathway targeted by CirA. Using this approach we demonstrated that the toxicity of CirA could be suppressed by overexpression of members of the Rho GTPase family, suggesting this is the pathway targeted by CirA. Rho GTPases are targeted by many bacterial effector proteins including *Yersinia pseudotuberculosis* YopE (11), *Salmonella typhimurium* SopE (30), *Vibrio cholerae* RTX toxin (93), and *Escherichia coli* EspH (27) indicating this is a conserved mechanism among many bacterial pathogens (58). Regulation of Rho activity by bacterial effector proteins have been shown to employ 1 of 3 methods (58): 1) Effectors

such as YopE, EspM2, and YopO control localization and activation indirectly by mimicking Rho GAPs, GEFs, or GDIs, respectively (3, 11). 2) Regulation can be directly through post-translational modification's including ADP-ribosylation (19), adenylation (74), deamidation (59), and glucosylation (102). 3) Lastly, effectors can target upstream regulators such as EspH that targets a PH-DH RhoGEF (27) or *Pasteurella multocida* toxin (PMT) that target heterotrimeric G-proteins (82). Bioinformatic analysis of CirA did not detect any GAP or GEF domains and it does not share homology with bacterial or mammalian GAPs or GEFs. Furthermore co-immunoprecipitation using RhoA or Cdc42 was unsuccessful in verifying an interaction with CirA. Together these results suggest that CirA does not regulate Rho GTPases indirectly by mimicking GAPs or GEFs, but instead could post-translationally modify the GTPase or act upstream.

To determine if CirA binds any proteins directly in a mammalian system, we used phage display as an alternative approach to characterize protein-protein interactions. Using this approach we identified RhoGAP 29 as a potential binding partner for CirA. RhoGAP 29, also known as PARG1, is a GTPase activator that has strong activity toward RhoA and weaker activity toward Cdc42 and Rac1 (75, 91). It acts in concert with RASIP1 to dampen Rho-associated protein kinase (ROCK) signaling. Overexpression of RhoGAP29 in NIH3T3 fibroblast leads to cell rounding, detachment, and reduced stress fiber formation (75), a phenotype comparable to cells overexpressing CirA. This finding suggests that the disruption of the cytoskeleton observed in cells overexpressing CirA, could be due to direct modulation of RhoGAP 29

that in turn dampens ROCK signaling through Rho GTPase activation, which ultimately resulting in reduced stress fiber formation. Currently we are testing the interaction between RhoGAP29 and CirA using co-immunoprecipitation and are also in the process of identifying a potential domain required for this interaction.

Many pathogenic bacteria target cytoskeletal components including actin, intermediate filaments, and microtubules to modulate invasion, establish a replicative niche, facilitate cell-to-cell spread through actin based motility, and disseminate (38). Specifically, several pathogens secrete T3S effectors that target Rho GTPases to modulate uptake. *Salmonella* releases at least 4 effector proteins to modulate actin rearrangements through Rho GTPases: SopE and SopE2 directly activate by mimicking Rho GEFs (42, 98), whereas SopB indirectly activates Rho GTPases through inositol phosphatase (103). Following actin polymerization, SptP down-regulates cytoskeletal rearrangements induced by other T3S effectors by acting as a Rac1 and Cdc42 GAP. This tightly balanced cycle acts to rebuild the cytoskeleton following invasion (30). In contrast to the model exemplified by *Salmonella, Yersina* secretes an array of antiphagocytic T3S effectors that disrupts the cytoskeleton to block uptake, most notable is YopE which targets RhoA, Rac1, and Cdc42 by mimicking Rho GAPs (11). While targeting of Rho GTPase to modulate uptake is a common theme among secreted effectors, it is unlikely to be the reason *C. burnetii* CirA targets this pathway. Similarly, it is that CirA co-opts cytoskeletal components for actin based motility to do its vacuolar localization and no defect in dissemination was noted for this mutant, suggesting CirA is not necessary for release from the host cell. Instead we propose that CirA is secreted by

the T4SS system after uptake, where it indirectly modulates RhoGTPases by engaging RhoGAP29 to regulate the size of the CCV (Fig. 3.6).

Figure 3.6 CirA's interaction with RhoGAPs is necessary to promote the formation of a spacious CCV. In the current study we demonstrate that CirA is a T4SS that is necessary for intracellular replication and for formation of the characteristically spacious CCV. Following endocytic maturation, CirA is secreted and interacts with RhoGAPs 29 and 33.

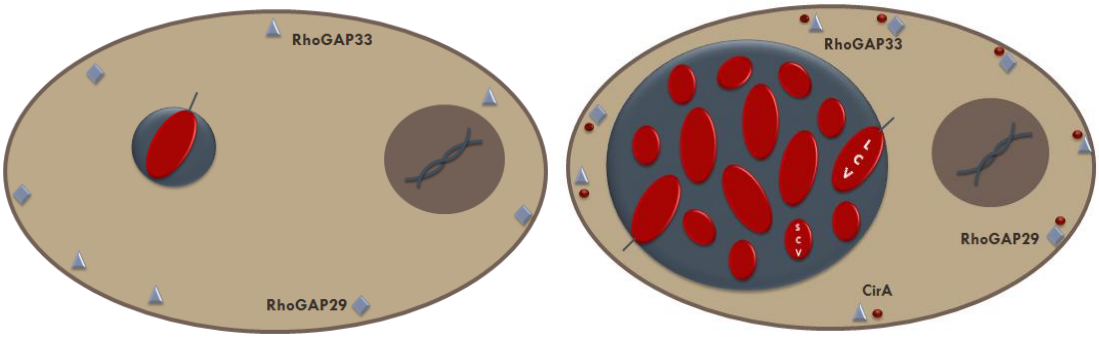

CHAPTER IV

CONCLUSIONS

Like many intracellular pathogens, *Coxiella burnetii* encodes a specialized secretion system that translocates numerous effector proteins into the host cell cytoplasm. In the current study, we used an enhanced bioinformatics screen to identify candidate substrates, which resulted in the identification of 85 novel secretion substrates (20, 113). Preliminary characterization of these substrates using large scale screens revealed these substrates traffic to distinct subcellular compartments; interfere with crucial host cell processes, and play an integral role in intracellular replication and CCV formation.

Many intracellular pathogens secrete effector proteins that traffic to the nucleus where they modify chromatin and modulate the transcriptional response. Post-translational modification of histones by SET domain containing methyltranferases *L. pneumophila* RomA and *C. trachomatis* Nue has been shown to play an crucial role in modulating the inflammatory response by direct histone methylation (85, 87). *H. pylori* also affects histone modifications by decreasing histone phosphorylation and acetylation in a *cag*PAI-dependent mechanism (26). AnkA, a secreted effector from *Anaplasma phagocytophilum*, binds to the *CYBB* promoter resulting in decreased H3 acetylation and *CYBB* expression, which ultimately leads to decreased oxidative burst (31, 32, 84). Expression of *C. burnetii* secretion substrates as C-terminal fusions to EGFP identified six substrates that traffic to the nucleus (20, 113). Bioinformatic analysis of these substrates revealed the presence of a nuclear localization signal (NLS), as evident by

arginine and lysine enrichment, in five of the secretion substrates (Cbu0388, Cbu1314, Cbu1524, Cbu0393, and Cbu0794). The finding that these substrates possess an NLS suggests that these substrates have the necessary information to enter the nucleus and likely function in the nucleus in *C. burnetii* infected cells (Fig. 4.1). Further analysis of these nuclear substrates revealed two substrates, Cbu1314 and Cbu0388, encode DNA binding domains. Furthermore, Cbu0388 possesses a C(X)5R motif, suggesting it maybe a phosphatase. The fact that many intracellular pathogens secrete effectors that modify histones coupled with ectopic localization, the presence of an NLS, DNA binding domain, and phosphatase domain suggests this effector may dephosphorylate histones. Current study is underway to determine if either Cbu1314 or Cbu0388 associate with host chromatin using ChIP-seq.

Infection of a host cell by *C. burnetii* leads to the formation of a spacious vacuole that surprisingly doesn't affect host viability, suggesting *C. burnetii* actively promotes host cell viability by the secretion of anti-apoptotic effectors. In a screen to identify anti-apoptotic proteins, three T4SS effectors; AnkG, CaeA, and CaeB were shown to block staurosporin apoptosis. AnkG inhibits apoptosis by binding pro-apoptotic gC1qR (p32) (60). CaeB was also found to inhibit the intrinsic apoptosis at the mitochondrial level in a pathway that does not require binding to p32, whereas the mechanism of CaeA inhibition of apoptosis is less clear (52). Ectopic expression and bioinformatics analysis of CaeA suggest it localizes to the nucleus (18, 20, 52, 113). It will be interesting to determine if modulation of apoptosis by this effector involves up-regulation of anti-apoptotic or down-regulation of pro-apoptotic factors caused by histone modifications.

While promoting host cell viability is of paramount importance to pathogen survival, the fusogenicity of the CCV is also critical for an effective infection. The use of a variety of inhibitors and overexpression constructs have demonstrated that the *C. burnetii* CCV interacts with vesicular pathways including endocytic (Rab5, Rab7), autophagic (LC3), and secretory (Rab1) (17, 36, 88, 107). Fusogenicity with these compartments is mediated by recruitment of *N*- ethylmaleimide-sensitive factor attachment protein receptors (SNARE) and importantly depletion of either Vamp7 and syntaxin-17 results in aberrant vacuole formation (16, 68). While interactions with many of these compartments require active protein synthesis and suggest these interactions could be mediated by secreted effector proteins, the identity of these effector proteins remains largely unknown. Recently the characterization of one effector, CvpA, demonstrated that this effector co-ops clathrin transport mechanisms in order to acquire endolysosomal membrane. Deletion of *cvpA* or inhibition of clathrin or AP2 lead to decreased intracellular replication and CCV formation, highlighting the importance of this pathway in normal development.

In the current study we identified and preliminarily characterized a T4SS effector, CirA, that when overexpressed, resulted in cell rounding, cell detachment, and disruption of the actin cytoskeleton through indirect modulation of Rho GTPases. Unlike other bacterial effector proteins that target Rho GTPases to modulate uptake, CirA is unique in that it is dispensable for uptake. Our results suggest that CirA may be involved in regulating size and formation of the spacious CCV as both F-actin and Rho GTPases are recruited to the CCV and are crucial for normal development (1). Studies have

shown that F-actin assembles on phagosomes, which serves as "tracks" on which lysosomes or late endosomes can progress to facilitate fusions with phagosomes (1, 50). This suggests that recruitment of both F-actin and Rho GTPases may facilitate heterotypic fusions with endosomes and lysosomes as well as homotypic fusions with other small CCVs and serve as a method for delivering membrane to the growing vacuole (1).

In addition to a crucial role for Rho GTPases in vacuole development, it is likely that other GTPases from the Ras superfamily could play an important role in facilitating interactions with other cellular compartments. This is exemplified by *L. pneumophila* which is a master manipulator of Rab function. Rab1, a GTPase that regulates protein transport from the endoplasmic reticulum to the golgi, is recruited to the *Legionella*-containing vacuole (LCV) by the Rab GEF DrrA/SidM (74). After two hours, Rab1 begins to dissociate from the LCV due to inactivation by the Rab GAP LepB (49). Rab1 activity is also tightly regulated by AMPylation by DrrA (72) and phosphocholination by AnkX (100). Post-translational modification of DrrA by these two effectors inhibits the activity of LepB and enhances accumulation on the LCV (41). These post-translational modifications are reversed by SidD that deadenylylates Rab1 (100) and Lem3 that is a dephosphocholinase (100). While *Coxiella* and *Legionella* replicate in distinct intracellular compartments, Rab1 is recruited to the CCV in a process dependent on active protein synthesis, suggesting an effector mediated event and is likely that it encodes effectors similar to those found in *Legionella* for Rab1 manipulation (17)

Ubiquitination is a reversible post-translational modification that is involved in protein degradation, signal transduction, host defense, and membrane trafficking (22). While bacteria do not encode ubiquitin (97), numerous bacteria pathogens including *Listeria monocytogenes*, *Salmonella typhimurium, Yersinia sp,* and *Legionella pneumophila* have evolved sophisticated mechanisms for subverting host ubiquitin for their own benefit. *Coxiella burnetii* encodes three T4SS substrates (Cbu1217, Cbu0814, and CbuA0014) with F-boxes, a eukaryotic domain that serves as a scaffold for the formation of a functional Skp-Cullin-F-box E3 ubiquitin ligase complex (28). Two *Legionella* F-box containing effectors, LegU1 and LegAU13, direct the ubiquitination of the host protein BAT3, which may reduce the ER stress response and inhibit apoptosis (28). Bacteria also use ubiquitination to modulate the host innate immune system. *Yersina* spp. employ the de-ubiquitination effectors YopJ/P to de-ubiquination of TRAF6. In contrast to targeting host proteins, the host ubiquitination pathway can be employed to regulate the activity of its own effectors. Ubiquitination of SopB serves to control the subcellular localization of this effector, in that prior to ubiquitination, SopB localizes to the plasma membrane, but then it is quickly mono-ubiquitinated causing it to associate with the *Salmonella* containing vacuole (SCV). Once associated with the SCV, SopB directs remodeling of the phagosome by recruiting high levels of phosphatidylinositol-3-phosphate (PI(3)P), which subverts the normal phagosome trafficking and inhibits lysosome fusion and acidification (22). LubX, a functional E3 ligase of *L. pneumophia*, regulates the activity of another *Legionella* T4SS effector, SidH, by ubquitinating it, thus targeting it for proteosomal degradation (55).

Autophagy plays an integral role in maintaining the quality of cellular components by delivering cytoplasmic proteins or damaged organelles to the lysosomes for degradation. Many pathogenic bacteria have evolved sophisticated mechanisms for inhibiting autophagic initiation, avoiding autophagic capture, suppressing maturation of the autolysosome, or for utilizing host autophagy (24). While it was originally believed that autophagy was detrimental to intracellular pathogens, it is now known that autophagic activation benefits some bacterial pathogens including *C. burnetii*, *L. pneumophila*, *A. phagocytophilum* and *Brucella abortus* by serving as a nutrient source, providing a replication niche that protects them from the endolysosomal pathway or by direct use of autophagic machinery (25). Within minutes of uptake, the CCV is decorated with LC3, indicating an interaction with the autophagic pathway (88, 107). The CCV also recruits Beclin1, which when overexpressed, delays the arrival of the lysosome, enhances bacterial replication and increases the number of infected cells. (107). Beclin1 has a BH3 domain that interacts with anti-apoptotic proteins such as Bcl-2 (24). Interaction between these two proteins and subsequent recruitment to the PV is intriguing given that interaction between Bcl-2 and Beclin1 has been demonstrated to dampen autophagy. Thus, co-recruitment of both may be a pathogenic mechanism to prevent excess autophagy that could lead to autophagic cell death (24, 25). LC3 recruitment to the PV occurs within minutes of uptake, so it is unlikely that the initial engagement of the autophagy pathway is dependent on a T4SS effector. However, a recent study by Voth et al. (109) identified a T4SS substrate, CpeB, that when

ectopically expressed co-localizes with LC3, which suggest that the T4SS does play a role in autophagy, possibly at later time points of infection cycle.

Host pathogen interactions are very complex, intricate proceses that require modulation and manipulation of numerous pathways. Many pathogens have evolved sophisticated methods for facilitating subversion; principle among them is secretion of effector proteins. To date over 100 secreted substrates of *C. burnetii* T4SS have been identified, representing approximately 5% of its proteome. As the field continues to advance and more genetic tools are developed, understanding the role of these proteins in pathogenesis will be of paramount importance.

Figure 4.1 Role of *C. burnetii* T4SS substrates in intracellular infection. Through a bacterial two-hybrid, bioinformatics, and genomic screens, over 100 *C. burnetii* T4SS substrates have been identified. Large-scale screens have identified 6 substrates (Cbu1314, Cbu0388, Cbu0129, Cbu1524, Cbu0794, and Cbu0393) that traffic to the nucleus and may play a role in transcriptional modulation. One effector, CvpA, was recently shown to associate with host clathrin and may serve as a source of membrane for the growing CCV. An additional effector, CirA, localizes to the plasma membrane and reduces stress fiber formation when overexpressed, possibly by interacting with RhoGAP 33. Three effectors (AnkG, CaeA, and CaeB) are capable of blocking exogenously stimulated apoptosis. An additional 3 effectors (CbuA0014, Cbu1217, and Cbu0814) possess an F-box motif and may mediate proteasomal degradation of host proteins. A plasmid encoded effector, CpeB, co-localizes with the autophagosomal marker LC3.

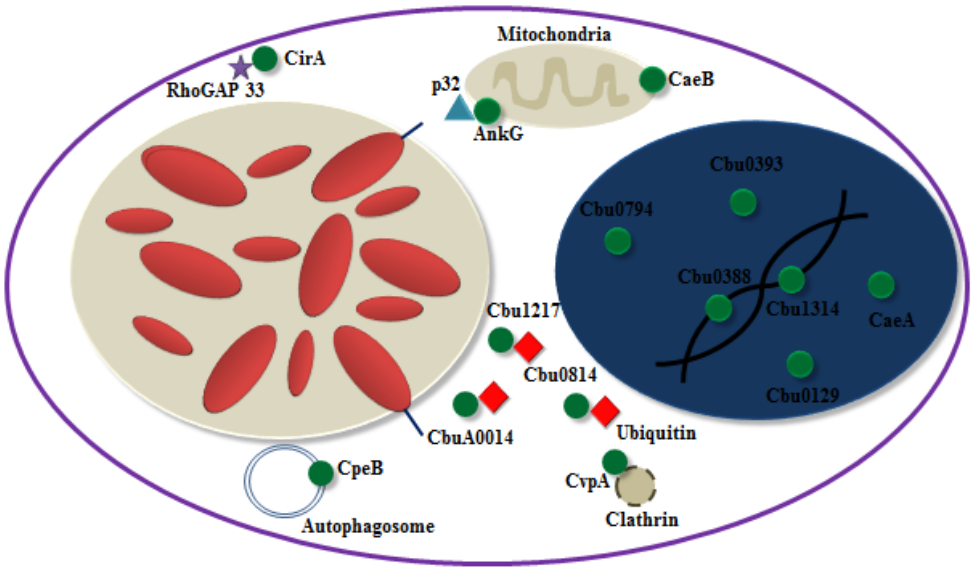

REFERENCES

1. **Aguilera M, Salinas R, Rosales E, Carminati S, Colombo MI, Berón W**. 2009. Actin dynamics and Rho GTPases regulate the size and formation of parasitophorous vacuoles containing *Coxiella burnetii*. Infect. Immun. **77**:4609–20.

2. **Al-Khodor S, Price CT, Habyarimana F, Kalia A, Abu Kwaik Y**. 2008. A Dot/Icm-translocated ankyrin protein of *Legionella pneumophila* is required for intracellular proliferation within human macrophages and protozoa. Mol. Microbiol. **70**:908–23.

3. **Arbeloa A, Garnett J, Lillington J, Bulgin RR, Berger CN, Lea SM, Matthews S, Frankel G**. 2010. EspM2 is a RhoA guanine nucleotide exchange factor. Cell Microbiol. **12**:654–664.

4. **Banga S, Gao P, Shen X, Fiscus V, Zong W-X, Chen L, Luo Z-Q**. 2007. *Legionella pneumophila* inhibits macrophage apoptosis by targeting pro-death members of the Bcl2 protein family. Proc. Natl. Acad. Sci. U. S. A. **104**:5121–6.

5. **Barbu EM, Ganesh VK, Gurusiddappa S, Mackenzie RC, Foster TJ, Sudhof TC, Höök M**. 2010. beta-Neurexin is a ligand for the *Staphylococcus aureus* MSCRAMM SdrC. PLoS Pathog. **6**:e1000726.

6. **Beare PA, Gilk SD, Larson CL, Hill J, Stead CM, Omsland A, Cockrell DC, Howe D, Voth DE, Heinzen RA**. 2011. Dot /Icm type IVB secretion system requirements for *Coxiella burnetii* growth in human macrophages. mBio. **2**:doi:10.1128/mBio.00175-11.

7. **Beare PA, Howe D, Cockrell DC, Omsland A, Hansen B, Heinzen RA**. 2009. Characterization of a *Coxiella burnetii ftsZ* mutant generated by *Himar1* transposon mutagenesis. J. Bacteriol. **191**:1369–81.

8. **Beare PA, Larson CL, Gilk SD, Heinzen RA**. 2012. Two systems for targeted gene deletion in *Coxiella burnetii*. Appl. Environ. Microbiol. **78**:4580–9.

9. **Beare PA, Unsworth N, Andoh M, Voth DE, Omsland A, Gilk SD, Williams KP, Sobral BW, Kupko JJ, Porcella SF, Samuel JE, Heinzen RA**. 2009. Comparative genomics reveal extensive transposon-mediated genomic plasticity and diversity among potential effector proteins within the genus *Coxiella*. Infect. Immun. **77**:642–56.

10. **Berger KH, Isberg RR**. 1993. Two distinct defects in intracellular growth complemented by a single genetic locus in *Legionella pneumophila*. Mol. Microbiol. **7**:7–19.

11. **Black DS, Bliska JB**. 2000. The RhoGAP activity of the *Yersinia pseudotuberculosis* cytotoxin YopE is required for antiphagocytic function and virulence. Mol. Microbiol. **37**:515–27.

12. **Brand BC, Sadosky AB, Shuman HA**. 1994. The *Legionella pneumophila* icm locus : a set of genes required for intracelluiar multiplication in human macrophages. Mol. Microbiol. **14**:797–808.

13. **Brennan RE, Samuel JE**. 2003. Evaluation of *Coxiella burnetii* antibiotic susceptibilities by real-time PCR Assay. J. Clin. Microbiol. **41**: 1869-1874.

14. **Burstein D, Zusman T, Degtyar E, Viner R, Segal G, Pupko T**. 2009. Genome-scale identification of *Legionella pneumophila* effectors using a machine learning approach. PLoS Pathog. **5**:e1000508.

15. **Campodonico EM, Chesnel L, Roy CR**. 2005. A yeast genetic system for the identification and characterization of substrate proteins transferred into host cells by the *Legionella pneumophila* Dot/Icm system. Mol. Microbiol. **56**:918–33.

16. **Campoy EM, Mansilla ME, Colombo MI**. 2013. Endocytic SNAREs are involved in optimal *Coxiella burnetii* vacuole development. Cell Microbiol. **15**:922–41.

17. **Campoy EM, Zoppino FCM, Colombo MI**. 2011. The early secretory pathway contributes to the growth of the *Coxiella*-replicative niche. Infect. Immun. **79**:402–13.

18. **Carey KL, Newton HJ, Lührmann A, Roy CR**. 2011. The *Coxiella burnetii* Dot/Icm system delivers a unique repertoire of type IV effectors into host cells and is required for intracellular replication. PLoS Pathog. **7**:e1002056.

19. **Cassel D, Pfeuffer T**. 1978. Mechanism of cholera toxin action: covalent modification of the guanyl nucleotide-binding protein of the adenylate cyclase system. Proc. Natl. Acad. Sci. U. S. A. **75**:2669–73.

20. **Chen C, Banga S, Mertens K, Weber MM, Gorbaslieva I, Tan Y, Luo Z-Q, Samuel JE**. 2010. Large-scale identification and translocation of type IV secretion substrates by *Coxiella burnetii*. Proc. Natl. Acad. Sci. U. S. A. **107**:21755–60.

21. **Coleman SA, Fischer ER, Howe D, Mead J, Heinzen RA, Mead DJ**. 2004. Temporal analysis of *Coxiella burnetii* morphological differentiation. J. Bacteriol. **186**: 7344-7352.

22. **Collins CA, Brown EJ**. 2010. Cytosol as battleground: ubiquitin as a weapon for both host and pathogen. Trends Cell Biol. **20**:205–13.

23. **De Felipe KS, Glover RT, Charpentier X, Anderson OR, Reyes M, Pericone CD, Shuman H a**. 2008. *Legionella* eukaryotic-like type IV substrates interfere with organelle trafficking. PLoS Pathog. **4**:e1000117.

24. **Deretic V**. 2011. Autophagy in immunity and cell-autonomous defense against intracellular microbes. Immunol. Rev. **240**:92–104.

25. **Deretic V, Levine B**. 2009. Autophagy, immunity, and microbial adaptations. Cell Host Microbe **5**:527–49.

26. **Ding S-Z, Fischer W, Kaparakis-Liaskos M, Liechti G, Merrell DS, Grant P a, Ferrero RL, Crowe SE, Haas R, Hatakeyama M, Goldberg JB**. 2010. *Helicobacter pylori*-induced histone modification, associated gene expression in gastric epithelial cells, and its implication in pathogenesis. PLoS One **5**:e9875.

27. **Dong N, Liu L, Shao F**. 2010. A bacterial effector targets host DH-PH domain RhoGEFs and antagonizes macrophage phagocytosis. EMBO J. **29**:1363–76.

28. **Ensminger AW, Isberg RR**. 2010. E3 ubiquitin ligase activity and targeting of BAT3 by multiple *Legionella pneumophila* translocated substrates. Infect. Immun. **78**:3905–19.

29. **Fan H, Cheng KK, Klein HL**. 1996. Mutations in the RNA polymerase II transcription machinery suppress the hyperrecombination mutant *hpr1Δ* of *Saccharomyces cerevisiae*. Genetics Society of America **142**: 749-759.

30. **Fu Y, Galán JE**. 1999. A *Salmonella* protein antagonizes Rac-1 and Cdc42 to mediate host-cell recovery after bacterial invasion. Nature **401**:293–7.

31. **Garcia-Garcia JC, Barat NC, Trembley SJ, Dumler JS**. 2009. Epigenetic silencing of host cell defense genes enhances intracellular survival of the rickettsial pathogen *Anaplasma phagocytophilum*. PLoS Pathog. **5**:e1000488.

32. **Garcia-Garcia JC, Rennoll-Bankert KE, Pelly S, Milstone AM, Dumler JS**. 2009. Silencing of host cell CYBB gene expression by the nuclear effector AnkA of the intracellular pathogen *Anaplasma phagocytophilum*. Infect. Immun. **77**:2385–91.

33. **Gietz, D, St Jean A, Woods RA, Schiestl RH**. 1992. Improved method for high efficiency transformation of intact yeast cells. Nucleic Acids Res. **20**:1425.

34. **Gillespie JJ, Wattam AR, Cammer SA, Gabbard JL, Shukla MP, Dalay O, Driscoll T, Hix D, Mane SP, Mao C, Nordberg EK, Scott M, Schulman JR, Snyder EE, Sullivan DE, Wang C, Warren A, Williams KP, Xue T, Yoo HS, Zhang C, Zhang Y, Will R, Kenyon RW, Sobral WB.** 2011. PATRIC : the comprehensive bacterial bioinformatics resource with a focus on human pathogenic species. Infect. Immun. **79**: 4286-4298.

35. **Guo Z, Stephenson R, Qiu J, Zheng S, Luo Z-Q**. 2013. A *Legionella* effector modulates host cytoskeletal structure by inhibiting actin polymerization. Microbes Infect. 1–12.

36. **Gutierrez MG, Vázquez CL, Munafó DB, Zoppino FCM, Berón W, Rabinovitch M, Colombo MI**. 2005. Autophagy induction favours the generation and maturation of the *Coxiella*-replicative vacuoles. Cell Microbiol. **7**:981–93.

37. **Hackstadt T, Peacock MG, Hitchcock PJ, Cole RL**. 1985. Lipopolysaccharide variation in *Coxiella burnetii*: intrastrain heterogeneity in structure and antigenicity Infect. Immun. **48**: 359-365.

38. **Haglund CM, Welch MD**. 2011. Pathogens and polymers: microbe-host interactions illuminate the cytoskeleton. J. Cell Biol. **195**:7–17.

39. **Hamon MA, Batsché E, Régnault B, Tham TN, Seveau S, Muchardt C, Cossart P**. 2007. Histone modifications induced by a family of bacterial toxins. Proc. Natl. Acad. Sci. U. S. A. **104**:13467–72.

40. **Hamon MA, Cossart P**. 2008. Histone modifications and chromatin remodeling during bacterial infections. Cell Host Microbe **4**:100–9.

41. **Hardiman CA, Mcdonough JA, Newton HJ, Roy CR**. 2012. The role of Rab GTPases in the transport of vacuoles containing *Legionella pneumophila* and *Coxiella burnetii*. Biochem. Soc. Tran.1353–1359.

42. **Hardt WD, Chen LM, Schuebel KE, Bustelo XR, Galán JE**. 1998. *S. typhimurium* encodes an activator of Rho GTPases that induces membrane ruffling and nuclear responses in host cells. Cell **93**:815–26.

43. **Heidtman M, Chen EJ, Moy M-Y, Isberg RR**. 2009. Large-scale identification of *Legionella pneumophila* Dot/Icm substrates that modulate host cell vesicle trafficking pathways. Cell Microbiol. **11**:230–48.

44. **Howe D, Mallavia LP**. 2000. *Coxiella burnetii* exhibits morphological change and delays phagolysosomal fusion after internalization by J774A.1 cells. Infect. Immun. **68**:3815–21.

45. **Howe D, Melnicáková J, Barák I, Heinzen RA**. 2003. Maturation of the *Coxiella burnetii* parasitophorous vacuole requires bacterial protein synthesis but not replication. Cell Microbiol. **5**:469–80.

46. **Huang L, Boyd D, Amyot WM, Hempstead AD, Luo Z-Q, O'Connor TJ, Chen C, Machner M, Montminy T, Isberg RR**. 2011. The E Block motif is associated with *Legionella pneumophila* translocated substrates. Cell Microbiol. **13**:227–45.

47. **Hubber A, Roy CR**. 2010. Modulation of host cell function by *Legionella pneumophila* type IV effectors. Annu. Rev. Cell Dev. Biol. **26**:261–83.

48. **Hussain SK, Broederdorf LJ, Sharma UM, Voth DE**. 2010. Host kinase activity is required for *Coxiella burnetii* parasitophorous vacuole formation. Front. Microbiol. **1**:137.

49. **Ingmundson A, Delprato A, Lambright DG, Roy CR**. 2007. *Legionella pneumophila* proteins that regulate Rab1 membrane cycling. Nature. **450**:365–9.

50. **Kjeken R, Egeberg M, Habermann A, Kuehnel M, Peyron P, Floetenmeyer M, Walther P, Jahraus A, Kuznetsov SA, Griffiths G**. 2004. Fusion between phagosomes , early and late endosomes : A role for actin in fusion between late , but not early endocytic organelles Mol. Biol. Cell. **15**:345–358.

51. **Klee SR, Tyczka J, Ellerbrok H, Franz T, Linke S, Baljer G, Appel B**. 2006. Highly sensitive real-time PCR for specific detection and quantification of *Coxiella burnetii*. BMC Microbiol. **6**:2.

52. **Klingenbeck L, Eckart RA, Berens C, Lührmann A**. 2012. The *Coxiella burnetii* type IV secretion system substrate CaeB inhibits intrinsic apoptosis at the mitochondrial level. Cell Microbiol. **32**: doi:10.1111/cmi.12066.

53. **Kosugi S, Hasebe M, Matsumura N, Takashima H, Miyamoto-Sato E, Tomita M, Yanagawa H**. 2009. Six classes of nuclear localization signals specific to different binding grooves of importin alpha. J. Biol. Chem. **284**:478–85.

54. **Kubori T, Hyakutake A, Nagai H**. 2008. *Legionella* translocates an E3 ubiquitin ligase that has multiple U-boxes with distinct functions. Mol. Microbiol. **67**:1307–19.

55. **Kubori T, Shinzawa N, Kanuka H, Nagai H**. 2010. *Legionella* metaeffector exploits host proteasome to temporally regulate cognate effector. PLoS Pathog. **6**:e1001216.

56. **Laguna RK, Creasey E a, Li Z, Valtz N, Isberg RR**. 2006. A *Legionella pneumophila*-translocated substrate that is required for growth within macrophages and protection from host cell death. Proc. Natl. Acad. Sci. U. S. A. **103**:18745–50.

57. **Larson CL, Beare PA, Howe H, Heinzen RA**. 2013. *Coxiella burnetii* effector protein subverts clathrin-mediated vesicular trafficking for pathogen vacuole biogenesis. Proc. Natl. Acad. Sci. U. S. A. **49**:e4770-9

58. **Lemichez E, Aktories K**. 2013. Hijacking of Rho GTPases during bacterial infection. Exp. Cell Res. **319**:2329–36.

59. **Lerm M, Selzer J, Hoffmeyer A, Rapp UR, Aktories K, Schmidt G**. 1999. Deamidation of Cdc42 and Rac by *Escherichia coli* cytotoxic necrotizing factor 1: activation of c-Jun N-terminal kinase in HeLa cells. Infect. Immun. **67**:496–503.

60. **Lührmann A, Nogueira C V, Carey KL, Roy CR**. 2010. Inhibition of pathogen-induced apoptosis by a *Coxiella burnetii* type IV effector protein. Proc. Natl. Acad. Sci. U. S. A. **107**:18997–9001.

61. **Luo Z-Q, Isberg RR**. 2004. Multiple substrates of the *Legionella pneumophila* Dot/Icm system identified by interbacterial protein transfer. Proc. Natl. Acad. Sci. U. S. A. **101**:841–6.

62. **Macdonald LJ, Graham JG, Kurten RC, Voth DE**. 2013. *Coxiella burnetii* exploits host cAMP-dependent protein kinase signalling to promote macrophage survival. Cell Microbiol. doi: 10.1111/cmi.12213.

63. **MacDonald LJ, Kurten RC, Voth DE**. 2012. *Coxiella burnetii* alters cyclic AMP-dependent protein kinase signaling during growth in macrophages. Infect. Immun. **80**:1980–6.

64. **Madariaga MG, Rezai K, Trenholme GM, Weinstein RA**. 2003. Review Q fever : a biological weapon in your backyard. Lancet. 709–721.

65. **Mahapatra S, Ayoubi P, Shaw EI**. 2010. *Coxiella burnetii* Nine Mile II proteins modulate gene expression of monocytic host cells during infection. BMC Microbiol. **10**:244.

66. **Marra A, Blander SJ, Horwitz MA, Shuman HA**. 1992. Identification of a *Legionella pneumophila* locus required for intracellular multiplication in human macrophages. Proc. Natl. Acad. Sci. U. S. A. **89**:9607–9611.

67. **Maturana P, Graham JG, Sharma UM, Voth DE**. 2013. Refining the plasmid-encoded type IV secretion system substrate repertoire of *Coxiella burnetii*. J. Bacteriol. **195**:3269–76.

68. **Mcdonough JA, Newton HJ, Klum S**. 2013. Host pathways important for *Coxiella burnetii* infection revealed by genome-wide RNA interference screening. mBio. **4**: e00606-12.

69. **Meconi S, Jacomo V, Boquet P, Mege J, Capo C, Jacomo R, Raoult D**. 1998. *Coxiella burnetii* induces reorganization of the actin cytoskeleton in human monocytes. Infect. Immun. **66**: 5527-5533.

70. **Miki T, Akiba K, Iguchi M, Danbara H, Okada N**. 2011. The *Chromobacterium violaceum* type III effector CopE, a guanine nucleotide exchange factor for Rac1 and Cdc42, is involved in bacterial invasion of epithelial cells and pathogenesis. Mol. Microbiol. **80**:1186–203.

71. **Moos A, Hackstadt T**. 1987. Comparative virulence of intra- and interstrain lipopolysaccharide variants of *Coxiella burnetii* in the guinea pig model. Infect. Immun. **55**:1144–50.

72. **Müller MP, Peters H, Blumer J, Blankenfeldt W, Goody RS, Itzen A**. 2014. The *Legionella* effector protein DrrA AMPylates the membrane traffic regulator Rab1b Science. **329**: 946-949.

73. **Mumberg D, Müller R, Funk M**. 1995. Yeast vectors for the controlled expression of heterologous proteins in different genetic backgrounds. Gene. **156**:119–22.

74. **Murata T, Delprato A, Ingmundson A, Toomre DK, Lambright DG, Roy CR**. 2006. The *Legionella pneumophila* effector protein DrrA is a Rab1 guanine nucleotide-exchange factor. Nat. Cell Biol. **8**:971–7.

75. **Myagmar B-E, Umikawa M, Asato T, Taira K, Oshiro M, Hino A, Takei K, Uezato H, Kariya K**. 2005. PARG1, a protein-tyrosine phosphatase-associated RhoGAP, as a putative Rap2 effector. Biochem. Biophys. Res. Commun. **329**:1046–52.

76. **Nagai H, Kubori T**. 2011. Type IVB secretion systems of *Legionella* and other Gram-negative bacteria. Front. Microbiol. **2**:136.

77. **Newton HJ, Ang DKY, van Driel IR, Hartland EL**. 2010. Molecular pathogenesis of infections caused by *Legionella pneumophila*. Clin. Microbiol. Rev. **23**:274–98.

78. **Newton HJ, McDonough JA, Roy CR**. 2013. Effector protein translocation by the *Coxiella burnetii* Dot/Icm type IV secretion system requires endocytic maturation of the pathogen-occupied vacuole. PLoS One. **8**:e54566.

79. **O'Connor TJ, Adepoju Y, Boyd D, Isberg RR**. 2011. Inaugural Article: Minimization of the *Legionella pneumophila* genome reveals chromosomal regions involved in host range expansion. Proc. Natl. Acad. Sci. U.S.A **108**: 14733-14740.

80. **Omsland A, Beare PA, Hill J, Cockrell DC, Howe D, Hansen B, Samuel JE, Heinzen RA**. 2011. Isolation from animal tissue and genetic transformation of *Coxiella burnetii* are facilitated by an improved axenic growth medium. Appl. Environ. Microbiol. **77**:3720–5.

81. **Omsland A, Heinzen RA**. 2011. Life on the outside: The rescue of *Coxiella burnetii* from its host cell. Annu. Rev. Microbiol. **15**:111–128.

82. **Orth JHC, Preuss I, Fester I, Schlosser A, Wilson BA, Aktories K**. 2009. *Pasteurella multocida* toxin activation of heterotrimeric G proteins by deamidation Proc. Natl. Acad. Sci. U.S.A. 2–7.

83. **Pan X, Lührmann A, Satoh A, Laskowski-Arce MA, Roy CR**. 2008. Ankyrin repeat proteins comprise a diverse family of bacterial type IV effectors. Science. **320**:1651–4.

84. **Park J, Kim KJ, Choi K, Grab DJ, Dumler JS**. 2004. *Anaplasma phagocytophilum* AnkA binds to granulocyte DNA and nuclear proteins. Cell Microbiol. **6**:743–51.

85. **Pennini ME, Perrinet S, Dautry-Varsat A, Subtil A**. 2010. Histone methylation by NUE, a novel nuclear effector of the intracellular pathogen *Chlamydia trachomatis*. PLoS Pathog. **6**:e1000995.

86. **Ridley AJ.** 2006. Rho GTPases and actin dynamics in membrane protrusions and vesicle trafficking. Trends Cell Biol. **16**:522–9.

87. **Rolando M, Sanulli S, Rusniok C, Gomez-Valero L, Bertholet C, Sahr T, Margueron R, Buchrieser C**. 2013. *Legionella pneumophila* effector RomA uniquely modifies host chromatin to repress gene expression and promote intracellular bacterial replication. Cell Host Microbe. **13**:395–405.

88. **Romano PS, Gutierrez MG, Berón W, Rabinovitch M, Colombo MI**. 2007. The autophagic pathway is actively modulated by phase II *Coxiella burnetii* to efficiently replicate in the host cell. Cell Microbiol. **9**:891–909.

89. **Russell-Lodrigue KE, Andoh M, Poels MWJ, Shive HR, Weeks BR, Zhang GQ, Tersteeg C, Masegi T, Hotta A, Yamaguchi T, Fukushi H, Hirai K, McMurray DN, Samuel JE**. 2009. *Coxiella burnetii* isolates cause genogroup-specific virulence in mouse and guinea pig models of acute Q fever. Infect. Immun. **77**:5640–50.

90. **Samuel JE, Frazier ME, Kahn ML, Thomashow LS, Mallavia LP**. 1983. Isolation and characterization of a plasmid from phase I *Coxiella burnetii*. Infect. Immun. **41**:488–93.

91. **Saras, J.** 1997. A Novel GTPase-activating protein for Rho interacts with a PDZ domain of the protein-tyrosine phosphatase PTPL1. J. Biol. Chem. **272**:24333–24338.

92. **Seshadri R, Paulsen IT, Eisen JA, Read TD, Nelson KE, Nelson WC, Ward NL, Tettelin H, Davidsen TM, Beanan MJ, Deboy RT, Daugherty SC, Brinkac LM, Madupu R, Dodson RJ, Khouri HM, Lee KH, Carty HA, Scanlan D, Heinzen RA, Thompson HA, Samuel JE, Fraser CM, Heidelberg JF**. 2003. Complete genome sequence of the Q-fever pathogen *Coxiella burnetii*. Proc. Natl. Acad. Sci. U. S. A. **100**:5455–60.

93. **Sheahan K-L, Satchell KJF**. 2007. Inactivation of small Rho GTPases by the multifunctional RTX toxin from *Vibrio cholerae*. Cell Microbiol. **9**:1324–35.

94. **Shohdy N, Efe JA, Emr SD, Shuman HA**. 2005. Pathogen effector protein screening in yeast identifies *Legionella* factors that interfere with membrane trafficking. Proc. Natl. Acad. Sci. U. S. A. **102**:4866–71.

95. **Sisko JL, Spaeth K, Kumar Y, Valdivia RH**. 2006. Multifunctional analysis of *Chlamydia*-specific genes in a yeast expression system. Mol. Microbiol. **60**:51–66.

96. **Spiering D, Hodgson L**. 2011. Dynamics of the Rho-family small GTPases in actin regulation and motility. Cell Adh. Migr. **5**:170–180.

97. **Steele-Mortimer O**. 2011. Exploitation of the ubiquitin system by invading bacteria. Traffic. **12**:162–9.

98. **Stender S, Friebel A, Linder S, Rohde M, Mirold S, Hardt WD**. 2000. Identification of SopE2 from *Salmonella typhimurium*, a conserved guanine

nucleotide exchange factor for Cdc42 of the host cell. Mol. Microbiol. **36**:1206–21.

99. **Stoenner HG, Lackman DB**. 1960. The Biologic Properties of *Coxiella burnetii* isolated from rodents collected in Utah. Am. J. Hyg. **71**:45–51.

100. **Tan Y, Arnold RJ, Luo Z-Q**. 2011. *Legionella pneumophila* regulates the small GTPase Rab1 activity by reversible phosphorylcholination. Proc. Natl. Acad. Sci. U. S. A. **108**:21212–21217.

101. **Tcherkezian J, Lamarche-Vane N**. 2007. Current knowledge of the large RhoGAP family of proteins. Biol. Cell. **99**:67–86.

102. **Teichert M, Tatge H, Schoentaube J, Just I, Gerhard R**. 2006. Application of mutated *Clostridium difficile* toxin A for determination of glucosyltransferase-dependent effects Infect. Immun. **74**:6006–6010.

103. **Terebiznik MR, Vieira OV, Marcus SL, Slade A, Yip CM, Trimble WS, Meyer T, Finlay BB, Grinstein S**. 2002. Elimination of host cell PtdIns(4,5)P(2) by bacterial SigD promotes membrane fission during invasion by *Salmonella*. Nat. Cell Biol. **4**:766–73.

104. **Valdivia RH.** 2004. MINIREVIEWS Modeling the function of bacterial virulence factors in *Saccharomyces cerevisiae*. Eukaryotic Cell. **3**:827–834.

105. **Van der Hoek W, Schneeberger PM, Oomen T, Wegdam-Blans MC, Dijkstra F, Notermans DQ, Bijlmer HA, Groeneveld K, Wijkmans CJ, Rietveld A, Kampschreur LM, van Duynhoven Y**. 2012. Shifting priorities in the aftermath of a Q fever epidemic in 2007 to 2009 in The Netherlands: from acute to chronic infection. Euro. Surveill. **17**:20059.

106. **Van Schaik EJ, Chen C, Mertens K, Weber MM, Samuel JE**. 2013. Molecular pathogenesis of the obligate intracellular bacterium *Coxiella burnetii*. Nat. Rev. **11**:561–73.

107. **Vázquez CL, Colombo MI**. 2010. *Coxiella burnetii* modulates Beclin 1 and Bcl-2, preventing host cell apoptosis to generate a persistent bacterial infection. Cell Death Differ. **17**:421–38.

108. **Viner R, Chetrit D, Ehrlich M, Segal G**. 2012. Identification of two *Legionella pneumophila* effectors that manipulate host phospholipids biosynthesis. PLoS Pathog. **8**:e1002988.

109. **Voth DE, Beare PA, Howe D, Sharma UM, Samoilis G, Cockrell DC, Omsland A, Heinzen RA**. 2011. The *Coxiella burnetii* cryptic plasmid is enriched in genes encoding type IV secretion system substrates. J. Bacteriol. **193**:1493–503.

110. **Voth DE, Heinzen RA**. 2009. Sustained activation of Akt and Erk1/2 is required for *Coxiella burnetii* antiapoptotic activity. Infect. Immun. **77**:205–13.

111. **Voth DE, Howe D, Beare PA, Vogel JP, Unsworth N, Samuel JE, Heinzen RA**. 2009. The *Coxiella burnetii* ankyrin repeat domain-containing protein family is heterogeneous, with C-terminal truncations that influence Dot/Icm-mediated secretion. J. Bacteriol. **191**:4232–42.

112. **Voth DE, Howe D, Heinzen RA**. 2007. *Coxiella burnetii* inhibits apoptosis in human THP-1 cells and monkey primary alveolar macrophages. Infect. Immun. **75**:4263–71.

113. **Weber MM, Chen C, Rowin K, Mertens K, Galvan G, Zhi H, Dealing CM, Roman VA, Banga S, Tan Y, Luo Z-Q, Samuel JE**. 2013. Identification of *C. burnetii* type IV secretion substrates required for intracellular replication and *Coxiella*-containing vacuole formation. J. Bacteriol. **195**:3914–24.

114. **Xu L, Shen X, Bryan A, Banga S, Swanson MS, Luo Z-Q**. 2010. Inhibition of host vacuolar H+-ATPase activity by a *Legionella pneumophila* effector. PLoS Pathog. **6**:e1000822.

115. **Zamboni DS, McGrath S, Rabinovitch M, Roy CR**. 2003. *Coxiella burnetii* express type IV secretion system proteins that function similarly to components of the *Legionella pneumophila* Dot/Icm system. Mol. Microbiol. **49**:965–976.

116. **Zhu B, Nethery KA, Kuriakose JA, Wakeel A, Zhang X, McBride JW**. 2009. Nuclear translocated *Ehrlichia chaffeensis* ankyrin protein interacts with a specific adenine-rich motif of host promoter and intronic Alu elements. Infect. Immun. **77**:4243–55.

117. **Zhu, W, Banga S, Tan Y, Zheng C, Stephenson R, Gately J, Luo Z-Q**. 2011. Comprehensive identification of protein substrates of the Dot/Icm type IV transporter of *Legionella pneumophila*. PLoS One. **6**:e17638.

118. **Zusman T, Aloni G, Halperin E, Kotzer H, Degtyar E, Feldman M, Segal G**. 2007. The response regulator PmrA is a major regulator of the icm/dot type IV secretion system in *Legionella pneumophila* and *Coxiella burnetii*. Mol. Microbiol. **63**:1508–23.